



Natural Resources
Canada

Ressources naturelles
Canada

**GEOLOGICAL SURVEY OF CANADA
OPEN FILE 8670**

**Palynological analysis of the two Labrador Shelf wells,
Petro-Canada et al. North Leif I-05 and Total Eastcan
et al. Skolp E-07, offshore eastern Canada: new age,
paleoenvironmental and lithostratigraphic interpretations**

L.T. Dafoe and G.L. Williams

2020

Canada



**GEOLOGICAL SURVEY OF CANADA
OPEN FILE 8670**

**Palynological analysis of the two Labrador Shelf wells,
Petro-Canada et al. North Leif I-05 and Total Eastcan et al.
Skolp E-07, offshore eastern Canada: new age,
paleoenvironmental and lithostratigraphic interpretations**

L.T. Dafoe and G.L. Williams

Geological Survey of Canada, 1 Challenger Drive, Dartmouth, Nova Scotia B2Y 4A2

2020

© Her Majesty the Queen in Right of Canada, as represented by the Minister of Natural Resources, 2020

Information contained in this publication or product may be reproduced, in part or in whole, and by any means, for personal or public non-commercial purposes, without charge or further permission, unless otherwise specified.

You are asked to:

- exercise due diligence in ensuring the accuracy of the materials reproduced;
- indicate the complete title of the materials reproduced, and the name of the author organization; and
- indicate that the reproduction is a copy of an official work that is published by Natural Resources Canada (NRCan) and that the reproduction has not been produced in affiliation with, or with the endorsement of, NRCan.

Commercial reproduction and distribution is prohibited except with written permission from NRCan. For more information, contact NRCan at nrcan.copyrightdroitdauteur.nrcan@canada.ca.

Permanent link: <https://doi.org/10.4095/321502>

This publication is available for free download through GEOSCAN (<https://geoscan.nrcan.gc.ca/>).

Recommended citation

Dafoe, L.T. and Williams, G.L., 2020. Palynological analysis of the two Labrador Shelf wells, Petro-Canada et al. North Leif I-05 and Total Eastcan et al. Skolp E-07, offshore eastern Canada: new age, paleoenvironmental and lithostratigraphic interpretations; Geological Survey of Canada, Open File 8670, 103 p.
<https://doi.org/10.4095/321502>

Publications in this series have not been edited; they are released as submitted by the author.

INTRODUCTION

Geophysical surveys in the 1960s revealed the existence of two major sedimentary basins in the Labrador Sea–Davis Strait area: these were the Hopedale Basin to the south and the Saglek Basin to the north. To investigate the hydrocarbon potential of the Hopedale Basin, Tenneco et al. drilled the Leif E-38 well in 1971. Subsequently, other companies undertook exploration programmes in the two basins, so that by the early 1980s there were 29 wells, 9 in the Saglek Basin and 20 in the Hopedale Basin. Two of these wells were North Leif I-05 and Skolp E-07, which were drilled in the Hopedale and Saglek basins, respectively (Fig. 1).

North Leif I-05 was drilled in a water depth of 144 m and the total depth of the well is 3513 m; at Skolp E-07 the water depth is 166.5 m and the total depth is 2992 m. North Leif I-05 penetrated Lower Cretaceous volcanics of the Alexis Formation from 3394 m to its total depth of 3513 m (Moir, 1989). According to Nøhr-Hansen et al. (2016), the Alexis was sequentially overlain by about 710 m of Lower Cretaceous, 270 m of Upper Cretaceous, 2040 m of Paleogene, and 60 m of Neogene strata. Skolp E-07, which reached total depth at 2992 m, encountered Precambrian gneiss at 2967 m (Moir, 1989). Nøhr-Hansen et al. (2016) identified the following strata overlying Precambrian basement: 490 m of Albian–Cenomanian section, a 1480 m Campanian–Maastrichtian interval, and 90 m of Paleocene–Eocene strata.

Although these two wells were studied in detail by Nøhr-Hansen et al. (2016), we considered that a restudy was merited because the stratigraphic control within the lower part of the Upper Cretaceous interval was still poorly understood in the region. We also wanted to test the possibility of building on the palynological event scheme developed by Nøhr-Hansen et al. (2016), which incorporated 169 last occurrence and 18 local/regional-peak/common-occurrence events based on fossil dinoflagellates (dinocysts), spores and pollen (miospores), fungal spores and the massulae of the freshwater fern *Azolla*. A third objective was the incorporation of results from the lithological and palynostratigraphic studies of the conventional core material from these and other wells on the Labrador Margin (Dafoe and Williams, in press), and to see if this new data could refine the palynomorph assemblages, and thus age at certain horizons. A final aim was to integrate new interpretations of ages and unconformities, together with an assessment of well logs and lithologies, allowing for refinement of the lithostratigraphic interpretations of the two wells. This study provides a critical contribution to an understanding of the overall succession along the Labrador margin and within the Hopedale and Saglek basins.

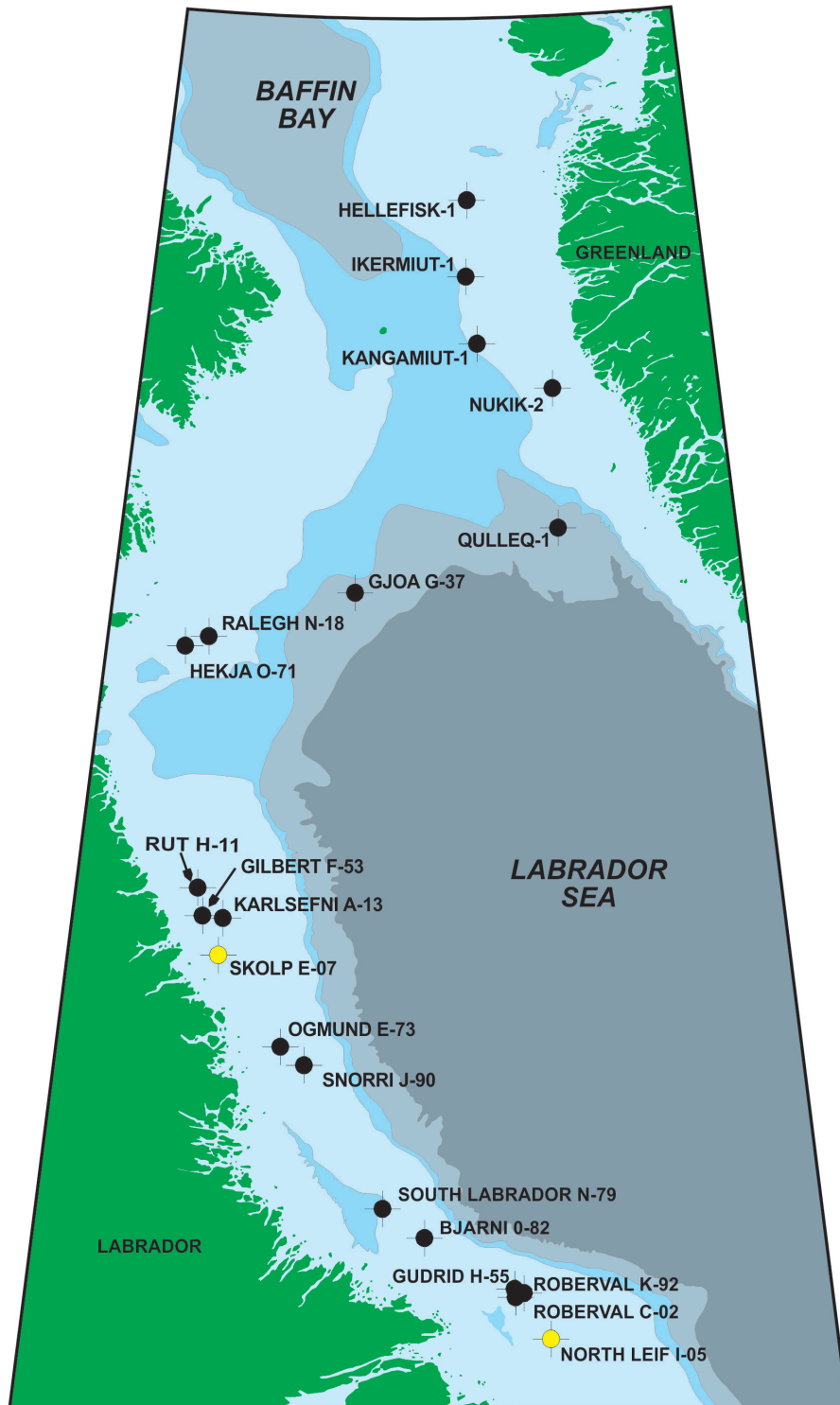


Figure 1: Map of the Labrador margin showing the Skolp E-07 and North Leif I-05 wells. The shelf at a maximum of 400 m water depth is shown in light blue. Not all wells for the Labrador margin are shown.

METHODOLOGY

Although our age and paleoenvironmental determinations for the North Leif I-05 and Skolp E-07 wells are based on cuttings, we further integrate the analyses of samples from two conventional cores based on the work of Dafoe and Williams (in press). For North Leif I-05, we analyzed two sets of slides from processed cutting samples: one set processed by the Geological Survey of Canada (GSC) and the other by the Geological Survey of Denmark and Greenland (GEUS). The total number of slides was 185, of which 81 were prepared at GSC (Atlantic) and 104 at GEUS. Each individual cuttings sample represents a 10 m interval, but samples were collected at more widely spaced intervals (e.g. every 30 m for the GSC set of slides). The conventional core samples from Dafoe and Williams (in press) for North Leif I-05 were processed by Global Geolabs Ltd of Medicine Hat, Alberta.

The cuttings samples processed from Skolp E-07 comprise 5 m intervals taken every thirty or fifteen metres, with samples more concentrated in the key intervals of interest from 1815–2010 m and 2415–2610 m. Additionally, we incorporated the analyses of seven conventional cores from this well, as reported in Dafoe and Williams (in press). All of the samples from Skolp E-07 were processed by Global Geolabs Ltd.

Processing

Processing of samples for palynomorphs was not markedly different in the three laboratories. The samples processed by Global Geolabs Ltd were treated as follows. The samples were first crushed, then treated with hydrochloric and hydrofluoric acids to remove carbonates and silicates, respectively, with thorough washing after both treatments. To allow for better heavy-liquid separation, a few drops of concentrated hydrochloric acid were added and the mixture was then centrifuged. Following this stage, a fraction of each sample was saved and then used to make a kerogen slide. Further concentration of the remaining fraction involved centrifuging in heavy liquid zinc bromide and oxidizing with Schulze solution. The samples were then placed in a 10% solution of ammonium hydroxide for a few minutes. On completion of this phase, a second slide was prepared from the unsieved material to allow for palynomorph counts to determine variations in abundances of taxa. Further processing involved sieving the samples through a 30 μm sieve, a technique that is invaluable for concentrating the dinocysts and larger miospores. Slides were then prepared from both the +30 and -30 μm fractions. Residues were smeared on a coverslip, which was inverted and placed on a slide using the mounting medium, clear casting resin.

The samples processed by the other two laboratories were also treated in hydrochloric and hydrofluoric acid. The GSC-Atlantic laboratory followed a similar procedure, the major difference involving the use of sieves of different mesh sizes. GEUS sieved the samples after the acid treatment, then oxidized the residue in concentrated nitric acid, followed usually by washing

in weak potassium hydroxide solution. The one significant difference was that GEUS sometimes mounted the residue in glycerine jelly. All of the slides were examined under a Zeiss Photomicroscope.

Age Determinations

Qualitative analyses were undertaken on the fractions of each sample and quantitative data generated from approximately every second sample. Where possible, we counted specimens from which plots were generated showing variations in the major palynomorph groups; these were miospores, dinocysts, acritarchs and what we loosely classed as others.

The results presented in this paper are based on the analysis of the palynomorph groups defined above, as well as the lithostratigraphy and well logs. We also discern bioevents, each generally representing the last occurrence (LO; the highest or youngest occurrence of a taxon in a well or surface section). First Occurrences (FOs) are not reliable indicators when deriving data from cuttings, so we have included only those derived from the conventional cores in both wells.

Although our ages are derived primarily from events recognized in Nøhr-Hansen et al. (2016), we have also incorporated other taxa. Age interpretations for the two wells are keyed to known stratigraphic ranges of dinocysts in European sections (Powell, 1992; Bujak et al., 1980; Bujak, 1994; Williams et al., 1999, 2004) and from older wells and coreholes from offshore eastern Canada and onshore and offshore West Greenland (Williams, 1975; Williams and Brideaux, 1975; Williams and Bujak, 1977; Barss et al., 1979; Williams et al., 1990; Sønderholm et al., 2003; Nøhr-Hansen, 2003, 2004; Fensome et al., 2016; Nøhr-Hansen et al., 2016; and Williams, 2017a, b). Throughout this study, we have attempted to adhere to the absolute age calibrations proposed by Gradstein et al. (2012).

Paleoenvironmental Interpretations

When interpreting paleoenvironments from well samples, it is desirable to have conventional or sidewall cores. These are rarely available for Labrador Shelf wells, so conclusions have to be primarily based on cuttings, which can be misleading because of contamination from caving and drilling mud.

Both qualitative and quantitative assessments are needed for paleoenvironmental interpretations, the former primarily providing stratigraphic control; however some individual taxa are excellent paleoenvironmental markers. Where quantitative analyses have to be determined from cuttings samples, the quality of the data has to be treated with caution. In quantitative analyses, the number of species (species richness) has some value, but the main emphasis has to be on proportions of specimens grouped into the following major categories: miospores excluding bisaccates, bisaccates, dinocysts, acritarchs, and other palynomorphs. We attempted to count 100 specimens for approximately every second sample using the unsieved slides, but the total count

varied with productivity. In addition, our plots of palynomorph groups outlined above represent percentages of the total, and where the total count was smaller, the resulting plots are likely slightly skewed due to a more limited count. Where there were insufficient total palynomorph counts, we report the counts as too low on the palynomorph ratio plots. We did not consider species richness or diversity, as we did not carry out species counts. The bias of the palynomorph ratio plots reflects that counts are only undertaken on the unsieved fractions of each sample. Sieving acts to concentrate dinocysts, which are generally larger than the miospores (with the exception of the bisaccates); accordingly, we invariably record other species from the sieved slides that are not documented in the counts.

The reliability of quantitative data varies with the fossil group(s) used. Benthic foraminifera are the most informative microfossils for predicting paleoenvironments. However, only one comprehensive report using these microfossils has been published on the Labrador Shelf wells (Bujak Davies Group, 1989a). Our database is restricted to palynomorphs, which can denote a significant range of paleoenvironments. By generating counts of the five major groups listed above, it is possible to determine a progressive sequence from nonmarine to open ocean. Samples containing only miospores are generally terrestrial, although some deep-sea sediments contain high concentrations of bisaccate pollen, which are derived mainly from conifers, due to long-range wind dispersal; for this reason we count bisaccates as a separate category.

Specific taxa or groups of dinocysts and acritarchs can indicate fresh water to open-ocean settings. However, dinocysts (and probably also acritarchs) represent the encysted stage of motile planktonic organisms. Dinoflagellates, and hence the corresponding dinocysts, show distinct environmental preferences, especially with regard to nutrient availability and salinity. This explains why individual dinocyst taxa can be concentrated in lagoonal, coastal, inner shelf, outer shelf, or open-ocean settings. Thus, paleoenvironmental determinations are possible as, for example, we generally assume open-ocean assemblages to represent deeper-water or bathyal environments.

Grouping dinocyst species often allows meaningful interpretation. One example is the gonyaulacacean/peridiniacean/ceratiacean ratio utilised by Lister and Batten (1988). In a study of the Priabonian of Italy, Brinkhuis (1992, 1994) selected genera characteristic of certain environments to illustrate lateral changes in dinocyst assemblages across a transect from lagoonal to open-ocean settings. We base our paleoenvironmental interpretations on a modified version of Brinkhuis's model, as published by Sluijs et al. (2005) and on the findings in Nøhr-Hansen et al. (2016) and Williams (2017a, b). However, paucity of assemblages in some cuttings samples limit paleoenvironmental determinations.

Lithostratigraphy

New age constraints and significant changes in paleoenvironmental settings have allowed refinement of the lithostratigraphic assignments of previous studies, most importantly the work of Moir (1989). We have used well logs (gamma-ray, sonic and resistivity) to study depositional trends, and have tied distinctive log changes to unconformities. We further used the lithology (Canadian Stratigraphic Services; Canstrat) to refining the placement of sandstone- and mudstone-dominated members as well as formation boundaries. Significant breaks in the section noted from the palynological analyses helped to determine the placement of formation tops and related unconformities where lithological constraints were less clear. Revised lithostratigraphic picks are provided for both wells.

NORTH LEIF I-05

Biostratigraphy

Figure 2 shows key well logs, lithology, cored intervals, select biostratigraphic studies, and lithostratigraphy from Moir (1989) and this study for the North Leif I-05 well. Range plots illustrate: the dinocysts recorded from the GSC slide set (Fig. 3); the dinocysts identified in the GEUS slide set (Fig. 4); the spores, pollen and other palynomorphs from the GSC slide set (Fig. 5); and the spores, pollen and other palynomorphs identified in the GEUS slide set (Fig. 6). Plates 1–8 illustrate some key palynomorph species from North Leif I-05 (more details are given in Appendix A for these plates). Ages are discussed in detail below and are summarized in Table 1. Previous biostratigraphic studies of North Leif I-05 include Petro-Canada Exploration Inc. (1980), Bujak Davies Group (1989b), Gradstein et al. (1994), Nøhr-Hansen (2004), Nøhr-Hansen et al. (2016) and Ainsworth et al. (2016). We compare our results to some of these previous studies.

According to Moir (1989), the interval 3513–3394 m of North Leif I-05 (119 m of section) represents the Alexis Formation, a unit named by Umpleby (1979). Despite the volcanic nature of this formation, the lowermost cuttings sample (3507–3500 m) contains the miospore species *Parvisaccites radiatus* and *Impardecispora? cf. apiverrucata*. Nøhr-Hansen et al. (2016) considered the LO of *Parvisaccites radiatus* to be around the top of the Aptian. However, Bujak Davies Group (1989a) defined a *Parvisaccites amplus* Zone, which they considered to be of early Albian age, with one of the key index species being *Parvisaccites radiatus*. Based on this zonation, the age would be early Albian. However, the presence of the miospore *Pilosiporites trichopapillosus* at 3460–3450 m and the miospore *Aequitriradites spinulosus* at 3380–3370 m suggest an older age. In a study of six Scotian Shelf wells, Williams (1975) considered *Pilosiporites trichopapillosus* to have its LO in the Aptian. In the Herjolf M-92 well, also located in the Hopedale Basin, a sample from core 3 at 3563.8 m contains a varied miospore assemblage

including *Aequitriradites spinulosus* and *Callialasporites dampieri* (Dafoe and Williams, in press). Nøhr-Hansen et al. (2016) placed the LO of *Callialasporites dampieri* within the Aptian, whereas Williams (2006) considered the LO of this species to be in the Barremian in the Hermine E-94 well in the Scotian Basin. Based on this evidence, Dafoe and Williams (in press) considered the sample from 3563.8 m in Herjolf M-92 to be close to the base of the Aptian. Taking into account the above findings, we consider the top of the Aptian in North Leif I-05 to be at about 3380–3370 m. This is in contrast to the Barremian–Aptian age of Bujak Davies Group (1989b), which was probably based on the presence of *Pseudoceratium pelliferum*. We have not recorded this species from the well, and no other studies have revealed rocks older than Albian except for Nøhr-Hansen et al. (2016), who considered the well to have reached total depth in upper ?Aptian–lower Albian rocks.

TOP (M)	BASE (M)	AGE
420	480	EARLY MIOCENE
480	1140	RUPELIAN
1140	1440	PRIABONIAN
1440	1860	BARTONIAN
1860	1935	EARLY LUTETIAN
1935	2130	YPRESIAN
2130	2220	EARLY YPRESIAN
2220	2340	THANETIAN
2340	2400	SELANDIAN
2400	2430	LATE DANIAN
2430	2520	EARLY DANIAN
2520	2550	LATE LATE MAASTRICHTIAN
2550	2610	EARLY LATE MAASTRICHTIAN
2610	2660	EARLY MAASTRICHTIAN
2690	2720	CAMPANIAN
2720	2820	CENOMANIAN–TURONIAN
2820	3210	ALBIAN
3210	3370	EARLY ALBIAN
3370	3507	APTIAN

Table 1: Summary of biostratigraphic ages for North Leif I-05 from this study.

The index species of the Bujak Davis Group's (1989a) lower Albian Zone, *Parvisaccites amplus*, has its LO in the cuttings sample from 3020–3010 m in North Leif I-05, but occurs consistently only down to the sample at 3220–3210 m. However, from analysis of samples from the conventional cores 1 and 2 between 3116.5 and 3110 m of the same well, Dafoe and Williams

(in press) determined that this interval is middle to late Albian in age due to the presence of *Parvisaccites amplus*, *Parvisaccites radiatus*, *Rugubivesiculites reductus* and *Rugubivesiculites rugosus*. This conclusion was based on two considerations: Pedersen and Nøhr-Hansen (2014) placed the FO of the genus *Rugubivesiculites* within the Albian; and the oldest occurrence of *Rugubivesiculites* is more significant than the LO of *Parvisaccites radiatus*. We thus conclude that 3370–3210 m is of early Albian age based on the presence of *Parvisaccites amplus* in the sample at 3220–3210 m and absence of *Rugubivesiculites amplus* and *Rugubivesiculites reductus*. This is about 150 m higher than the boundary designated by Nøhr-Hansen (2004) and Nøhr-Hansen et al. (2016), who assigned the interval below 3360 m to the late ?Aptian–early Albian. In Nøhr-Hansen (2004) and Nøhr-Hansen et al. (2016), the event marking the early–middle Albian boundary in North Leif I-05 was the LO of *Vesperopsis longicornis*. In their general Cretaceous event scheme, Nøhr-Hansen et al. (2016), placed the LO of *Vesperopsis longicornis* in approximately the middle of the Albian in North Leif I-05, but the conventional core data was not available at the time for either Nøhr-Hansen (2004) nor Nøhr-Hansen et al. (2016).

In previous studies, Nøhr-Hansen (2004) and Nøhr-Hansen et al. (2016) subdivided the Albian of North Leif I-05 into three units, recognizing both middle and late Albian intervals. Nøhr-Hansen et al. (2016) placed the boundary between the middle and late Albian in North Leif I-05 at 3120 m, marked by the LO of *Nyktericysta davisii*, with the LO of *Pseudoceratium pelliferum* occurring just below at 3150 m. However, in their general Cretaceous events scheme, Nøhr-Hansen et al. (2016) considered the LO of *Nyktericysta davisii* to be at the Albian–Cenomanian boundary and did not utilize *Pseudoceratium pelliferum* as an index species, but plotted the LO of *Pseudoceratium* sp. within the Aptian. Based on our analyses, we are unable to resolve a middle to late Albian boundary, but we place the top of the Albian at 2830–2820 m based on the LO of the dinocysts *Nyktericysta davisii*, *Odontochitina ancala* and *Oligosphaeridium albertense*. *Nyktericysta davisii* and *Odontochitina ancala* were described from the upper Albian Kiowa Formation of Kansas by Bint (1986). *Nyktericysta* is a ceratioid genus that is indicative of brackish-water paleoenvironments and is common in the Albian. Another dinocyst species having its LO at 2830–2820 m and also in the Albian is *Canningia reticulata* sensu Nøhr-Hansen, 2004. A single specimen of *Kiokansium williamsii*, is present in the cuttings sample from 2890–2880 m in North Leif I-05: according to Nøhr-Hansen et al. (2016) the LO of the species is in the early Cenomanian; however, as only one specimen was found, it does not provide convincing evidence of lower Cenomanian at this depth. Nøhr-Hansen et al. (2016) proposed that an unconformity at 2790 m, separated the Albian from the overlying upper Cenomanian–lower Turonian based on the LO of *Canningia reticulata* sensu Nøhr-Hansen, 2004, *Odontochitina ancala* and *Oligosphaeridium albertense*. We found the same index species above our sample at 2830–2820 m, but a significant well-log change at about 2820 m (see details below) best conforms with the top of the Lower Cretaceous, and reworking could explain the presence of Albian palynomorphs in overlying sedimentary rocks.

A key marker for the Cenomanian is the dinocyst *Cyclonephelium vannophorum* sensu Williams, 1975, which has its LO in the cuttings sample from 2800–2790 m in North Leif I-05. Williams (1975) considered this taxon to have its LO in the Turonian, but to peak in the Cenomanian. *Rugubivesiculites convolutus* and *Rugubivesiculites rugosus* have their LOs in the cuttings sample at 2740–2730 m. Nøhr-Hansen et al. (2016) placed the LO of *Rugubivesiculites* within the Turonian. Thus, it seems reasonable to designate the interval 2820–2720 m as Cenomanian–Turonian, also taking into account the log changes at both the top and base of the interval (see ‘Correlation to Lithostratigraphy’ section). Nøhr-Hansen et al. (2016) dated the interval 2790–2730 m as late Cenomanian–early Turonian, with the top based on the LOs of *Heterosphaeridium difficile* and *Rugubivesiculites rugosus*. The conclusions of these authors closely parallel our findings, as do those of Bujak Davies Group (1989b). Ainsworth et al. (2016) also observed an abundance of *Cyclonephelium* between 2765 and 2730 m, but gave that interval a late Albian–early Cenomanian age.

The Upper Cretaceous section is condensed, perhaps explaining why we did not identify a Coniacian or Santonian interval; but Campanian rocks are present. Nøhr-Hansen et al. (2016) recognized Maastrichtian sediments at 2730 m, directly overlying their upper Cenomanian–lower Turonian section. Our interpretation is slightly different since we dated the cuttings sample at 2700–2690 m as Campanian, based on the presence of *Odontochitina operculata*. Williams et al. (2004) placed the LO of this species within the basal Maastrichtian, but the closely related *Odontochitina costata* is considered to have its LO in the latest Campanian (Nøhr-Hansen et al. 2016). That the section from 2720 to 2690 m is Campanian is further supported by the LO of *Tenua* cf. *hystrix* in the cuttings sample at 2710–2700 m. *Tenua* cf. *hystrix* (previously recorded as *Cerbia* cf. *tabulata*) has been recorded from the Campanian of other Labrador Shelf wells including South Labrador N-79 (Williams, 2007a) and Roberval K-92 (Williams, 2017b), so its LO appears to have some validity as an index marker for this stage. Our interpretation of a Campanian age for 2720–2690 m agrees well with the assessment by Bujak Davies Group (1989b), but is younger than the Santonian age interpreted by Ainsworth et al. (2016).

In the well, we subdivide the Maastrichtian into early, early late and late late. The early Maastrichtian extends from 2660–2610 m, with the top marked by the LO of *Isabelidinium cooksoniae*, which has its LO in the early Maastrichtian according to Nøhr-Hansen (2004). One especially good index species for the early late Maastrichtian is *Isabelidinium cretaceum*, which has its LO in the cuttings sample from 2560–2550 m. This species has been recorded from several Labrador Shelf wells (Nøhr-Hansen et al., 2016). Askin (1988), in a study of dinocysts from the Campanian to Paleocene of Seymour and adjacent islands, Antarctica, defined a Zone 1 that was characterized by *Isabelidinium cretaceum* and considered it to be late Campanian. Based on revised data from the same locality, Bowman et al. (2012) revised the age as questionable late Maastrichtian but recognized two younger Maastrichtian zones. Therefore, the LO of *Isabelidinium cretaceum* can be considered as early late Maastrichtian as in Nøhr-Hansen

et al. (2016). Based on the occurrence of *Isabelidinium cretaceum* in North Leif I-05, we have assigned the interval 2610–2550 m to the early late Maastrichtian. From our study, other dinocyst taxa having their LO in this interval include Chorate cyst 9 Nøhr-Hansen (2004) and *Impagidinium cf. victorianum*.

A cuttings sample from 2530–2520 m contains the dinocyst *Palynodinium grillator*. Nøhr-Hansen in Sønderholm et al. (2003) defined a *Palynodinium grillator* interval for the latest Maastrichtian, characterized by the LOs of *Palynodinium grillator* and the pollen *Wodehouseia spinata*. Williams et al. (2004) placed the FO of *Palynodinium grillator* in northern mid-latitudes at the Maastrichtian–Danian boundary and its LO at the same latitude as within the basal Danian. Nøhr-Hansen et al. (2016) plotted the LO of *Palynodinium grillator* at the top of the Maastrichtian, and we agree with this age determination. Accordingly, we find the late late Maastrichtian in North Leif I-05 to extend from 2550–2520 m.

Nøhr-Hansen (2004), came to similar conclusions regarding the extent and subdivision of the Maastrichtian in North Leif I-05. He recognized an early and a late Maastrichtian, subdividing the latter into three zones: these were the *Isabelidinium cooksoniae* Zone, the *Chatangiella biapertura* Zone and the *Palynodinium grillator* Zone. The early Maastrichtian, defined by the *Alterbidinium acutulum* Zone, extended from 2730 to 2670 m. This was sequentially overlain by the *Isabelidinium cooksoniae* Zone (2670–2610 m), the *Chatangiella biapertura* Zone (2610–2550 m), and the *Palynodinium grillator* Zone (2550–2520 m). Thus the top of our early Maastrichtian at 2610 m is above that of the top of the *Alterbidinium acutulum* Zone but is at the same depth as the top of Nøhr-Hansen's (2004) *Isabelidinium cooksoniae* Zone. There is agreement, however, that the top of the Maastrichtian occurs at 2520 m, which is also in accord with the findings of Bujak Davies Group (1989b) and Nøhr-Hansen et al. (2016).

We assign the interval 2520–2430 m to the early Danian based on the LO of the dinocyst species *Tanyosphaeridium xanthiopyxides* in the cuttings sample from 2440–2430 m, although a single, possibly reworked, specimen of that species occurs at 2410–2400 m. Also in the North Leif I-05 well, Nøhr-Hansen (2004) placed the LO of *Spongodinium delitiense*, *Tanyosphaeridium xanthiopyxides* and *Trithyrodinium evitti* approximately at the top of the early Danian. This would explain the consistent occurrence of *Spongodinium delitiense* as high as the sample from 2490–2480 m; however, a single specimen of this species occurred in the cuttings sample from 2385–2375 m.

The cuttings sample from 2410–2400 m contains the LO of *Phelodinium kozlowskii*. According to Nøhr-Hansen (2004), the Danian is marked by the LOs of the dinocyst species *Cerodinium diebelii*, *Phelodinium kozlowskii*, *Senoniasphaera inornata*, *Spongodinium delitiense*, *Tanyosphaeridium xanthiopyxides* and *Trithyrodinium evittii*. Therefore, we are assigning the interval 2430–2400 m to the late Danian. In contrast to our results, Nøhr-Hansen (2004) suggested that the Danian extends from 2520 to 2370 m, where he indicated a hiatus, based on

his belief that Selandian rocks were absent in North Leif I-05. The top of his Danian interval was defined on the LO of several dinocyst taxa, including *Cerodinium diebelii*, *Spongodinium delitiense* and *Trithyrodinium evittii*, the last-named being a zonal index species.

In common with several other Labrador Shelf wells, the Selandian in North Leif I-05 is characterized by the presence of *Impletosphaeridium apodastum*. This species was described by Fensome et al. (2016), who noted its LO in the late Selandian. In North Leif I-05, several specimens of this species occur in the cuttings sample from 2350 to 2340 m. This leads us to conclude that the interval 2400–2340 m is Selandian. The LO of *Palaeoperidinium pyrophorum*, also having its LO in the late Selandian (Nøhr-Hansen et al., 2016), appears to be in the sample at 2380–2370 m, although single specimens can be found in higher samples.

We date the cuttings sample at 2260–2250 m as Thanetian based on LOs of *Cerodinium speciosum* and *Cerodinium dartmoorium*, which have their LOs at the Thanetian–Ypresian boundary. Gradstein and Williams (1976) and Bujak Davies Group (1989a) both defined a *Cerodinium speciosum* Zone, which they considered to be Late Paleocene. In his study of the North Leif I-05 well, Nøhr-Hansen (2004) plotted the LO of *Cerodinium glabrum* (as *Cerodinium speciosum* subsp. *glabrum*) within the late Thanetian. Similarly, Nøhr-Hansen et al. (2016) placed the LO of *Cerodinium glabrum* at the top of the Thanetian. However, countering this conclusion is the presence of a specimen of *Apectodinium augustum* in the sample at 2230–2220 m. In a study of *Apectodinium* species of northwestern Europe, Harland (1979) restricted *Apectodinium augustum* to the latest Paleocene, but Nøhr-Hansen et al. (2016) suggested that *Apectodinium* had its LO in the basal Ypresian. But we consider the presence of *Cerodinium speciosum* more compelling. Dinocyst taxa having their LOs within 2230–2220 m are *Areoligera gippingensis*, *Cerodinium glabrum* and *Cordosphaeridium fibrospinosum*. Nøhr-Hansen et al. (2016) erected an *Areoligera gippingensis* Zone, which they dated as Thanetian, and agrees with our findings. The Late Paleocene of Bujak Davies Group (1989b) and Nøhr-Hansen et al. (2016) generally matches our results. From the above, we conclude that the Thanetian extends from 2340 to 2220 m.

Between 2320–2280 and 2260–2220 m, the relative abundances of species of *Apectodinium*, especially *Apectodinium homomorphum*, dramatically increase. We equate these abundances with warmer seawater temperatures, associated with the Paleocene–Eocene Thermal Maximum (PETM). Bujak and Brinkhuis (1998) considered *Apectodinium homomorphum* to be a warmer-water species, a finding verified in studies of stable isotope and biogeochemical paleotemperature indicators (Sluijs et al., 2006; Zachos et al., 2006; Schoon et al., 2013). Crouch et al. (2001) demonstrated that the earliest appearance of *Apectodinium*-dominated assemblages appears to be synchronous on a global scale, with the major peak possibly occurring during the PETM. Therefore, we are placing the PETM within the cuttings samples at 2260–2220 m, with a preceding peak at 2320–2280 m, and another within the basal Ypresian. Nøhr-

Hansen (2004) also recorded an *Apectodinium* acme between 2250 and 2220 m in North Leif I-05, but they did not note the peak of similar magnitude between 2320–2280 m. This author placed the Thanetian–Ypresian boundary at 2220 m, and Nøhr-Hansen et al. (2016) included the interval 2250–2220 m in the *Apectodinium* Acme Zone.

We have differentiated an early Ypresian interval between 2220 and 2130 m based on the LO of the dinocyst species *Petalodinium condylos* and *Adnatosphaeridium robustum* in the cuttings sample at 2140–2130 m. Bujak (1994) presented a dinocyst zonation for the Eocene of the North Sea in which he placed the consistent LO of *Petalodinium condylos* at the top of his E2b Subzone. The E2b Subzone equates with the lower part of the NP12 Zone within the Ypresian. Nøhr-Hansen et al. (2016) plotted the top of their early Ypresian *Petalodinium condylos* Zone at 2130 m in the North Leif I-05 well. This zone is equivalent to the E2b zone of Nøhr-Hansen (2004). As further demonstration of the stratigraphic significance of *Petalodinium condylos*, Nøhr-Hansen et al. (2016) placed its LO at approximately the top of the early Ypresian in other Labrador Shelf wells. Morgenroth (1966) described *Adnatosphaeridium* (as *Cannosphaeropsis*) *robustum* from the Ypresian of northwestern Europe.

We include the interval 2220–1935 m in the Ypresian. We base the top of this stage on the occurrences of *Heteraulacacysta pustulosa*, *Homotryblium tenuispinosum* and *Hystrichosphaeridium tubiferum*, which have their LOs in the cuttings sample at 1990–1980 m. *Heteraulacacysta pustulosa* was described from the Paleocene–Early Eocene of Nigeria by Jan du Chêne and Adediran (1985). Nøhr-Hansen et al. (2016) placed the LO of *Hystrichosphaeridium tubiferum* within the lowermost Lutetian. *Apectodinium homomorphum* and *Apectodinium quinquelatum* have their LOs in the cuttings sample from 1960–1950 m and 1945–1935 m, respectively. Nøhr-Hansen et al. (2016) placed the LO of *Apectodinium quinquelatum* within the Early Eocene. Therefore, the evidence seems to indicate that the Ypresian/Lutetian boundary is approximately at 1945–1935 m.

Nøhr-Hansen (2004) recognized three zones in the Ypresian of North Leif I-05. The oldest, discussed above, is the E2b or *Petalodinium condylos* Zone. The two other zones are respectively the E3a or *Eatonicysta furensis* Zone and the E3b or *Piladinium columna* Zone. Nøhr-Hansen (2004) and Nøhr-Hansen et al. (2016) recorded the LO of *Eatonicysta furensis* in the cuttings sample at 2080–2070 m, but placed the top of the *Eatonicysta furensis* Zone in the cuttings sample at 2050–2040 m. This top appears to have been based on the LO of *Achilleodinium biformoides*. According to Nøhr-Hansen (2004) and Nøhr-Hansen et al. (2016), the top of the overlying E3b *Piladinium columna* Zone, based on the LO of the index species, is in the cuttings sample from 1990–1980 m in North Leif I-05, which is slightly at odds with our pick for the Ypresian–Lutetian boundary at 1935 m. Although we did not record *Piladinium columna*, it is an excellent marker for the Ypresian–Lutetian boundary.

Overlying the Ypresian is a Lutetian section that extends from 1935 to 1860 m and appears to represent only the early part of the stage. A key taxon is *Glaphyrocysta* cf. *vicina*, which has its LO in the sample at 1870–1860 m. Williams (2017b) recorded this form from 2025 m in the Roberval C-02 well, an interval which he designated as Lutetian; he further noted that the taxon may be a useful marker for the Lutetian. Other taxa with their LOs in the Lutetian are *Deflandrea* sp. B sensu Williams and Bujak (1977) and *Diphyes colligerum* (basal Lutetian). Nøhr-Hansen (2004) recognized three zones in the Lutetian of North Leif I-05. These were from oldest to youngest: the E4 or *Diphyes ficusoides* Zone from 1980 to 1800 m; the E5-E6a Zone from 1800 to 1560 m; and the E6b-E6c Zone from 1560 to 1470 m. Species with their LOs at the top of the *Diphyes ficusoides* zone were *Tetraporina* sp. B of Fensome et al. (2016) and *Thalassiphora patula*. The LO of *Sophismatia tenuivirgula* marked the top of the E5-E6c Zone, and the LO of *Chiropteridium gilbertii* coincides with the Lutetian/Bartonian boundary. *Chiropteridium gilbertii*, named by Fensome et al. (2016), is known only from wells on the Labrador Shelf (Williams, 2007b, used the informal name *Hystrichokolpoma* “*gilbertii*” for this taxon). In their event scheme, Nøhr-Hansen et al. (2016) placed the LO of this species in the Bartonian. The use of *Chiropteridium gilbertii* to mark the Lutetian/Bartonian boundary, suggests that Nøhr-Hansen (2004) and Nøhr-Hansen et al. (2016) placed the Lutetian/Bartonian boundary too high in North Leif I-05.

We consider that Bartonian rocks cover the interval 1860–1440 m. This conclusion is based on the LO of the dinocyst *Chiropteridium gilbertii*, which has its LO established in the Bartonian (Nøhr-Hansen et al., 2016). Several specimens of this species are present in three samples between 1510 and 1440 m. One notable LO in this interval is that of *Sophismatia tenuitabulata*, which has its LO in the cuttings sample at 1570–1560 m. Nøhr-Hansen (2004) and Nøhr-Hansen et al. (2016) placed the LO of this species within, rather than at the top of the Lutetian, which accounts for their Lutetian interval extending nearly to the top of the interval we define as Bartonian. This discrepancy may be explained by new knowledge from the nearby Roberval K-92 and C-02 wells where *Chiropteridium gilbertii* is also a good Bartonian marker (Williams, 2017b).

The LO of the dinocyst *Lentinia serrata* in the cuttings sample at 1240–1230 m confirms that the overlying Priabonian extends from 1440 to at least 1230 m. The LO of *Lentinia serrata* appears to define the top of the Priabonian in some Grand Banks wells (e.g. Williams, 2003a, b). Support for the use of this event to determine the top of the Priabonian is provided by Williams et al. (2004), who placed it just above the Priabonian/Rupelian boundary. *Lentinia serrata* is found in several wells on the Labrador Shelf, including Gilbert F-53, North Leif I-05, Raleigh N-18 and South Labrador N-79 (Nøhr-Hansen et al., 2016). Designation of a Priabonian age is supported by the LOs of *Phthanoperidinium alectrolophum*, *Phthanoperidinium levimurum* and *Rhombodinium draco* also in the sample at 1240–1230 m. Nøhr-Hansen et al. (2016) placed the LO of *Phthanoperidinium levimurum* in the late Priabonian. Powell (1992) considered the LO of

Rhombodinium draco to be in the Rupelian, but Nøhr-Hansen et al. (2016) plotted the LO of this species within the Priabonian. *Lingulodinium funginum*, which is also usually a good indicator for the Priabonian, occurs in the cuttings samples between 1395 and 1265 m. In the sample at 1180–1170 m, *Phthanoperidinium echinatum* is present, and at 1150–1140 m, *Trithyrodinium conservatum* is present. From this we conclude that the Priabonian extends to 1140 m.

In contrast to our results, Nøhr-Hansen et al. (2016) delineated the Bartonian–Priabonian boundary at 700–690 m, as marked by the LOs of *Phthanoperidinium geminatum*, *Phthanoperidinium stockmansii* and *Phthanoperidinium* spp. We recorded specimens of *Phthanoperidinium coreoides* in this sample but none of the other species observed by Nøhr-Hansen et al. (2016). They further placed the Priabonian–Rupelian boundary in the cuttings sample at 550–540 m, based on the LO of the dinocyst *Lentinia serrata* and the alga (or acritarch) *Tetraporina*. As noted earlier, we did not record *Lentinia serrata* above 1240–1230 m: neither did we record *Phthanoperidinium alectrolophum*, *Phthanoperidinium levimurum* or *Rhombodinium draco*. This explains the difference in the placement of the top Bartonian and top Priabonian as recorded by Nøhr-Hansen et al. (2016) and this study.

Rupelian sediments extend from 1140 to 480 m in North Leif I-05, as confirmed by the presence of the dinocyst ?*Licracysta semicirculata* in the cuttings sample at 490–480 m. Further confirmation of the presence of a thick Oligocene section is indicated by the presence of the dinocyst *Enneadocysta magna* in the uppermost cuttings sample at 490–480 m. In their study of the Labrador–Baffin Seaway, Nøhr-Hansen et al. (2016) placed the LO of both *Licracysta semicirculata* and *Enneadocysta magna* at the Rupelian–Chattian boundary. Other species with their LOs in the Rupelian of North Leif I-05 include the dinocysts *Chiropteridium galea*, *Deflandrea heterophlycta*, *Deflandrea phosphoritica* and *Membranophoridium aspinatum* and the miospores *Corsinipollenites oculusnoctis* and *Zlavisporites* sp. Nøhr-Hansen et al. (2016) considered the miospore *Corsinipollenites oculusnoctis* to have its LO in the Bartonian; however, Williams (1986) placed the LO of this species (as *Jussiaea* sp.) in the Early Oligocene (Rupelian), a conclusion supported by observations from the Labrador Shelf well Roberval C-02 by Williams (2017b). According to Nøhr-Hansen et al. (2016), *Zlavisporites* sp. also has its LO in the Rupelian. Reworked palynomorphs are common in most Rupelian samples, including the Cretaceous dinocysts *Chatangiella tripartita*, *Isabelidinium cooksoniae*, *Nyktericysta* sp. and *Ovoidinium verrucosum*. Reworked Cretaceous miospores in the same interval include *Appendicisporites* sp., *Aquilapollenites* sp., *Rugubivesiculites reductus* and *Rugubivesiculites rugosus*. While the base of our Rupelian interval differs greatly from that of Nøhr-Hansen et al. (2016) for reasons discussed above, we agree with those authors regarding the top of the stage.

The interval 480–420 m appears to be Early Miocene based on the LO of the trilete spore *Osmundacidites wellmannii* in the uppermost sample at 430–420 m. Nøhr-Hansen et al. (2016) considered *Osmundacidites wellmannii* to have its LO in the Burdigalian. Other palynomorphs

with their LOs in the Miocene are the pollen *Tiliaepollenites* and the dinocysts *Cleistosphaeridium diversispinosum*, *Dapsilidinium pseudocolligerum* and *Spiniferites ovatus*. As in the underlying Rupelian, the samples in this interval contain reworked Early Cretaceous palynomorphs. Nøhr-Hansen et al. (2016) considered the section 480–420 m to be Early–Middle Miocene, and our results show good agreement with that conclusion.

Paleoenvironments

A plot showing the relative percentages of dinocysts, miospores (excluding bisaccates), bisaccates, acritarchs and other organic-walled microfossils in North Leif I-05 is provided in Figure 7. This plot illustrates paleoenvironmental changes, which are interpreted in Table 2. Previous paleoenvironmental studies of North Leif I-05 were undertaken by Petro-Canada (1980), Bujak Davies Group (1989b), Miller and d’Eon (1987) and Ainsworth et al. (2016). Miller and d’Eon (1987) based their interpretations on lithologic analyses, and the other authors utilized planktonic foraminifera. Bujak Davies Group (1989b) also utilized palynomorphs.

TOP (M)	BASE (M)	PALEOENVIRONMENT
420	1290	INNER NERITIC
1290	1920	INNER NERITIC
1920	2140	OUTER NERITIC SHALLOWING TO INNER NERITIC
2160	2200	INNER NERITIC
2220	2340	NERITIC
2340	2620	OUTER NERITIC TO OPEN OCEAN
2620	2710	OPEN OCEAN
2730	2770	OUTER NERITIC TO OPEN OCEAN
2790	3000	NERITIC
3000	3507	NONMARINE TO MARGINAL MARINE TO COASTAL

Table 2: Summary of paleoenvironments in the North Leif I-05 well from this study.

Figure 7 reveals the dominance of miospores in most of the section, with values commonly exceeding 80% from 3507 to 3000 m in the Aptian–Albian, the oldest sedimentary rocks in the well. We interpret these Aptian–Albian rocks as being deposited in fluctuating nonmarine to marginal marine or coastal paleoenvironments. This is consistent with that of Dafoe and Williams (in press) who found that the core 1 and 2 intervals (3117.1–3110 m) reflected distal delta front and prodeltaic deposits, respectively. In the cuttings samples, marginal marine interludes are indicated by periodic occurrences of the dinocysts *Nyktericysta* and

Quantouendinium in the interval 3507–2820 m. *Nyktericysta* has been recorded from several wells on the Labrador margin, in offshore West Greenland, and in samples from Nuussuaq and Disko in the Nuussuaq Basin of onshore West Greenland (Nøhr-Hansen, 2008; Pedersen and Nøhr-Hansen, 2014). Our findings confirm that the paleoenvironments in North Leif I-05 in the Aptian–Albian must have been shallow marine to lagoonal or lacustrine. Some of the interval could be nonmarine, as demonstrated by the absence of dinocysts and acritarchs in the samples from conventional cores 1 and 2 in North Leif I-05 from 3116.5, 3115.0, 3113.66, 3113.25, 3112.55, 3111.05, and 3110.0 m (Dafoe and Williams, in press). However, sedimentological and ichnological analyses from these core intervals in the same study show a shallow marine, but brackish setting that was likely inhospitable to dinoflagellates. Bujak Davies Group (1989b) considered the interval 3424–3410 m to be middle to outer neritic and 3380–2850 m to be questionable outer neritic to upper bathyal. This is at odds with our findings and those of Miller and d’Eon (1987), who interpreted 3513–3280 m as representing nonmarine, fluvial settings, and 3280–2926 m as representing marginal marine to nonmarine settings.

From 3000 to 2580 m dinocysts become much more abundant and diverse. The dinocyst taxa found in the interval 3000–2790 m include species of *Odontochitina*, *Oligosphaeridium* and *Tenua*, plus *Alterbidinium* and other peridiniaceans. Such an assemblage indicates a neritic setting, shallower than the questionable outer neritic to upper bathyal of Bujak Davies Group (1989b), but possibly deeper than Miller and d’Eon’s (1987) inner shelf.

The presence of *Impagidinium* in the samples from 2770–2730 m seems to denote a change to an outer neritic to open-ocean setting. This is more consistent with the upper bathyal setting of Bujak Davies Group (1989b), but deeper than the questionable inner shelf reported by Miller and d’Eon (1987). *Impagidinium* is one of the few dinocyst genera that appear to be restricted to open ocean, deeper-water environments. Wall et al. (1977) were the first to recognize that *Impagidinium* species (then included in *Leptodinium*) were indicative of oceanic realm environments. Brinkhuis (1992, 1994) incorporated this concept into his Priabonian model, and Dale (1996) confirmed the prominence of *Impagidinium* among organic-walled dinocysts in the oceanic realm. The “*Impagidinium* signal” has been used to indicate open-water or deeper-water paleoenvironments in studies of other Labrador Sea wells (Nøhr-Hansen et al., 2016), for example South Labrador N-79 (Williams, 2007a). From 2710 to 2620 m in North Leif I-05, which includes the Campanian and Maastrichtian, the presence of *Impagidinium* species denotes open-ocean conditions, in agreement with bathyal settings interpreted in previous studies (Miller and d’Eon, 1987; Bujak Davies Group, 1989b).

Dinocysts relative to miospores increase to about 80% between 2620 and 2400 m, but then begin a gradual decline until at 1930–1920 m, where they constitute less than 10% of the assemblage. This reduction in abundance of dinocysts generally persists throughout the upper part of the well. Samples between 2620–2340 m contain several specimens of *Hystrichosphaeridium*,

Impletosphaeridium apodastum and *Palaeoperidinium pyrophorum*, with the occasional *Impagidinium* up to 2340 m. We consider this assemblage as indicative of an outer neritic to open-ocean paleoenvironment, which is similar to the bathyal interpretations of previous authors (Miller and d'Eon, 1987; Bujak Davies Group, 1989b).

From 2340–2130 m, *Apectodinium* and *Areoligera gippingensis* are present and sometimes abundant, indicating a neritic setting. Abundances of *Areoligera gippingensis* have been interpreted in two different ways by Heilmann-Clausen (1994) and Powell et al. (1996), respectively. Heilmann-Clausen (1994) considered *Areoligera gippingensis* to be indicative of offshore paleoenvironments. However, Powell et al. (1996) described an *Areoligera* assemblage, probably primarily composed of *Areoligera gippingensis*, with the most concentrated samples being from restricted, high-energy, marginal marine settings typical of a transgressive regime. *Apectodinium* abundance peaks around the PETM may simply reflect the age of the sediments rather than the nature of the paleoenvironmental setting. Another possibility is that specimens of *Apectodinium* were transported into the Labrador–Baffin Seaway because of the onset of deeper-water conditions. Foraminiferal and lithological studies by Bujak Davies Group (1989b), Miller and d'Eon (1987), and Ainsworth et al. (2016) have indicated that this section was bathyal only. However, the interval from 2200–2160 m is characterized by a marked increase in miospores and acritarchs. An increase in acritarch abundance often equates with a more inner neritic setting as noted by Staplin (1961), so we consider 2200–2160 m to be inner neritic. This shallowing trend to neritic and inner neritic paleoenvironments in the Thanetian and early Ypresian is not discerned in previous studies. However, our conclusions are supported by those of Dafoe and Williams (in press), who interpreted shallow marine settings for the Gudrid Formation on the basis of cores from three different wells.

In the interval from 2140–1920 m, a dramatic rise in the percentage of miospores occurs; in the sample from 1930–1920 m, they constitute almost 100% of the palynomorphs. The lowermost part of this interval represents outer neritic conditions based on the dominance of gonyaulacalean over peridinialean dinocysts and then shallows upward to inner neritic conditions. The shallowing trend indicated in sample 1930–1920 m seems to persist to 1300–1290 m based on the miospore/dinocyst ratio and the variability of the dinocyst assemblages. In many samples, the relative percentage of dinocysts is 5% or less, consistent with a continued inner neritic environment. Above 1275–1260 m, species of the dinocyst genus *Phthanoperidinium* become common, indicating that they are in place. Brinkhuis et al. (2003) and Sluijs et al. (2003) demonstrated a relationship between lithological, geochemical, grain size and diatom data and high abundances of *Phthanoperidinium*, which appeared to indicate an inner neritic setting. Based on this and the relative percentages of the palynomorph groups, we are postulating a continued inner neritic environment between 1260 and 420 m. Unlike our postulated neritic settings, Miller and d'Eon (1987) and Bujak Davies Group (1989b) did not report shallowing to

shelfal or neritic conditions until 1476 and 1150 m, respectively. However, there is general agreement on middle shelf/neritic or shallower conditions persisting above 1110 m (Fig. 3).

In summary, the interval from about 3507–2790 m, was deposited in fluctuating nonmarine to marginal marine paleoenvironments with increasing water depth to neritic settings, an interpretation generally consistent with other studies. Outer neritic to open ocean paleoenvironments persisted from about 2770 to 2340 m. This was followed by shallowing to neritic and inner neritic between 2340–2160 m, a trend not noted by previous studies of North Leif I-05, but consistent with results from the Gudrid Formation in general (Dafoe and Williams, in press). A short-lived, renewed deepening to outer neritic conditions is followed by shallowing to inner neritic conditions persisting from 1920–430 m. Shallowing above 1110 m was noted by Miller and d’Eon (1987) and Bujak Davies Group (1989b), but both reports interpreted more extensive bathyal conditions than we did during the latest Cretaceous and early Paleogene.

Correlation to Lithostratigraphy

The lithostratigraphy of the Labrador margin is based on the original stratigraphic framework developed by Umpleby (1979) and revised by McWhae et al. (1980), which consists of the eight formations still recognized today: Alexis, Bjarni, Markland, Cartwright, Gudrid, Kenamu, Mokami and Saglek. The lithostratigraphic interpretations for North Leif I-05 in Figure 2 are derived from Moir (1989). However, other studies have refined the lithostratigraphic assignments, including those by the Canada–Newfoundland and Labrador Offshore Petroleum Board (C–NLOPB, 2007) and Ainsworth et al. (2016). Below we discuss further refinements to some units.

Formation	Moir (1989)		This study	
	Base (m)	Top (m)	Base (m)	Top (m)
Saglek Formation	547	319	547	396
Mokami Formation	1476	547	1476	547
Kenamu Formation	2124	1476	2141	1476
Leif Member	1586	1524	1588	1476
Gudrid Formation (upper)	2228	2124	2220	2141
Cartwright Formation	2326	2228	2348	2220
Gudrid Formation (lower)	2340	2326		
Markland Formation	2820	2340	2820	2348
Bjarni Formation	3394	2820	3394	2820
Snorri Member	3354	2820	3354	2820
Alexis Formation	3513	3394	3513	3394

Table 3: Lithostratigraphy of the North Leif I-05 well from Moir (1989) and showing revised picks from this study.

According to Moir (1989) and Ainsworth et al. (2016), North Leif I-05 reached total depth at 3513 m in the Alexis Formation. The Alexis Formation in this well comprises volcanic rocks from 3513–3444 m and tuff from 3444–3394 m (C–NLOPB, 2007). Based on detailed cuttings reports, a tuffaceous character from 3444–3432 m seems likely; however, the interval 3432–3394 m includes shales, coal fragments and sandstones intermixed with weathered volcanic clasts, suggesting volcanoclastic sedimentation atypical for the Alexis Formation. No ages were derived from core 3 at 3512.5–3507 m, but Umpleby (1979) suggested an Early Cretaceous age for the formation in general, and McWhae et al. (1980) proposed a Berriasian or Valanginian to Barremian age. Our results from cuttings indicate an Aptian age, but cavings could have led us to misleading interpretations, especially within the basaltic interval at the base of the well. Nevertheless, the presence of sedimentary material from 3432–3394 m could be the source of the palynomorphs recovered.

The overlying Bjarni Formation consists of sandstones, conglomerates, carbonaceous shales and thin coal seams (Umpleby, 1979; McWhae et al., 1980). Opinions differ on the thickness of the Bjarni Formation and whether the Snorri Member is present in North Leif I-05. Moir (1989) considered the Bjarni Formation to extend from 3394 to 2820 m, with the Snorri Member occurring between 3354 and 2820 m. The C–NLOPB (2007) included the interval 3394–2722 m in the Bjarni Formation and did not designate an interval for the Snorri Member. Ainsworth et al. (2016) recognized an unconformity at 3393 m, with the Bjarni Formation having its base at this level and extending to 2721.5 m, and placed the Snorri Member at 3357.5 m (possibly indicating only the base of the member). A major log change at 2820 m best correlates with the prominent top Bjarni Formation unconformity noted in seismic data (Dickie et al., 2011— their unconformity 2). We’ve correlated our top Albian pick to 2820 m with a significant log change to a more shale-dominated overlying unit with an increased calcareous component. Accordingly, in North Leif I-05, we consider the Bjarni Formation to be Aptian–Albian. The Snorri Member is a shale-dominated unit with thin silty and sandy intervals, coal seams and plant detritus (Umpleby, 1979). Moir’s (1989) designation appears reasonable, but Ainsworth et al.’s (2016) pick is unclear. The paleoenvironment in the lower part of the Bjarni Formation is nonmarine to marginal marine or coastal, becoming neritic in the upper part.

Overlying the Bjarni Formation is the Markland Formation, a unit formally proposed by McWhae et al. (1980) for a sequence of shales, silty shale, rare siltstone and sandstone and thin dolomitic limestone of Cenomanian–Turonian to Danian age on the Labrador Shelf. Moir (1989) extended the Markland Formation in North Leif I-05 from 2820 to 2340 m. The C–NLOPB (2007) included the interval 2722–2339 m in the Markland Formation, similar to the pick of Ainsworth et al. (2016), except that the latter gave the top as 2350 m. The log change in gamma-ray signature, resistivity and density logs at 2348 m appears to correspond to a significant lithological change consistent with the top of the Markland Formation. With this revised top, we date the Markland Formation as Cenomanian–Turonian to Selandian. Nøhr-Hansen et al. (2016)

identified an unconformity at 2730 m, between their upper Cenomanian–lower Turonian and lower Maastrichtian, and Ainsworth et al. (2016) picked an unconformity at 2721.25 m based on log character and presumably separating their upper Albian–lower Cenomanian from Santonian. However, we note a log change at 2720 m that corresponds to a break in section between our Cenomanian–Turonian and Campanian, indicating Coniacian and Santonian rocks are absent or highly condensed. This stratigraphic break would correlate to the 2' unconformity of Dickie et al. (2011), which separates a thin interval of rocks lying above the top Bjarni Formation horizon in the lower part of the Markland Formation. A condensed uppermost Maastrichtian is consistent with findings from other Labrador shelf wells (Dafoe et al., 2017b). The lower Upper Cretaceous is neritic to outer neritic to open ocean, with progressive deepening upward within that interval. Our findings for the Upper Cretaceous show outer neritic to open ocean settings, with overall shallowing upward.

Umpleby (1979) defined the Cartwright Formation as a broad lithostratigraphic interval, but it was later restricted by McWhae et al. (1980) to the Middle Paleocene to Early Eocene. McWhae et al. (1980) described the formation as consisting of brown-grey claystone, silty claystone, and siltstone with thin sandstones and carbonate beds. A sandstone interval correlative to the Cartwright Formation, was defined as the Gudrid Sand Member by Umpleby (1979), but McWhae et al. (1980) elevated the Gudrid to formation status. The Gudrid Formation consists of quartzose and feldspathic sandstone, often poorly sorted, with glauconite and traces of coal (Umpleby, 1979; McWhae et al., 1980). Moir (1989) identified the lower part of the Gudrid Formation as the interval from 2340 to 2326 m, the Cartwright Formation as the interval from 2326 to 2228 m, and the upper part of the Gudrid Formation as the interval from 2228 to 2124 m. The C–NLOPB (2007) identified the top of the Cartwright Formation at 2141 m and the Gudrid as two informal members. Similarly, Ainsworth et al. (2016) considered the Gudrid to represent members within the Cartwright Formation, with the top of the formation at 2109 m. The significant log change at the top of the sandstone unit at 2141 m appears to be the most logical top for the Gudrid, and we retain its formation status. However, within the Cartwright–Gudrid succession in North Leif I-05, sandstones only dominate the upper portion of the succession. Accordingly, we disagree with assignment of a lower Gudrid Formation by Moir (1989), but we assign the upper Gudrid Formation to 2220–2141 m. In addition, although Umpleby (1979), Balkwill and McMillan (1990) and Dafoe and Williams (in press) have interpreted the Gudrid as representing a shallow marine setting, this is only true for the upper interval (i.e. the only unit identified as Gudrid Formation herein). However, the sandy shale development at 2340–2311 m could be a distal equivalent of the Gudrid Formation, with a minor marine flooding event at the top. Accordingly, the Cartwright Formation extends from 2348–2220 m.

The Cartwright Formation is of Selandian to Thanetian age and reflects outer neritic to open ocean shallowing to neritic conditions. Overlying the Cartwright is the Gudrid Formation, which is early Ypresian in age and represents an inner neritic setting. The top of the lower Gudrid

equivalent at 2311 m is within the Thanetian. At 2220 m, the PETM forms the base of the upper Gudrid Formation.

The Kenamu Formation was described by McWhae et al. (1980) as an Eocene shale, siltstone, and sandstone sequence, in part glauconitic and calcareous. Umpleby (1979) named the Leif Sand Member (of the Saglek Formation), and McWhae et al. (1980) subsequently retained this unit as the Leif Member within the Kenamu Formation. This member comprises fine-grained, quartzose, white to light-grey-brown sandstone, often glauconitic, with some interbedded siltstone and mudstone (Umpleby, 1979; McWhae et al., 1980). Up to three stacked, coarsening-upward units may be present locally (Balkwill and McMillan, 1990). In North Leif I-05, Moir (1989) assigned the interval 2124–1476 m to the Kenamu Formation and the interval 1586–1524 m to the Leif Member. C–NLOPB (2007) and Ainsworth et al. (2016), picked the top of the Kenamu Formation at similar depths, but defined the Leif Member interval as a thinner unit (1588–1562 m) and a thicker (1697.5–1475.5 m) unit, respectively. Ainsworth et al. (2016) named the interval 1815.5–1765 m as the Roberval member, but this unit has not been described formally. We pick the base of the Kenamu Formation at 2141 m, with the gamma-ray and sonic log changes at 1476 m marking the distinctive top, characteristic of other wells in the region. The Leif Member, is a sandstone-dominated interval and we agree with the base at 1588 m (C–NLOPB, 2007), but bring the top to 1476 m, thus including three roughly coarsening-upward intervals. According to our results, the age of the Kenamu Formation is early Ypresian to Bartonian and shows shallowing from outer to inner neritic upwards. The Leif Member is middle to late Bartonian and was deposited under inner neritic conditions. While the palynology may not discern fine details, it agrees with the interpretation of a shallow marine setting for the Leif Member by several previous authors (Umpleby, 1979; McWhae et al., 1980; Gradstein and Srivastava, 1980; Miller and d’Eon, 1987; Dafoe et al., 2017a, 2018).

Sequentially overlying the Kenamu Formation are beds of the Mokami and Saglek formations. McWhae et al. (1980) defined the Mokami Formation as a predominantly claystone and soft shale unit with thinner beds of siltstone, sandstone, and limestone. McWhae et al. (1980) restricted Umpleby’s (1979) original designation of the Saglek Formation to very porous, unconsolidated, feldspathic and cherty sandstone that is poorly sorted, fine- to coarse-grained and locally conglomeratic with bivalve fragments, lignite, and glauconite, as well as lesser siltstone and claystone interbeds. In the North Leif I-05 well, Moir (1989), C–NLOPB (2007), and Ainsworth et al. (2016) gave remarkably consistent picks for the Mokami and Saglek formations, with the top of the Mokami Formation at 548–547 m; we agree with a 547 m pick for the top of the Mokami as there is a distinctive log change there. It is unclear why all three studies place the top of the Saglek Formation above the cuttings samples and logs; we place the top at 396 m. Our palynological analyses indicate that the Mokami Formation is of latest Bartonian to late Rupelian age and that the Saglek Formation is latest Rupelian to Early Miocene in age. However, the top of the well is cased and so we do not have samples from younger Saglek

Formation strata. Both formations were deposited in inner neritic settings. The presence of reworked Cretaceous palynomorphs in the Rupelian to Lower Miocene section is likely related to erosion at the base of large clinothems that form the Saglek Formation (Balkwill and McMillan, 1990; Dickie et al., 2011).

Summary

North Leif I-05 was drilled to test the Bjarni Formation onlapping a northward-plunging anticlinal nose (Petro-Canada Exploration Inc., 1980). The well, a dry hole, bottomed in volcanics of the Alexis Formation at 3513 m. Our age control is based primarily on dinocysts but the spores and pollen were informative, especially in the Aptian and Albian.

An intriguing aspect of the well is the Cretaceous section, with Aptian, Albian, Cenomanian–Turonian, Campanian and Maastrichtian sediments being present. This represents one of the more complete Cretaceous successions on the Labrador margin and preserves one of the few records of the lower Markland Formation. However, Coniacian and Santonian sediments appear to be absent, and the Cenomanian–Turonian and Campanian are attenuated. Regardless, North Leif I-05 is one of the few wells on the Labrador Shelf that appears to have a more-or-less continuous section across the Cretaceous–Cenozoic boundary, providing good preservation of the uppermost Markland Formation and excellent correlation of the dinocysts with coeval assemblages in Europe.

In the Cenozoic, there is a major dinocyst event marking the Paleocene–Eocene Thermal Maximum (PETM), denoted by floods of the dinocyst genus *Apectodinium* at the base of the Gudrid Formation. This genus proliferated in warmer waters, migrating northwards from equatorial waters during the Late Paleocene warming. North Leif I-05 is the first Labrador Shelf well to show this distinctive concentration of *Apectodinium*, offering new evidence for climatic conditions in the Late Paleocene–Early Eocene and insights into paleo-oceanic currents.

North Leif I-05 has a thick Eocene section of the Kenamu Formation, totalling 1090 m. The Rupelian and Lower Miocene sediments successively overlie the Priabonian, forming a thick Mokami Formation and thin Saglek Formation. The one major hiatus in this interval is between the Rupelian and the Early Miocene, which is consistent with other wells in the Hopedale Basin (e.g. South Labrador N-79: Williams, 2007b).

Paleoenvironments in North Leif I-05 include: nonmarine, marginal marine, inner neritic, and outer neritic to open ocean, with deepening in the Early Cretaceous into the early Late Cretaceous. This is followed by shallowing in the latest Cretaceous to Ypresian, then a slight deepening and final shallowing to inner neritic for much of the Eocene to Early Miocene.

Oversized Figure Captions

Figure 2: Plot of the North Leif I-05 well showing key wireline logs, lithology (Canstrat), conventional core locations and key biostratigraphic studies, paleoenvironmental interpretations, and lithostratigraphy.

Figure 3: Range plot of dinocysts for the North Leif I-05 well from GSC samples.

Figure 4: Range plot of dinocysts for the North Leif I-05 well from GEUS samples.

Figure 5: Range plot of spores, pollen, and other palynomorphs for the North Leif I-05 well from GSC samples.

Figure 6: Range plot of spores, pollen, and other palynomorphs for the North Leif I-05 well from GEUS samples.

Figure 7: Palynomorph ratio plot for the North Leif I-05 well from this study. Bisaccates are shown separately from other spores and pollen.

SKOLP E-07

Biostratigraphy

The Skolp E-07 well is illustrated in Figure 8, showing key well logs, lithology, cored intervals, a reference section (Moir, 1989), select biostratigraphic studies and lithostratigraphy from Moir (1989) and this study. Range plots illustrate: the dinocysts recorded (Fig. 9); and the spores, pollen and other palynomorphs (Fig. 10). Plates 9–21 illustrate specimens from the Skolp E-07 well (more details are given in Appendix A for the plates). Ages are discussed in detail below and summarized in Table 4. Previous biostratigraphic studies of the Skolp E-07 well include those by Price and Thorne (1978), Williams (1980), Gradstein et al. (1994), Nøhr-Hansen in Sønderholm et al. (2003), and Nøhr-Hansen et al. (2016).

The Skolp E-07 well penetrated 25 m of Precambrian gneiss before reaching total depth at 2992 m (Moir, 1989). Dafoe and Williams (in press) provided a lithological description of conventional core 7 from 2992–2988 m, which recovered 3.96 m of gneiss of Archean age (Wasteneys et al., 1996).

TOP (M)	BASE (M)	AGE
540	545	SERRAVALLIAN
570	600	AQUITANIAN-EARLY BURDIGALIAN
600	630	CHATTIAN?
630	870	RUPELIAN
870	875	BARTONIAN
900	990	EARLY YPRESIAN
990	1020	EARLY DANIAN
1020	1080	LATE LATE MAASTRICHTIAN
1080	1260	EARLY LATE MAASTRICHTIAN
1260	1450	EARLY MAASTRICHTIAN
1450	1650	LATE CAMPANIAN
1650	1845	EARLY CAMPANIAN
1845	1980	SANTONIAN
1980	2080	CONIACIAN
2080	2400	TURONIAN
2400	2460	CENOMANIAN
2460	2917.1	EARLY ALBIAN
2917.1	2967	APTIAN

Table 4: Summary of biostratigraphic ages for Skolp E-07 from this study.

Overlying the gneiss is the Bjarni Formation, from which we have cuttings and conventional core samples. The lowest cuttings sample at 2990–2985 m contains the bisaccate *Rugubivesiculites rugosus* plus some Cenozoic pollen (sourced from cavings). However, in the cuttings sample from 2970–2965 m is the bisaccate *Parvisaccites radiatus* and the trilete *Matonisporites “skolpii”*. In the cuttings sample from 2940–2935 m, we recorded the miospores *Cicatricosporites auritus* and *Rugubivesiculites rugosus*. It is difficult to determine an age from the above miospores. However, Dafoe and Williams (in press) analyzed three samples from the conventional core from 2918.77–2915.5 m. The sample at 2917.1 m contained the pollen *Callialasporites dampieri* and *Vitreisporites pallidus* and the spore *Camarozonosporites* sp. Nøhr-Hansen et al. (2016) placed the LO of *Callialasporites dampieri* within the Aptian, and Dafoe and Williams (in press) accordingly dated this sample as Aptian.

Our analyses indicate that the section from the base of the Bjarni Formation at 2967 m to 2917.1 m is of Aptian age, the latter depth marking the top of this stage. However, Nøhr-Hansen et al. (2016) did not recognize any Aptian rocks in Skolp E-07, giving an age of Albian–Cenomanian for the interval 2985–2495 m, above which they identified early Campanian sediments. In contrast, Williams (1980) considered 2967–2875 m to be ?Barremian–Aptian and 2855–2485 m to be Albian–Cenomanian. The oldest sedimentary rocks recognized were dated Neocomian by Price and Thorne (1978).

The cuttings sample at 2465–2460 m appears to mark the top of the Albian, as determined from the LO of *Parvocavatus radiatus*, as well as the miospore *Matonisporites “skolpii”*. Bujak Davies Group (1989a) defined a *Parvisaccites amplus* Zone, which they considered early Albian. One of their key index species was *Parvisaccites radiatus*. Thus, the age of the interval 2917.1–2460 m would appear to be early Albian. The LOs of the miospores *Cicatricosporites auritus*, *Distaltriangulisporites irregularis* and *Distaltriangulisporites perplexus* in the cuttings sample at 2480–2475 m further confirm an Albian age. Other miospore taxa in the interval 2910–2905 include *Appendicisporites potomacensis*, *Appendicisporites tricornitatus*, *Cicatricosisporites subrotundus* and *Vitreisporites pallidus*. These species occur in Albian or older rocks in many Labrador Shelf wells (Nøhr-Hansen et al. 2016). If our age assignment is correct, then upper Albian rocks must be absent in Skolp E-07.

The interval 2450–2080 m contains rich palynomorph assemblages, especially species of *Alterbidinium* and *Isabelidinium*. We are tentatively picking the top of the Cenomanian in the cuttings sample at 2405–2400 m, because of the presence of *Eurydinium glomeratum* and *Isabelidinium “skolpense.”* *Eurydinium glomeratum* was described from the Cenomanian of Saskatchewan by Davey (1970). Thus the thickness of this stage is only about 60 m, indicating that much of the stage is likely missing in Skolp E-07.

According to Nøhr-Hansen et al. (2016), *Rugubivesiculites rugosus* has its LO in the Turonian. In Skolp E-07, this species has its LO in the cuttings sample at 2085–2080 m. Therefore, the

Turonian extends from 2400 to 2080 m in the well. A dinocyst species having its LO in this interval is *Batioladinium jaegeri*, which has its LO in the Campanian according to Nøhr-Hansen et al. (2016). However, we consider the evidence from *Rugubivesiculites rugosus* more convincing. Williams (1980) considered 2465–2155 m to be Coniacian, with the Cenomanian and Turonian being absent. Nøhr-Hansen et al. (2016) found the age to be even younger with lower Campanian strata from 2495–2225 and upper Campanian from 2225–1430 m.

Stover et al. (1996) cited the LO of the dinocyst *Scriniodinium campanula* as top Coniacian. In Skolp E-07, this species has its LO in the cuttings sample from 1985–1980 m. Taking the sample to mark the top of the Coniacian would mean that the stage is approximately 100 m thick.

Several dinocyst taxa have their LOs in the interval 1925–1920 to 1850–1845 m. These include, with depths in parentheses: *Chlamyдохorella grossa* and *Odontochitina “skolpensis”* (1925–1920 m); *Endoscrinium obscurum* (1895–1890 m); and *Odontochitina porifera* (1850–1845 m). The LO of *Odontochitina porifera* is generally considered to be within the Santonian (Stover et al. 1996), thus we consider from 1980 to 1845 m in Skolp E-07 to be Santonian. Nøhr-Hansen et al. (2016) assigned this interval to the late Campanian, but Williams (1980) dated it as early Santonian with 1835–1645 m being Santonian–early Campanian.

The sample at 1655–1650 m contains the LOs of the following four dinocyst taxa — *Alterbidinium “rotundum”*, *Chlamyдохorella nyei*, *Heterosphaeridium “elegantulum”* and *Tenua cf. hystrix* (recorded as *Cerbia cf. tabulata* in some wells). *Tenua cf. hystrix* has been recorded from the Campanian of other Labrador Shelf wells including South Labrador N-79 and Roberval K-92 (Williams, 2007b, 2017b), so its LO appears to have some validity as an index marker for this stage. Nøhr-Hansen et al. (2016) placed the LO of *Chlamyдохorella nyei* within the Coniacian. However, this does not accord with our findings in Skolp E-07, where we consider the interval 1845 to 1650 m to be early Campanian. Other dinocyst species with their LOs in the Campanian are *Palaeohystrichophora infusorioides* and *Trichodinium castanea*. Nøhr-Hansen et al. (2016) plotted the LO of *Palaeohystrichosphaera infusorioides* in the early Campanian and the LO of *Trichodinium castanea* towards the top of the Campanian, which show close agreement with our findings. Williams (1980) assigned the interval 1835–1645 to the Santonian–early Campanian, and Nøhr-Hansen et al. (2016) reported an extensive upper Campanian section from 2225–1430 m.

We are including from 1650 to 1450 m in the late Campanian, the top being picked after analysis of the conventional core from 1454.32–1450 m by Dafoe and Williams (in press). Key taxa in the cuttings samples with their LOs in this interval (depths in parentheses) are: *Kleithriasphaeridium loffrense* (1595–1590 m); *Microdinium ornatum* (1535–1530 m); and *Callaiosphaeridium asymmetricum* and *Chatangiella ditissima* (1475–1470 m). In the conventional core, Dafoe and Williams (in press) studied four samples and noted the presence of key dinocyst species, including: *Gillinia hymenophora*, *Hystrichosphaeridium quadratum*,

Heterosphaeridium bellii, *Senoniasphaera rotundata*, and *Odontochitina costata*. Stover et al. (1996) found *Gillinia hymenophora* to have a late Campanian to Maastrichtian range, and the presence of *Hystrichosphaeridium quadratum* indicates an age of no older than Campanian. Nøhr-Hansen et al. (2016) restricted *Heterosphaeridium bellii* to the late Campanian and indicated that the LO of *Odontochitina costata* roughly equates with the Campanian–Maastrichtian boundary. Our placement of the Campanian–Maastrichtian boundary is very close to that indicated by both Williams (1980) and Nøhr-Hansen et al. (2016).

Skolp E-07 is one of the few Labrador Shelf wells in which the Maastrichtian can be subdivided and in which there seems to be a relatively continuous section across the Cretaceous–Cenozoic boundary. The top of the lower Maastrichtian is at 1265–1260 m, based on the LO of *Laciniadinium williamsii*, which Fensome et al. (2016) considered to be a taxonomic junior synonym of *Laciniadinium arcticum*. Confirmation of our age determination is provided by Nøhr-Hansen et al. (2016), who placed the LO of the latter species at approximately the middle of the Maastrichtian. Thus, we postulate that the lower Maastrichtian extends from 1450 to 1260 m. This compares well with the lower Maastrichtian pick of Williams (1980). Other dinocyst taxa with their LOs in this interval are (with depths in parentheses): *Phelodinium kozlowskii* and *Trigonopyxidia ginella* (1325–1320 m); *Areoligera medusettiformis* (1295–1290 m); and *Leberocysta chlamydata* and *Elytrocysta druggii* (1265–1260 m).

Further confirmation of the presence of a lower Maastrichtian interval comes from the conventional core samples analyzed by Dafoe and Williams (in press): core 3 from 1289–1290 m, core 2 from 1280–1276.5 m, and core 1 from 1276.5–1276.3 m. In these samples, key dinocysts include *Isabelidinium cooksoniae*, *Cerodinium diebelii*, *Palaeoperidinium pyrophorum*, and *Cannosphaeropsis utinensis*. The most convincing evidence comes from the LO of *Isabelidinium cooksoniae*, which Nøhr-Hansen et al. (2016) placed at about the top of the early Maastrichtian. Furthermore, Williams et al. (2004) considered *Cannosphaeropsis utinensis* to be restricted to the Maastrichtian. The FO of *Cerodinium diebelii* is considered to be at the base of the Maastrichtian in higher northern latitudes (McIntyre, 1974; Nøhr-Hansen et al., 2016), and the FO of *Palaeoperidinium pyrophorum* is at 73.7 Ma in mid-northern latitudes near the Campanian–Maastrichtian boundary (Williams et al., 2004).

The lower upper Maastrichtian seems to extend from 1260 to 1080 m. We base this conclusion on the LO of *Isabelidinium cretaceum* in the cuttings sample from 1085–1080 m. This species has been recorded from several Labrador Shelf wells by Nøhr-Hansen et al. (2016), who placed its LO within the late Maastrichtian. Askin (1988), in a study of dinocysts from the Campanian to Paleocene of Seymour and adjacent islands in Antarctica, defined a Zone 1, which was characterized by *Isabelidinium cretaceum*. She considered the zone to be late Campanian. Bowman et al. (2012) cited the age to be of questionable late Maastrichtian age but recognized two younger Maastrichtian zones. Thus, the LO of *Isabelidinium cretaceum* can be considered as

early late Maastrichtian. This taxon is a key index species for determining whether part of the upper Maastrichtian is missing in the Labrador–Baffin Seaway. Williams (2017b) stated that the LO of *Isabelidium cretaceum* in Labrador Shelf wells equated approximately with the top of the early Maastrichtian. But it is probably more accurate to regard it as marking the early late Maastrichtian. Dinocyst taxa with their LOs in the early late Maastrichtian in Skolp E-07 are (with depth in parentheses) *Membranosphaera maastrichtia* and *Spiniferites porosus* (1145–1140 m), and *Circulodinium distinctum* (1115–1110 m), as well as the pollen *Porosipollis porosus* (1085–1080 m). Our placement of the base of the early late Maastrichtian is slightly different from that of Nøhr-Hansen et al. (2016), who considered the top of the early Maastrichtian to be at 1295 m and did not subdivide the late Maastrichtian. Williams (1980) placed the top of the early Maastrichtian at 1255 m.

We consider the top of the Maastrichtian to be in the cuttings sample at 1025–1020 m. Several dinocyst species have their LOs in this interval, including *Cerodinium diebelii*, *Impagidinium* cf. *victorianum*, *Palynodinium grallator*, *Senoniasphaera inornata* and *Spinidinium echinoideum*. Nøhr-Hansen in Sønderholm et al. (2003) defined a *Palynodinium grallator* interval for the uppermost Maastrichtian. This was characterized by the LOs of *Palynodinium grallator* and the pollen *Wodehouseia spinata*. Williams et al. (2004) placed the FO of *Palynodinium grallator* in northern mid-latitudes at the Maastrichtian–Danian boundary and its LO in southern mid-latitudes within the earliest Danian. Nøhr-Hansen et al. (2016) also plotted the LO at the Maastrichtian–Danian boundary, which they placed at 1015 m in North Leif I-05; so considering the top of the Maastrichtian to be at 1025–1020 m in Skolp E-07 agrees closely with previous interpretations.

The lower Danian section is abbreviated, as indicated by the dinocysts in the sample at 995–990 m. Species with their LO in this sample are *Alterbidinium “obscurum”*, *Cerodinium glabrum*, *Cerodinium speciosum*, *Cerodinium striatum*, *Hystrichosphaeridium quadratum*, *Hystrichosphaeridium salpingophorum*, *Hystrichosphaeridium tubiferum*, *Palaeoperidinium pyrophorum*, *Spongodinium delitiense* and *Trithyrodinium evittii*. Nøhr-Hansen et al. (2016) placed the LO of *Spongodinium delitiense* and *Trithyrodinium evittii* at around the top of the early Danian, thus showing good agreement with the present work. These authors also determined the top of the Danian to be at 995 m in Skolp E-07, very close to our pick. This contrasts somewhat with Williams (1980), who assigned the interval 1025–1015 m to the Early Paleocene.

Overlying the lower Danian are lower Ypresian sediments, indicating a major hiatus above the cuttings sample at 995–990 m. However, the sample at 995–990 m contains a specimen of the dinocyst *Palaeocystodinium bulliforme*, which may indicate a condensed or reworked Selandian interval. Lower Ypresian sediments extend to the cuttings sample at 905–900 m based on the LO of the dinocyst *Petalodinium condylos* in the sample at 965–960 m and *Cerodinium wardenense*

in the sample at 905–900 m. Nøhr-Hansen in Sønderholm et al. (2003) erected a *Petalodinium condylos* Zone, marked by the LO of the nominal species. Thus he considered the zone to be early Ypresian. Also having its LO in this sample is the dinocyst *Cordosphaeridium gracile*. The interval 965–960 m has several specimens of *Azolla*, a characteristic feature of the Ypresian (Nøhr-Hansen et al., 2016). In the topmost sample at 905–900 m are the LOs of the dinocysts *Cerodinium wardenense*, *Diphyes ficusoides* and *Eatonicysta ursulae*. Williams et al. (2004) plotted the LO of *Cerodinium wardenense* at 53.1 Ma for mid-latitudes of the Northern Hemisphere. Therefore, it appears that upper Ypresian sediments are absent or attenuated at Skolp E-07. The uppermost sample studied by Nøhr-Hansen et al. (2016) in Skolp E-07 was at 925 m, which they dated as Ypresian, and thus similar to our findings. Williams (1980) also included the sample at 925 m in the Ypresian.

The sample at 875–870 m appears to be Bartonian, judging by the predominance of *Lingulodinium funginum*, a species common in the Middle Eocene of other Labrador Shelf wells (Nøhr-Hansen et al., 2016). If the Ypresian extends to 900 m and the Bartonian is at 875–870 m, the Lutetian and some of the Bartonian are highly condensed or absent.

The overlying Rupelian subsequently extends from 870 to 630 m. We pick the top of the Rupelian at 635–630 m on the LOs of two pollen grains, *Corsinipollenites oculusnoctis* and *Boisduvalia clavitites*. Nøhr-Hansen et al. (2016) considered *Corsinipollenites oculusnoctis* to have its LO in the Bartonian. However, Williams (1986) placed the LO of this species (as *Jussiaea* sp.) in the Early Oligocene (Rupelian). In his analyses of samples from Roberval C-02, Williams (2017b) agreed with extending the LO of *Corsinipollenites oculusnoctis* into the Rupelian in agreement with Williams's (1986) findings. Williams (1986) also gave a LO of Rupelian for *Boisduvalia clavitites*, which fits with our findings in Skolp E-07. Williams (1980) did not recognize Rupelian sediments in Skolp E-07, including 905–775 m in the Early Miocene, 775–685 in the Middle–Late Miocene and 665–535 m in the Plio-Pleistocene.

One specimen of the dinocyst *Chiropteridium galea* has been recovered from the sample at 605–600 m. This could denote a thin interval of Chattian sediments between 630 and 600 m, since Nøhr-Hansen et al. (2016) placed the LO of *Chiropteridium galea* at the Chattian–Aquitanian boundary, but it could also be reworked. More convincing is the Aquitanian–Burdigalian age for the next higher sample at 575–570 m, which has the LO of the trilete spore *Osmundacidites wellmannii*. Nøhr-Hansen et al. (2016) placed the LO of this species within the Burdigalian, indicating that the interval is Aquitanian–early Burdigalian.

The uppermost sample from 545–540 m contains the pollen *Tiliaepollenites crassipites* and the dinocyst *Cleistosphaeridium diversispinosum*. These two taxa have their LOs close to the top of the Serravallian (Nøhr-Hansen et al., 2016), so we are assigning the sample at 545–540 m to this stage. Accordingly, between 570–545 m, the Lower to Middle Miocene must be condensed or absent.

Paleoenvironments

A plot showing the relative percentages of dinocysts, miospores, acritarchs and other organic-walled microfossils in Skolp E-07 is given in Figure 11. This plot is used to describe paleoenvironmental changes, which are interpreted in Table 5. Previous paleoenvironmental studies of the Skolp E-07 well were undertaken by Price and Thorne (1978) using foraminifera and Miller and d'Eon (1987) based on lithologic analyses. Their paleoenvironments are compared in Figure 5 against our results.

TOP (M)	BASE (M)	PALEOENVIRONMENT
540	700	MARGINAL MARINE TO OCCASIONALLY NONMARINE
720	965	MARGINAL MARINE TO INNER NERITIC, UPWARD SHALLOWING
990	1685	INNER NERITIC
1710	1715	MIDDLE NERITIC
1740	2145	INNER NERITIC
2160	2230	OUTER NERITIC?
2250	2370	INNER NERITIC
2400	2495	MARGINAL MARINE TO INNER NERITIC
2530	2940	NONMARINE

Table 5: Summary of paleoenvironments in the Skolp E-07 well from this study.

The plot in Figure 11 reveals the dominance of miospores in the lower part of the section from sample 2990–2985 to 2405–2400 m (only the lowermost sample reflects cavings), which is Aptian, Albian, and Cenomanian in age. Dafoe and Williams (in press) noted that the lowest part of the Bjarni Formation, which includes core 6 (2918.77–2915.5 m), is nonmarine based on the presence of only miospores and no dinocysts. From 2940 m to a cuttings sample at 2535–2530 m, the dominance of miospores, including bisaccate pollen, and the almost complete absence of dinocysts and acritarchs indicate generally nonmarine paleoenvironments. Marginal marine to increasingly inner neritic paleoenvironments seem to be present between samples 2495–2490 and 2405–2400 m, judging by the increase in relative percentages of dinocysts and acritarchs upwards. Price and Thorne (1978) had similar results of continental strata overlain by restricted marine or marginal marine deposits, but with fluctuations to nonmarine conditions. However, Miller and d'Eon (1987) found nonmarine conditions to continue upwards in the well to 2152 m, including lacustrine facies.

The interval 2370–2365 to 1175–1170 m contains a much greater percentage of dinocysts and, in several samples, acritarchs. Paleoenvironments between 2370 and 2250 m are inner neritic with *Cyclonephelium* and peridinioids, including *Isabelidinium*, being frequent to common and spores and pollen being common. The presence of *Impagidinium* in two samples in the interval 2230–2225 to 2165–2160 m suggests deeper water, possibly outer neritic, but this is contradicted by

the high relative percentage of acritarchs. These interpretations roughly equate to those of Price and Thorne (1978) of restricted marine and open marine environments, but again contrast with the nonmarine, lacustrine setting proposed by Miller and d'Eon (1987).

Based on the common and consistent occurrence of peridinioids and acritarchs, we consider the interval from 2145–2140 to 1745–1740 m to represent an inner neritic paleoenvironment, with a change to middle neritic at 1715–1710, where dinocysts attain their maximum relative percentages in Skolp E-07, *Spiniferites* increase in abundance, and acritarchs are absent. Our interpretations for this interval indicate initially shallower and then deeper settings than those of Price and Thorne (1978), who considered the paleoenvironment to have been open marine and then shallow restricted marine. Conversely, Miller and d'Eon (1987) interpreted initially nonmarine to marginal marine settings followed by a questionable shelf setting.

Acritarchs are present in increasing numbers in the samples from 1685–1680 to 815–810 m and peridiniaceans are often common, with acritarchs reaching a peak in the sample at 1235–1230 m. This suggests an extended interval from 1685–990 m when inner neritic paleoenvironments predominated. Confirmation of this comes from the conventional cores studied by Dafoe and Williams (in press), who determined fluctuating shoreface to distal outer shelf settings for cores 1 to 5. The detailed palynological analyses from these cores generally indicated neritic deposition, not too far from shore and possibly in the vicinity of a delta due to a high degree of vitrinite in the samples. However, the presence of *Impagidinium* in core 5 indicated an outer shelf or open ocean, deeper water paleoenvironment at that particular level in the well. Obvious fluctuations in the paleoenvironment took place during deposition of the interval 1459–1276.3 m which circumscribes the cores 1 through 5; however, the paleoenvironmental settings are averaged by the cuttings and interpretations appear to tend towards shallower settings. Although, there is a consistent occurrence of the dinocyst *Impagidinium* cf. *victorianum* in the interval 1385–1380 to 1025–1020 m implying more open-marine paleoenvironments. The interval we identify as inner neritic (1685–990 m), Price and Thorne (1978) interpreted as shallow to restricted marine, and Miller and d'Eon (1987) considered deepening from marginal marine/inner shelf to middle shelf and questionable outer shelf. Both interpretations are reasonably similar to our results.

From 965–960 m to the topmost sample in the well at 545–540 m, non-bisaccate miospores are the dominant palynomorphs, with bisaccates as a minor element. The relative percentage of dinocysts is minimal, with the group being absent from many samples, although acritarchs are still common and generally decrease upwards. We interpret the interval 965–960 to 725–720 m as being deposited in a marginal marine to inner neritic paleoenvironment, with upwards shallowing. Samples from 700–695 to 545–540 m reflect marginal marine to occasionally nonmarine settings, with several reworked Late Cretaceous palynomorphs in the sample at 700–

695 m. These interpretations are similar to those of both Price and Thorne (1978) and Miller and d'Eon (1987).

An overall assessment of paleoenvironments at Skolp E-07 during the Cretaceous and Cenozoic shows a transition from nonmarine to marginal marine in the late early Albian, inner neritic deepening to outer neritic in the Cenomanian–Turonian and a return to inner neritic in the later Turonian through early Campanian. This is followed by brief middle neritic conditions and resumed inner neritic paleoenvironments prevailing in the late early Campanian–early Danian. Shallow marine to nonmarine settings then take over in the Ypresian through Serravallian, but with significant stratigraphic breaks. Thus, in Skolp E-07 paleoenvironments are shallower than in most other Labrador Shelf wells; however, the general trends seem to be similar. Our paleoenvironmental interpretations show general agreement with Price and Thorne (1978) and Miller and d'Eon (1987), the major exception being that for the early Late Cretaceous.

Correlation to Lithostratigraphy

The lithostratigraphic interpretations for Skolp E-07 in Figure 5 are based on Moir (1989). However, other studies have refined the lithostratigraphic assignments for the well, including C–NLOPB (2007). Below we discuss further refinements to some units, which are summarized in Table 6. The historical development of the formal lithostratigraphic units is described under the “Correlation to Lithostratigraphy” section for the North Leif I-05 well. The only interval not discussed there was the Freydis Member, and we provide context for the designation of only this unit below.

According to Moir (1989) the well penetrates Precambrian gneiss basement from its total depth of 2992 m up to 2967 m. U-Pb age dating places the age of the migmatitic quartz-diorite gneiss at about 3213 (+21/-3.6) Ma (Wasteneys et al., 1996).

Overlying basement gneiss is the Bjarni Formation, which Moir (1989) proposed to extend from 2967–2472 m, but the C–NLOPB (2007) cited the interval as 2968–2473 m. In Skolp E-07, neither of these formation tops occur as a distinctive change in lithological or well log properties as they fall within a shaly interval in the well. However, our biostratigraphic results indicate that the top of the formation should be placed slightly higher at 2460 m, where we pick the top of the lower Albian and a significant break in section with the upper Albian missing. This depth corresponds to a gamma-ray high in the wells logs and a general change in log character to more ragged gamma-ray, resistivity and sonic log character above, signifying a more heterolithic lithology. Accordingly, we find the Bjarni Formation to be of Aptian–early Albian age in this well. Notably, we consider the Bjarni Formation to only extend into the Albian. However, Nøhr-Hansen et al. (2016) and Williams (1980) both considered much of the formation to include Albian–Cenomanian strata. The paleoenvironment during Bjarni Formation deposition was nonmarine, but became marine at the end of the early Albian.

Formation	Moir (1989)		This Study	
	Base (m)	Top (m)	Base (m)	Top (m)
Saglek Formation	685	350	685	505
Mokami Formation	855	685	870	685
Kenamu Formation	974	855	990	870
Leif Member	974	937		
Gudrid Formation (upper)	986	974		
Markland Formation	2472	986	2460	990
Freydis Member	2472	1355		
Freydis Member (upper)	*1707	*1355	1707	1243
Freydis Member (lower)	*2472	*2008	2460	2022
Bjarni Formation	2967	2472	2967	2460
Snorri Member	2924	2472	2915	2460
Unnamed Precambrian	2992	2967	2992	2967

Table 6: Lithostratigraphy of the Skolp E-07 well from Moir (1989) and showing revised picks from this study (* indicates lithostratigraphic picks from Moir (1987)).

Opinions differ as to whether the Snorri Member is present in Skolp E-07. Moir (1989) considered the member to occur between 2924 and 2472 m, but the C–NLOPB (2007) did not designate an interval for it. While sandstones are present, much of the Bjarni Formation in Skolp E-07 is shale-dominated with significant coaly intervals, consistent with the Snorri Member designated by Umpleby (1979). The base of the formation, however, contains thick sandstone and conglomerate intervals, including that in core 6 (see Dafoe and Williams, in press). Accordingly, we assign the interval above these coarse-grained rocks from 2915 m to 2460 m to the Snorri Member. This member is thus early Albian in age in Skolp E-07 and generally nonmarine, but with a marginal marine to inner neritic signature at the very top.

Moir (1989) and the C–NLOPB (2007) showed slight differences in their assignments for the overlying Markland Formation. The former author considered the Markland Formation to extend from 2472 to 986 m, whereas the latter restricted the formation to 2473–1051 m. Based on the unconformity described above, we place the base of the formation at 2460 m. The top of the formation is not as distinctive as it is in the Hopedale Basin where the Gudrid Formation sandstones are well developed (e.g., in the Roberval C-02 and K-92 wells; Williams, 2017b). The Paleocene is also not well developed, with significant section representing the upper Danian through Thanetian missing; this is in contrast to the situation in North Leif I-05. However, our revised biostratigraphy provides constraints for another major unconformity at 990 m, at the top of the lower Danian; this is relatively consistent with a hiatus documented in previous studies. At this level in the well, a subtle change occurs in the resistivity log to increased values, above

which the gamma-ray and sonic logs both show a more ragged character consistent with the heterolithic lithology. Accordingly, we pick the Markland Formation from 2460 m to 990 m, similar to that of Moir (1989). The age of the formation in this well is Cenomanian to early Danian, older than the base interpreted as Coniacian by Williams (1980) and as early Campanian by Nøhr-Hansen et al. (2016). The paleoenvironment is shallower than seen elsewhere, such as in North Leif I-05, and generally ranges from inner to outer neritic.

The Freydis Member, initially proposed by Umpleby (1979) as the Freydis Sand Member within his Cartwright Formation, was described by McWhae et al. (1980) to be light grey, fine- to coarse-grained, quartzose sandstone and poorly sorted arkosic sandstone with an argillaceous matrix and lesser siltstones and shale of Late Cretaceous age. Depths for the Freydis Member in Skolp E-07 vary in previous studies: Moir (1989) gave a thickness of 1117 m with the interval from 2472–1355 m and the C–NLOPB (2007) gave a thickness of 1018 m with the interval from 2373–1355 m. However, Moir (1987) suggested two Freydis Member tongues, the first from 2472–2008 m and the second from 1707–1355 m. We agree with the assignment of two separate Freydis Member intervals based on the lithology seen in the well: a shale-dominated interval notably separates two thick, sandstone-dominated intervals. It is unclear why Moir (1989) brought the lower member up to 2008 m; in contrast, we propose a lower Freydis Member sandstone interval to extend from 2460–2022 m. We agree with the base of Moir’s (1987) upper member at 1707 m, but suggest that it extends upwards to 1243 m, to the top of the thick sandstones. The conventional core intervals that intersect the upper Freydis Member include shales, mudstones and fine-grained sandstones indicating fluctuations in the paleoenvironment (Dafoe and Williams, in press). These authors reported shoreface to outer shelf settings with the sandstones representing shoreface conditions consistent with the Freydis Member (McWhae et al., 1980; Balkwill and McMillan, 1990; Dafoe and Williams, in press). Overall, Freydis Member sandstones are Cenomanian–early Coniacian and early Campanian–early late Maastrichtian in age and generally reflect inner neritic conditions.

Sequentially overlying the Markland Formation according to Moir (1989) are (with depths given in parentheses): the Gudrid Formation (upper: 986–974 m); the Kenamu Formation (974–855 m); and the Leif Member of the Kenamu Formation (974–937 m). The C–NLOPB (2007) did not pick the Gudrid Formation in this well, but designated the section 1051–855 m as the Kenamu Formation and that from 986–938 m as the Leif Member. Despite the early Ypresian age, which is consistent with the upper Gudrid Formation seen elsewhere (e.g., Dafoe and Williams, in press), we agree with the C–NLOPB (2007) that the formation is not present. The rationale here is that the Gudrid Formation represents a significant regression (Balkwill, 1987; Balkwill and McMillan, 1990; Dafoe and Williams, in press) and would not be typically preserved in proximal Labrador Shelf wells where there would have been exposure and erosion rather than deposition as the shoreline moved basinward. While the age of the Kenamu Formation is considered to be Early to Late Eocene (McWhae et al., 1980), the Leif Member is generally considered to be

restricted to the Middle or Late Eocene (McWhae et al., 1980; Dickie et al., 2011). Accordingly, the Leif Member designation of Moir (1989) and C–NLOPB (2007) are rather early Ypresian in age and not consistent with the formal designation, so we do not consider these sandier rocks of the Kenamu Formation to be within the Leif Member. Considering the gap between the lower Ypresian and Bartonian, this appears to reflect a condensed interval of the Kenamu Formation, possibly indicative of erosion during the shoreline regression in the Bartonian that develops the Leif Member sandstone. At 870 m there is an increase in the gamma-ray log that persists up section in the well. This correlates to subtle decreases in sonic velocity and resistivity. Based on this, we place the Kenamu Formation from 990–870 m in Skolp E-07. The lower Ypresian sandstones can be related to the Ypresian-aged proximal clinoform of Dafoe et al. (2017a) within the lower part of the Kenamu Formation, which represents a landward-situated shoreline facies during major transgression of the margin. While the Bartonian interval is also sandy, and would be consistent with the Leif Member, we cannot definitively assign it to the member as the Bartonian is highly condensed. In general, the paleoenvironment is marginal marine to inner neritic for the Kenamu Formation.

Above the Kenamu Formation, Moir (1989) picked the Mokami Formation from 855–685 m and the C–NLOPB (2007) gave the interval 855–687 m. We agree with the top of Mokami Formation at 685 m, but place the base at 870 m. This results in a Rupelian age, which falls within the Late Eocene to Middle–Late Miocene age proposed by Balkwill and McMillan (1990). The top of this formation is defined in the well logs by a sudden decrease in gamma-ray, decrease in sonic velocity, and increase in resistivity. The setting was relatively shallow for the Mokami Formation at marginal marine to inner neritic.

The Saglek Formation sits at the top of the well and was defined by Moir (1989) as the interval from 685–350 m and by the C–NLOPB as 687–350 m. We agree with the base at 685 m, but restrict the top to 505 m at the top of the well logs. The Saglek Formation is uncharacteristically heterolithic, unlike typical occurrences in the Hopedale Basin (e.g. Williams, 2017b). This may be explained by the paleoenvironment fluctuating from marginal marine to nonmarine, which may have included lagoonal or floodplain settings that account for the claystone accumulations. The Rupelian through Serravallian age is relatively consistent with previous studies (Dickie et al., 2011; Williams, 2017b), however the stages are generally condensed in Skolp E-07.

Summary

Skolp E-07 was drilled to test sedimentary units absent in Karlsefni A-13 (Prim et al., 1978): total depth was 2992 m. The well, a dry hole, encountered Precambrian gneiss at 2967 m (Moir, 1989). As in our study of North Leif I-05, age control is based primarily on dinocysts but the spores and pollen were informative, especially in the Aptian and early Albian.

The well shows a surprisingly complete Cretaceous section, with Aptian, early Albian, Cenomanian, Turonian, Coniacian, Santonian, Campanian and Maastrichtian sediments present. A significant hiatus is apparent at the top of the Bjarni Formation with the late Albian missing. Especially intriguing is the development of two thick Freydis Member sandstones, the presence of a Maastrichtian section of more than 400 m, and recognition of the Maastrichtian–Danian boundary. Thus Skolp E-07, like North Leif I-05, is one of the few wells on the Labrador Shelf, which appears to have a relatively continuous section across the Cretaceous–Cenozoic boundary, providing excellent correlation of the dinocysts with coeval assemblages in Europe.

Much of the Paleogene is missing, especially in the Paleocene and Eocene, with only lower Danian, lower Ypresian, Bartonian, Rupelian and ?Chattian sediments identified. These gaps indicate that there are major hiatuses in Skolp E-07. It is possible that there are some condensed intervals, but specimens indicating these were not seen in the cuttings samples. We have revised the lithostratigraphy to reflect this by indicating only the presence of the Kenamu, Mokami and Saglek formations.

Paleoenvironments in Skolp E-07 ranged from nonmarine, marginal marine, inner neritic to possibly outer neritic in the Cretaceous, with gradual shallowing in the Cenozoic giving rise to marginal marine to nonmarine paleoenvironments in the Miocene. Skolp E-07 preserves a unique succession, both in the presence of a relatively complete Cretaceous section from the Aptian to Maastrichtian and in the relative shallowness of the paleoenvironments compared to most of the other wells along the Labrador margin, consistent with its proximal location on the Labrador Shelf.

Oversized Figure Captions

Figure 8: Plot of the Skolp E-07 well showing key wireline logs, lithology (Canstrat), conventional core locations, reference section (Moir, 1989), and key biostratigraphic studies, paleoenvironmental interpretations, and lithostratigraphy.

Figure 9: Range plot for dinocysts from the Skolp E-07 well.

Figure 10: Range plot for spores, pollen, and other palynomorphs from the Skolp E-07 well.

Figure 11: Palynomorph ratio plot for the Skolp E-07 well from this study. Bisaccates are shown separately from other spores and pollen.

ACKNOWLEDGEMENTS

The authors would like to thank GEUS for their gracious loan of slides for the North Leif I-05 well. Thanks to Paul Lake for compiling the range plots for both wells and to Bill MacMillan for compiling the plates. A special thanks to Rob Fensome for his detailed and valuable critical review. Also thanks to Lori Campbell for her effort in the coordination of new palynomorph processing that was undertaken to complete this study.

REFERENCES

- Ainsworth, N.R., Riley, A., Bailey, H.W., and Gueinn, K.J., 2016. Cretaceous–Tertiary stratigraphy of the Labrador Shelf wells: Freydis B-87, Hopedale E-33, Karlsefni A-34, North Leif I-05 and South Hopedale L-39. Riley Geoscience Ltd., 31 p.
- Askin, R.A., 1988. Campanian to Paleocene palynological succession of Seymour and adjacent islands, northeastern Antarctic Peninsula. In: Feldmann, R.M., and Woodburne, M.O. (eds): *Geology and paleontology of Seymour Island, Antarctic Peninsula*. Geological Society of America Memoir 169, p. 131–153.
- Balkwill, H.R., 1987. Labrador basin: structural and stratigraphic style. In: *Sedimentary Basins and Basin-Forming Mechanisms*, (ed) C. Beaumont and A.J. Tankard. Canadian Society of Petroleum Geologists, Memoir, v. 12, p. 17–43.
- Balkwill, H.R. and McMillan, N.J., 1990. Mesozoic-Cenozoic geology of the Labrador Shelf, Chapter 7 (part 1). In: *Geology of the Continental Margin of Eastern Canada*, vol. 2., (ed) M.J. Keen and G.L. Williams. Geological Survey of Canada, Geology of Canada, p. 295-324. (also Geological Society of America, *The Geology of North America*, V. I-1).
- Barss, M.S., Bujak, J.P., and Williams, G.L., 1979. Palynological zonation and correlation of sixty-seven wells, eastern Canada. Geological Survey of Canada Paper 78(24), p. 1–118.
- Bint, A.N., 1986. Fossil Ceratiaceae: a restudy and new taxa from the mid-Cretaceous of the western interior, U.S.A. *Palynology*, v. 10, p.135-180.
- Bowman, V.E., Francis, J.E., Riding, J.B., Hunter, S.J., and Haywood, A.M., 2012. A latest Cretaceous to earliest Paleogene dinoflagellate cyst zonation from Antarctica, and implications for phytoprovincialism in the high latitudes. *Review of Palaeobotany and Palynology*, v. 171, p. 40–56.
- Brinkhuis, H., 1992. Late Eocene to early Oligocene dinoflagellate cysts from central and northeast Italy. Unpublished Ph.D. thesis, University of Utrecht, 169 p.
- Brinkhuis, H., 1994. Late Eocene to early Oligocene dinoflagellate cysts from the Priabonian type-area (northeast Italy) — biostratigraphy and paleoenvironmental interpretation. *Palaeogeography, Palaeoclimatology, Palaeoecology*, v. 107, no. 1–2, p.121–163.
- Brinkhuis, H., Sengers, S., Sluijs, A., Warnaar, J., and Williams, G.L., 2003. Chapter 3. Latest Cretaceous–earliest Oligocene and Quaternary dinoflagellate cysts, ODP Site 1172, East Tasman Plateau. In: Exon, N.F., Kennett, J.P. and Malome, M.J. (eds), *Proceedings of the Ocean Drilling Program, Scientific Results*, v. 189, p.1-48.
- Bujak, J.P., 1994. New dinocyst taxa from the Eocene of the North Sea. *Journal of Micropalaeontology*, v. 13, p.119–131.
- Bujak, J.P. and Brinkhuis, H., 1998. Global warming and dinocyst changes across the Paleocene/Eocene epoch boundary. In: Aubry, M.-P. *et al.* (eds), *Late Paleocene–early Eocene*

biotic and climate events in the marine and terrestrial records. New York, Columbia University Press, p. 277–295.

Bujak, J.P., Downie, C., Eaton, G.L., and Williams, G.L., 1980. Dinoflagellate cysts and acritarchs from the Eocene of southern England. *Special Papers in Palaeontology*, no. 24, 100 p.

Bujak Davies Group, 1989a. Biostratigraphy and maturation of 17 Labrador and Baffin Shelf wells. Volume 1: Scope, methodology, format and recommendations. Geological Survey of Canada, Open File 1929, 95 p.

Bujak Davies Group, 1989b. Biostratigraphy and Maturation of 17 Labrador and Baffin Shelf wells, Volume 6: North Leif I-05 and Ogmund E-72. Geological Survey of Canada, Open File Report, 1934, 91 p.

Canada–Newfoundland and Labrador Offshore Petroleum Board (C–NLOPB), 2007. Schedule of wells: Newfoundland and Labrador offshore area. <https://www.cnlopb.ca/>.

Crouch, E.M., Heilmann-Clausen, C., Brinkhuis, H., Morgans, H.E.G., Rogers, K.M., Egger, H. and Schmitz, B., 2001. Global dinoflagellate event associated with the Late Paleocene Thermal Maximum. *Geology*, v. 29, p.315–318.

Dafoe, L.T. and Williams, G.L., in press. Lithological, sedimentological, ichnological, and palynological analysis of 37 conventional core intervals from 15 wells, offshore Labrador, Canada. Geological Survey of Canada, Bulletin 613.

Dafoe, L.T., Dickie, K., Williams, G.L., and Keen, C.E., 2017a. A late rift to post-rift shoreline clinoform and shelf-edge model for the offshore Labrador margin, Canada. 5th Atlantic Conjugate Margins Conference, 1 p (abstract).

Dafoe, L.T., Dickie, K., Williams, G.L., and Keen, C.E., 2017b. Regional Cenozoic stratigraphic correlations on the passive margin of the North Atlantic Ocean: comparison between Orphan Basin and the Labrador Margin. Atlantic Geoscience Society, Annual Colloquium, p. 24 (abstract).

Dafoe, L.T., Dickie, K., and Williams, G.L., 2018. A clinoform trajectory model for Late Cretaceous and Cenozoic sedimentation on the Labrador-Baffin Island Margins. Conjugate Margins Conference, Program and Abstracts, p. 74.

Dale, B., 1996. Chapter 31. Dinoflagellate cyst ecology: modelling and geological applications. In: Jansonius, J. and McGregor, D.C. (eds), *Palynology: principles and applications*, 3. American Association of Stratigraphic Palynologists Foundation, Dallas, p. 1249–1275.

Davey, R.J., 1970. Non-calcareous microplankton from the Cenomanian of England, northern France and North America, part II. *British Museum (Natural History) Geology, Bulletin*, 18 (8), p. 333–397.

Dickie, K., Keen, C.E., Williams, G.L., and Dehler, S.A., 2011. Tectonostratigraphic evolution of the Labrador Margin, Atlantic Canada. *Marine and Petroleum Geology*, v. 28, p. 1663–1675. doi:10.1016/j.marpetgeo.2011.05.009

- Fensome, R.A., Nøhr-Hansen, H., and Williams, G.L., 2016. Cretaceous and Cenozoic dinoflagellate cysts and other palynomorphs from the western and eastern margins of the Labrador-Baffin Seaway. *Grønlands Geologiske Undersøgelse, Bulletin* 36, 143 p.
- Gradstein, F.M. and Williams, G.L., 1976. Biostratigraphy of the Labrador Shelf. Geological Survey of Canada, Open File 349, 39 p.
- Gradstein, F.M. and Srivastava, S.P., 1980. Aspects of Cenozoic stratigraphy and paleoceanography of the Labrador Sea and Baffin Bay. *Paleogeography, Paleoclimatology, Paleoecology*, v. 30, p. 261-295.
- Gradstein, F.M., Kaminski, M.A., Berggren, W.A., Kristiansen, I.L., and D’Orio, M.A., 1994. Cenozoic biostratigraphy of the North Sea and Labrador Shelf. *Micropaleontology*, 40, suppl., 152 p.
- Gradstein, F.M., Ogg, J.G., Schmitz, M.D., and Ogg, G.M., 2012. The geologic time scale 2012. Elsevier, 1176 p.
- Harland, R., 1979. The *Wetzelilla (Apectodinium) homomorphum* plexus from the Palaeogene/earliest Eocene of north-west Europe. In: Fourth International Palynology Conference, Lucknow, 1976-1977, Proceedings, v. 2, p. 59–70.
- Heilmann-Clausen, C., 1994. Review of Paleocene dinoflagellates from the North Sea region. Stockholm, Geological Society of Sweden, GFF116, p. 51–53.
- Jan du Chêne, R.E. and Adediran, S.A., 1985. Late Paleocene to Early Eocene dinoflagellates from Nigeria. *Cahiers de micropaléontologie, Centre nationale de la recherche scientifique*, no. 1984-3, p. 5–38.
- Lister, J.K. and Batten, D.J., 1988. Stratigraphic and palaeoenvironmental distribution of Early Cretaceous dinoflagellate cysts in the Hurlands Farm Borehole, West Sussex, England. *Palaeontographica, Abteilung B*, 210, p. 9–89.
- McIntyre, D.J., 1974. Palynology of an Upper Cretaceous section, Horton River, District of Mackenzie, Northwest Territories. Geological Survey of Canada, Paper 74-14, p.1–57.
- McWhae, J.R.H., Elie, R., Laughton, D.C., and Gunther, P.R., 1980. Stratigraphy and petroleum prospects of the Labrador Shelf. *Bulletin of Canadian Petroleum Geology*, v. 28, no. 4, p.460–488.
- Miller, P.E. and d’Eon, G.J., 1987. Labrador Shelf palaeoenvironments. Geological Survey of Canada, Open File 1722, 186 p.
- Moir, P.N., 1987. Stratigraphic picks, Total-Eastcan et al. Skolp E-07. Geological Survey of Canada (Atlantic), Internal Report No. EPGS-STRAT.27-87PNM, 2 p.
- Moir, P.N., 1989. Lithostratigraphy 1. Review and type sections. In: Geological Survey of Canada, Atlantic Geoscience Centre, East Coast Basin Atlas Series, Labrador Shelf, p. 26.

- Morgenroth, P., 1966. Mikrofossilien und Konkretionen des nordwesteuropäischen Untereozäns. *Palaeontographica*, Abteilung B, v. 119, no. 1–3, p. 1–53.
- Nøhr-Hansen, H., 2003. Dinoflagellate cyst stratigraphy of the Palaeogene strata from the wells Hellefisk-1, Ikermiut-1, Kangâmiut-1, Nukik-1, Nukik-2 and Qulleq-1, offshore West Greenland. *Marine and Petroleum Geology*, v. 20, p. 987–1016.
- Nøhr-Hansen, H., 2004. Dinoflagellate cyst stratigraphy of the North Leif I-05 well, Hopedale Basin, Labrador Shelf, offshore eastern Canada. *Danmarks og Grønlands Geologiske Undersøgelse Rapport 2004/109*, 117 p, 2 Enclosures.
- Nøhr-Hansen, H., 2008. Morphological variability within brackish water to marginal marine dinoflagellate cyst assemblages from mid-Cretaceous, West Greenland. *DINO8 – 8th International conference on modern and fossil dinoflagellates*, Montreal, Canada, 4-10 May, 2008. GEOTOP- UQAM, Canada, Abstract volume, p. 41–42.
- Nøhr-Hansen, Williams, G.L., and H., Fensome, R.A., 2016. Biostratigraphic correlation of the western and eastern margins of the Labrador-Baffin Seaway and implications for the regional geology. *Grønlands Geologiske Undersøgelse Bulletin 37*, 74 p.
- Pedersen, G.K. and Nøhr-Hansen, H., 2014. Sedimentary successions and paleoevent stratigraphy from the non-marine Lower Cretaceous to the marine Upper Cretaceous of the Nuussuaq Basin, West Greenland. *Bulletin of Canadian Petroleum Geology*, v. 62, no. 4, p. 216–244.
- Petro-Canada Exploration Inc., 1980. Well history report Petro-Canada et al North Leif I-05. On file at the Canada–Newfoundland and Labrador Offshore Petroleum Board, 218 p.
- Powell, A.J. (ed.), 1992. A stratigraphic index of dinoflagellate cysts. *British Micropaleontological Society, Publication Series*, Chapman and Hall, London, U.K., 290 p.
- Powell, A.J., Brinkhuis, H., and Bujak, J.P., 1996. Upper Paleocene–lower Eocene dinoflagellate cyst sequence biostratigraphy of southeast England. In: Knox, R.W.O.B. et al. (eds), *Correlation of the early Paleogene in northwest Europe*. Geological Society Special Publication (London), v. 101, p. 145–183.
- Price, R.J. and Thorne, B.V.A., 1978. The micropalaeontology, palynology and stratigraphy of the Total Eastcan Skolp E-7 well, Labrador Shelf, offshore eastern Canada. On file at the Canada–Newfoundland and Labrador Offshore Petroleum Board, 29 p.
- Prim, M., Cadel, M., Ameller, J.H., and Plé, C., 1978. Well history report Total Eastcan et al – Skolp E-07. Total Eastcan Exploration Ltd., Calgary, Alberta. On file at the Canada–Newfoundland and Labrador Offshore Petroleum Board, 154 p.
- Schoon, P.L., Heilmann-Clausen, C., Pagh Schultz, B., Sluijs, A., Sinninghe, D., 2013. Recognition of early Eocene global carbon isotope excursions using lipids of marine Thaumarchaeota. *Earth and Planetary Science Letters*, v. 373, p. 160–168.
- Sluijs, A., Brinkhuis, H., Stickley, C.E., Warnaar, J., Williams, G.L., and Fuller, M., 2003. Dinoflagellate cysts from Eocene-Oligocene transition in the Southern Ocean; results from ODP

Leg 189. In: Exon, N.F., Kennett, J.P., and Malome, M.J. (eds), Proceedings of the Ocean Drilling Program, Scientific Results, 189 p.

Sluijs, A., Pross, J., and Brinkhuis, H., 2005. From greenhouse to icehouse; organic-walled dinoflagellate cysts as paleoenvironmental indicators in the Paleogene. *Earth-Science Reviews*, v. 68, no. 3–4, p. 281–315.

Sluijs, A. et al., 2006. Subtropical Arctic Ocean temperatures during the Palaeocene-Eocene thermal maximum. *Nature*, v. 441, p. 610–613.

Sønderholm, M., Nøhr-Hansen, H., Bojesen-Koefoed, J.A., Dalhoff, F., and Rasmussen, J.A., 2003. Regional correlation of Mesozoic–Palaeogene sequences across the Greenland-Canada boundary. *Danmarks og Grønlands Geologiske Undersøgelse Rapport 2003/25*, 175 p.

Staplin, F.L., 1961. Reef controlled distribution of Devonian microplankton in Alberta. *Palaeontology*, v. 4, no. 3, p. 392–424.

Stover, L.E. *et al.*, 1996. Chapter 19. Mesozoic–Tertiary dinoflagellates, acritarchs and prasinophytes. In: Jansonius, J. and McGregor, D.C. (eds), *Palynology: principles and applications*, v. 2. American Association of Stratigraphic Palynologists Foundation, Dallas, p. 641–750.

Umpleby, D.C., 1979. Geology of the Labrador Shelf. Geological Survey of Canada Paper 79-13, 34 p.

Wall, D., Dale, B., Lohmann, G.P., and Smith, W.K., 1977. The environmental and climatic distribution of dinoflagellate cysts in modern marine sediments from regions in the North and South Atlantic Oceans and adjacent areas. *Marine Micropaleontology*, v. 2, p. 121–200.

Wasteneys, H.A., Wardle, R.J., and Krogh, T.E., 1996. Extrapolation of tectonic boundaries across the Labrador shelf: U-Pb geochronology of well samples. *Canadian Journal of Earth Science*, v. 33, p. 1308–1324.

Williams, G.L., 1975. Dinoflagellate and spore stratigraphy of the Mesozoic–Cenozoic, offshore eastern Canada. In: van der Linden, W.J.M. and Wade, J.A. (eds), *Offshore Geology of Eastern Canada*, volume 2, Regional Geology. Geological Survey of Canada Paper 2, p. 107–161.

Williams, G.L., 1980. Palynological analysis of Eastcan et al. Skolp E-07, Labrador Shelf. Geological Survey of Canada, Internal Report No. EPGs-PAL.6-80GLW, 3 p.

Williams, G.L., 2003a. Palynological analysis of Amoco-Imperial-Skelly Skua E-41, Carson Basin, Grand Banks of Newfoundland. Geological Survey of Canada, Open File Report 1658, 23 p.

Williams, G.L., 2003b. Palynological analysis of Petro-Canada et al. Terra Nova K-18, Jeanne d’Arc Basin, Grand Banks of Newfoundland. Geological Survey of Canada, Open File Report 1659, 21 p.

- Williams, G.L., 2006. Palynological analysis of Elf Hermine E-94, Scotian Basin. Geological Survey of Canada, Open File 4976, 22 p.
- Williams, G.L., 2007a. Palynological analysis of Chevron *et al.* South Labrador N-79, Hopedale Basin, Labrador Shelf. Geological Survey of Canada, Open File Report 5446, 26 p.
- Williams, G.L., 2007b. Palynological analysis of Total Eastcan *et al.* Gilbert F-53, Saglek Basin, Labrador Shelf. Geological Survey of Canada, Open File Report 5450, 22 p.
- Williams, G.L., 2017a. Palynological Analysis of the Two Labrador Shelf Wells, Petro-Canada *et al.* Corte Real P-85 and Petro-Canada *et al.* Pothurst P-19, Offshore Newfoundland and Labrador. Geological Survey of Canada, Open File Report 8182, 50 p.
- Williams, G.L., 2017b. Palynological analysis of the two Labrador Shelf wells, Petro-Canada *et al.* Roberval C-02 and Total Eastcan *et al.* Roberval K-92, offshore Newfoundland and Labrador. Geological Survey of Canada, Open File Report 8183, 63 p.
- Williams, G.L. and Brideaux, W.W., 1975. Palynological analysis of upper Mesozoic and Cenozoic Rocks of the Grand Banks, Atlantic Continental Margin. Geological Survey of Canada, Bulletin 236, 163 p.
- Williams, G.L. and Bujak, J.P., 1977. Cenozoic palynostratigraphy of offshore eastern Canada. American Association of Stratigraphic Palynologists, Contribution Series 5A, p. 14–47.
- Williams, G.L., Ascoli, P., Barss, M.S., Bujak, J.P., Davies, E.H., Fensome, R.A. and Williamson, M.A., 1990. Chapter 3. Biostratigraphy and related studies. In: Keen, M.J. and Williams, G.L. (eds), Geology of the continental margin of eastern Canada; Geological Survey of Canada, Geology of Canada, no. 2 (also Geological Society of America, the Geology of North America, v. I 1), p. 87–137.
- Williams, G.L., Bujak, J.P., Brinkhuis, H., Fensome, R.A., and Weegink, J.W., 1999. Mesozoic–Cenozoic dinoflagellate cyst course, Urbino, Italy, May 17–22, 1999 (unpublished short course manual).
- Williams, G.L., Brinkhuis, H., Pearce, M.A., Fensome, R.A., and Weegink, J.W., 2004. Southern Ocean and global dinoflagellate cyst events compared: index events for the Late Cretaceous–Neogene. In: Exon, N.F. *et al.* (eds), Proceedings of the Ocean Drilling Program, Scientific Results, v. 189, p. 1–98.
- Williams, V.E., 1986. Palynological study of the continental shelf sediments of the Labrador Sea. University of British Columbia, Vancouver, B.C., Canada, unpublished Ph.D. thesis, 210 p.
- Zachos, J.C., Schouten, S., Bohary, S., Quattlebaum, T., Sluijs, A., Brinkhuis, H., Gibbs, S.J., and Bralower, T.J., 2006. Extreme warming of mid-latitude coastal ocean during the Paleocene–Eocene Thermal Maximum: inferences from TEX₈₆ and isotope data. *Geology*, v. 34, no. 9, p. 737–744.

SPECIES CITATIONS

Citations for dinocysts are presented in Williams et al. (2017) and the online DINOFLAJ3 database: http://dinoflaj.smu.ca/dinoflaj3/index.php/Main_Page.

Dinocysts

- Achilleodinium biformoides* (Eisenack 1954) Eaton 1976
- Achomosphaera ramulifera* (Deflandre 1937b) Evitt 1963
- Adnatosphaeridium robustum* (Morgenroth 1966a) de Coninck 1975
- Alterbidinium* Lentin and Williams 1985
- Alterbidinium acutulum* (Wilson 1967b) Lentin and Williams 1985,
- Alterbidinium? bicellulum* (Islam 1983a) Lentin and Williams 1985
- Alterbidinium* “*rotundum*”; informal species name
- Apectodinium* (Costa and Downie 1976) Lentin and Williams 1977b
- Apectodinium homomorphum* (Deflandre and Cookson 1955) Lentin and Williams 1977b
- Areoligera* Lejeune-Carpentier 1938a
- Areoligera gippingensis* Jolley 1992
- Areoligera medusettiformis* Wetzel, 1933b ex Lejeune-Carpentier 1938a
- Axiodinium augustum* (Harland 1979c) Williams et al. 2015
- Batioladinium jaegeri* (Alberti 1961) Brideaux 1975
- Callaiosphaeridium asymmetricum* (Deflandre and Courteville 1939) Davey and Williams, 1966b
- Canningia reticulata* Cookson and Eisenack 1960b
- Cerbia* cf. *tabulata* (Davey and Verdier 1974) Below 1981a
- Cerodinium dartmoorium* (Cookson and Eisenack 1965b) Lentin and Williams 1987
- Cerodinium diebelii*. (Alberti 1959) Lentin and Williams 1987
- Cerodinium glabrum* (Gocht 1969) Fensome *et al.* 2009
- Cerodinium speciosum* (Alberti 1959) Lentin and Williams 1987
- Cerodinium striatum* (Drugg 1967) Lentin and Williams 1987
- Cerodinium wardenense* (Williams and Downie 1966c) Lentin and Williams 1987

Chatangiella biapertura (McIntyre 1975) Lentin and Williams 1976
Chatangiella madura Lentin and Williams 1976
Chatangiella tripartita (Cookson and Eisenack 1960a) Lentin and Williams 1976
Chiropteridium galea (Maier 1959) Sarjeant 1983
Chiropteridium gilbertii Fensome et al. 2017
Chlamydothorella nyei Cookson and Eisenack 1958
Chlamydothorella? grossa Manum and Cookson 1964
Chorate cyst 9 of Nøhr-Hansen 2004
Circulodinium distinctum Deflandre and Cookson 1955) Jansonius 1986
Cleistosphaeridium diversispinosum Davey et al. 1966
Cordosphaeridium fibrospinosum Davey and Williams 1966b
Cordosphaeridium gracile (Eisenack 1954) Davey and Williams 1966b
Cribopteridium wetzelii (Lejeune-Carpentier 1939) Helenes 1984
Cyclonephelium Deflandre and Cookson 1955
Cyclonephelium vannophorum Davey 1969a
Dapsilidinium pseudocolligerum (Stover 1977) Bujak et al. 1980
Deflandrea heterophlycta Deflandre and Cookson 1955
Deflandrea phosphoritica Eisenack 1938
Diphyes colligerum (Deflandre and Cookson 1955) Cookson 1965a
Diphyes ficusoides Islam 1983b
Distatodinium Eaton 1976
Downiesphaeridium? aciculare Davey 1969a Islam 1993
Eatonicysta ursulae (Morgenroth 1966a) Stover and Evitt 1978
Elytrocysta druggii Stover and Evitt 1978
Endoscrinium campanula Gocht 1959
Endoscrinium obscurum (Manum and Cookson 1964) Riding and Fensome 2003
Enneadocysta magna Fensome et al. 2007
Eurydinium glomeratum (Davey 1970) Stover and Evitt 1978
Gillinia hymenophora Cookson and Eisenack 1960a

Glaphyrocysta divaricata (Williams and Downie 1966b) Stover and Evitt 1978
Glapyrocysta intricata (Eaton 1971) Stover and Evitt 1978
Glaphyrocysta semitecta (Bujak in Bujak et al. 1980) Lentin and Williams 1981
Heterosphaeridium bellii Radmacher et al. 2014
Heterosphaeridium difficile (Manum and Cookson 1963) Ioannides 1986
Heterosphaeridium “*elegantulum*”; informal species name
Heteraulacacysta pustulosa Jan du Chêne and Adediran 1985
Homotryblium tenuispinosum Davey and Williams 1966b
Hystrichosphaeridium Deflandre 1937b
Hystrichosphaeridium quadratum Fensome et al. 2016
Hystrichosphaeridium salpingophorum Deflandre 1935 ex Deflandre 1937b
Hystrichosphaeridium tubiferum subsp. *brevispinum* (Davey and Williams 1966b) Lentin and Williams 1973
Impagidinium Stover and Evitt 1978
Impagidinium victorianum (Cookson and Eisenack 1965a) Stover and Evitt 1978
Impletosphaeridium apodastum Fensome et al. 2016
Isabelidinium Lentin and Williams 1977a
Isabelidinium amphiatum (McIntyre 1975) Lentin and Williams 1977a
Isabelidinium cooksoniae (Alberti 1959b) Lentin and Williams 1977a
Isabelidinium cretaceum (Cookson 1956) Lentin and Williams 1977a
Isabelidinium “*skolpense*”; informal species name
Kiokansium williamsii Singh 1983
Kleithriasphaeridium loffrense Davey and Verdier 1976
Laciniadinium arcticum (Manum and Cookson 1964) Lentin and Williams 1980
Laciniadinium williamsii Ioannides 1986
Leberidocysta chlamydata (Cookson and Eisenack 1962b) Stover and Evitt 1978
Lentinia serrata Bujak in Bujak et al. 1980
Leptodinium Klement 1960
Licracysta? *semicirculata* Fensome et al. 2007

Lingulodinium funginum (Morgenroth 1966a) Islam 1983a
Membranilarnacia Eisenack 1963a
Membranophoridium aspinatum Gerlach 1961
Membranosphaera maastrichtia Samoilovitch in Samoilovitch and Mtchedlishvili 1961
Microdinium ornatum Cookson and Eisenack 1960a
Nyktericysta Bint 1986
Nyktericysta davisii Bint 1986
Odontochitina Deflandre 1937b
Odontochitina ancala Bint 1986
Odontochitina costata Alberti 1961
Odontochitina operculata (Wetzel 1933a) Deflandre and Cookson 1955
Odontochitina porifera Cookson 1956
Odontochitina “*skolpensis*”; informal species name
Oligosphaeridium Davey and Williams 1966b
Oligosphaeridium albertense (Pocock 1962) Davey and Williams 1969
Oligosphaeridium complex (White 1842) Davey and Williams 1966b
Ovoidinium verrucosum (Cookson and Hughes 1964) Davey 1970
Palaeocystodinium bulliforme Ioannides 1986
Palaeocystodinium lidiae (Gorka 1963) Davey 1969b
Palaeohystrichophora infusorioides Deflandre 1935
Palaeoperidinium pyrophorum (Ehrenberg 1838 ex Wetzel 1933a) Sarjeant 1967
Palynodinium grallator Gocht 1970
Petalodinium condylos (Williams and Downie 1966a) Williams et al. 2015
Phelodinium kozlowskii (Gorka 1963) Lindgren 1984
Phthanoperidinium Drugg and Loeblich Jr. 1967
Phthanoperidinium coreoides (Benedek 1972) Lentin and Williams 1976
Phthanoperidinium geminatum Bujak in Bujak et al. 1980
Phthanoperidinium levimurum Bujak in Bujak et al. 1980
Phthanoperidinium stockmansii (de Coninck 1975) Lentin and Williams 1977b

Piladinium columna (Michoux 1988) Williams et al. 2015
Pseudoceratium Gocht 1957
Pseudoceratium pelliferum Gocht 1957
Pterodinium cingulatum (Wetzel 1933b) Below 1981a
Quantouendinium Mao Shaozhi et al. 1999
Quantouendinium dictyophorum (He Chengquan et al. 1992) Mao Shaozhi et al. 1999
Rhombodinium draco Gocht 1955
Schematophora speciose Deflandre and Cookson 1955
Senoniasphaera inornata (Drugg 1970) Stover and Evitt 1978
Senoniasphaera rotundata Clarke and Verdier 1967
Sophismatia tenuivirgula (Williams and Downie 1966a) Williams et al. 2015
Spinidinium echinoideum (Cookson and Eisenack 1960a) Lentin and Williams 1976
Spiniferites ovatus Matsuoka 1983b
Spiniferites porosus (Manum and Cookson 1964) Harland 1973
Spiniferites ramosus (Ehrenberg 1838) Mantell 1854
Spiniferites scabrosus (Clarke and Verdier 1967) Lentin and Williams 1975
Spongiodinium delitiense (Ehrenberg 1838) Deflandre 1936
Tanyosphaeridium xanthiopyxides (Wetzel 1933b ex Deflandre 1937) Stover and Evitt 1978
Tenua cf. hystrix Eisenack 1958
Thalassiphora patula (Williams and Downie 1966) Stover and Evitt 1978
Thalassiphora pelagica (Eisenack 1954b) Eisenack and Gocht 1960
Trichodinium castanea Deflandre 1935 ex Clarke and Verdier 1967
Trigonopyxidia ginella (Cookson and Eisenack 1960a) Downie and Sarjeant 1965
Trithyrodinium evittii Drugg 1967
Vesperopsis longicornis Bint 1986
Xenascus Cookson and Eisenack 1969

Acritarchs

Fromea chytra (Drugg 1967) Stover and Evitt 1978

Fromea fragilis (Cookson and Eisenack 1962a) Stover and Evitt 1978

Fromea madurensis Cookson and Eisenack 1982

Micrhystridium stellatum Deflandre 1945a

Veryhachium trispinosum (Eisenack 1938a) Stockmans and Willièrè 1962a

Miospores

Aequitriradites spinulosus (Cookson and Dettmann 1958) Cookson and Dettmann 1961

Appendicisporites potomacensis Brenner 1963

Appendicisporites tricornitatus Weyland and Greifeld 1953

Aquilapollenites Rouse 1957

Aquilapollenites augustus Srivastava 1969

Boisduvalia clavitites Piel 1971

Callialasporites dampieri (Balme 1957) Dev 1961

Camarozonosporites Danzé-Corsin and Laveine 1963

Caryapollenites Raatz (1937) ex Potonié 1960

Cicatricosisporites annulatus Archangelsky and Gamarro 1966

Cicatricosisporites auritus Singh 1971

Cicatricosisporites subrotundus Brenner 1963

Corsinipollenites oculusnoctis (Thiergart 1940) Nakoman 1965

Coryluspollenites Raatz 1937

Costatoperforosporites fistulosus Deák 1962

Densoisporites Weyland and Krieger 1953

Distaltriangulisporites perplexus (Singh 1964) Singh 1971

Extratropopollenites Pflug in Thomson and Pflug 1952

Hazaria Srivastava 1971

Impardecispora apiverrucata (Couper 1958) Venkatachala et al. 1969

Laevigatisporites Dybova and Jachowicz 1957

Lycopodiumsporites Thiergart 1938 ex Delcourt and Sprumont 1955

Matonisporites Couper 1958

Matonisorites “*skolpii*”; informal species name
Momipites Wodehouse 1933
Osmundacidites Couper 1953
Osmundacidites wellmannii Couper 1953
Parvisaccites amplus Brenner 1963
Parvisaccites radiatus Couper 1958
Pinuspollenites Raatz 1938 ex Potonié 1958
Porospollenites porosus (Mchedlishvili 1961) Krutzsch 1969
Rugubivesiculites convolutus Pierce 1961
Rugubivesiculites reductus Pierce 1961
Rugubivesiculites rugosus Pierce 1961
Tiliaepollenites Potonié 1931
Tiliaepollenites crassipites (Wodehouse 1933) Fensome et al. 2016
Vitreisporites pallidus (Reissinger) Nilsson 1958
Wodehouseia spinata Stanley 1961

Others

Azolla Lamarck in Lamarck et al. 1783
Tasmanites Newton 1875
Tetraporina Naumova 1939

PLATES

The palynological plates contain the following information: Taxon name, comment (where appropriate). Depth. Curation number, slide type (where applicable).

Plate 1

Dinocysts from the North Leif I-05 well. Scale bar represents 20 microns.

1. *Adnatosphaeridium vittatum*. 2130–2140 metres. YD17-600-2.
2. *Adnatosphaeridium vittatum*. 2400–2410 metres. YD17-609-2.
3. *Adnatosphaeridium robustum*. 2220–2230 metres. YD17-603-2.
4. *Alisocysta margarita*. 2335–2345 metres. P22077-01.
5. *Alisocysta margarita*. 2335–2345 metres. P22077-01.
6. *Alisocysta margarita*. 2335–2345 metres. P22077-01.
7. *Alisocysta margarita*. 2455–2465 metres. YD17-611-2.
8. *Alisocysta margarita*. 2455–2465 metres. YD17-611-2.
9. *Alterbidinium acutulum*. 2730–2740 metres. YD17-620-2.
10. *Alterbidinium* sp. 2455–2465 metres. YD17-611-2.
11. *Apectodinium homomorphum*. 2040–2050 metres. YD17-597-2.
12. *Apectodinium parvum*. 2160–2170 metres. YD17-601-2.
13. *Areoligera gippingensis*. 2335–2345 metres. P22077-01.
14. *Areoligera gippingensis*. 2335–2345 metres. P22077-01.
15. *Areoligera gippingensis*. 2335–2345 metres. P22077-01.
16. *Areoligera gippingensis*. 2340–2350 metres. YD17-607-2.
17. *Areoligera gippingensis*. 2340–2350 metres. YD17-607-2.
18. *Axiodinium augustum*. 2250–2260 metres. YD17-604-2.
19. *Caligodinium aceras*. 2730–2740 metres. YD17-602-2.
20. *Cerbia* cf. *tabulata*. 2700–2710 metres. YD17-619-2.

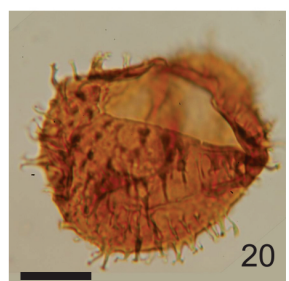
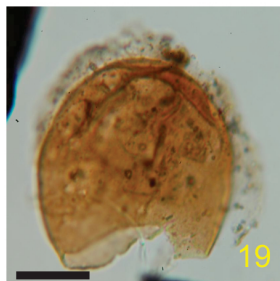
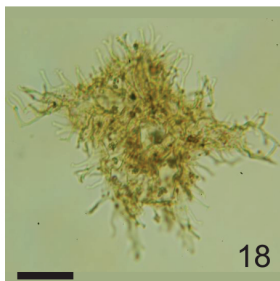
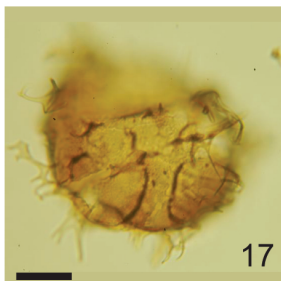
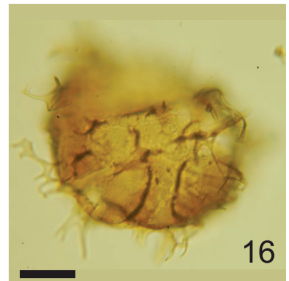
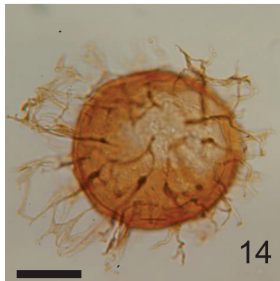
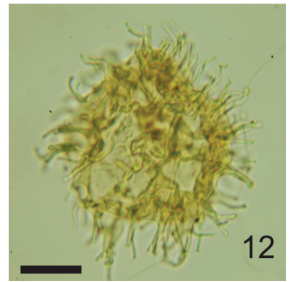
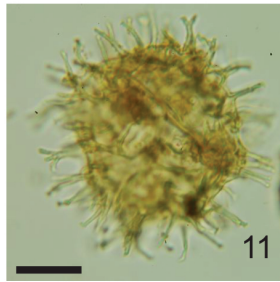
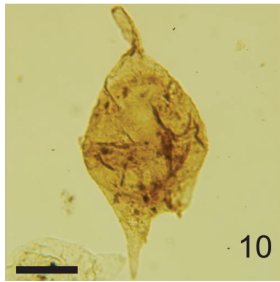
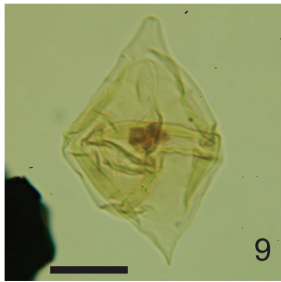
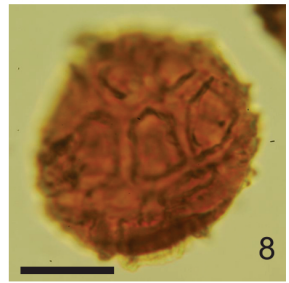
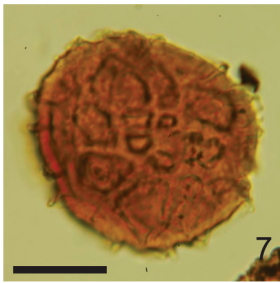
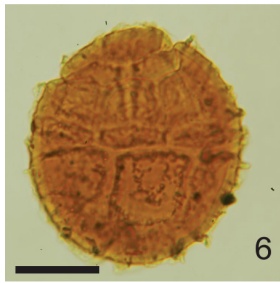
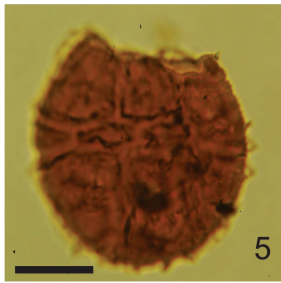
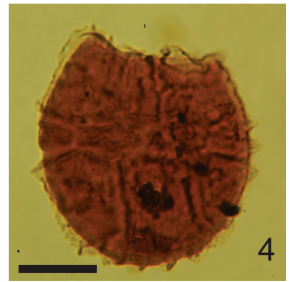
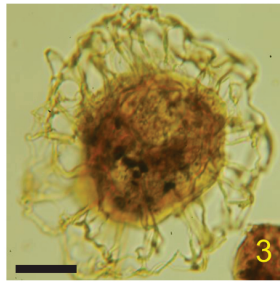
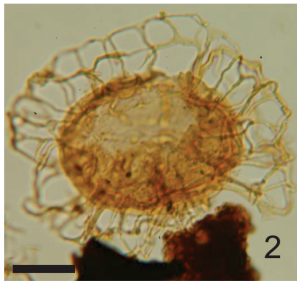


Plate 2

Dinocysts from the North Leif I-05 well. Scale bar represents 20 microns.

1. *Cerbia* cf. *tabulata*. 2700–2710 metres. YD17-619-2.
2. *Impagidinium* sp. 2700–2710 metres. YD17-619-2.
3. *Cerebrocysta bartonensis*. 1800–1810 metres. YD17-589-2.
4. *Cerebrocysta* sp. 2010–2200 metres. YD17-596-2.
5. *Cerodinium diebelii*. 2700–2710 metres. YD-619-2.
6. *Cerodinium speciosum*. 2580–2590 metres. YD17-615-2.
7. *Cerodinium striatum*. 2520–2530 metres. YD17-613-2.
8. *Cleistosphaeridium elegantulum*. 1885–1895 metres. P22066-01.
9. *Cometodinium* sp. 2730–2740 metres. P22087-01.
10. *Cometodinium* sp. 2730–2740 metres. P22087-01.
11. *Operculodinium* sp. 2535–2545 metres. P22082-01.
12. *Corrudinium* sp. 600–610 metres. YD17-549-2.
13. *Corrudinium* sp. 600–610 metres. YD17-549-2.
14. *Cribroperidinium* cf. *orthoceras*. 430–440 metres. P22029-01.
15. *Cribroperidinium* sp. 2445–2455 metres. P22080-01.
16. *Tenua hystrix*. 2930–2940 metres. P22092-01.
17. *Cyclonephelium compactum*. 2930–2940 metres. P22092-01.
18. *Cyclonephelium vannophorum* of Williams. 3390–3400 metres. YD17-642-2.
19. *Danea californica*. 2520–2530 metres. YD17-613-2.
20. *Deflandrea oebisfeldensis*. 2520–2530 metres. YD17-613-2.

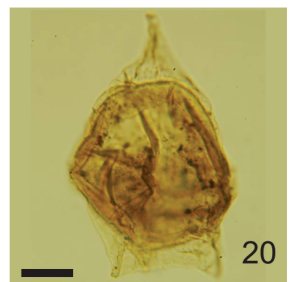
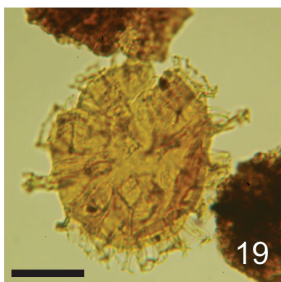
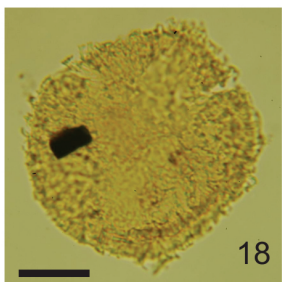
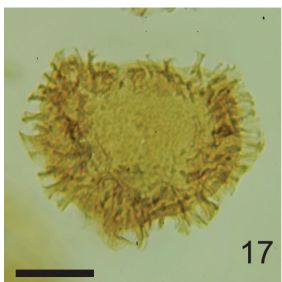
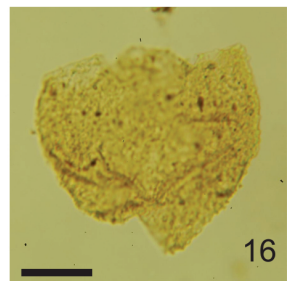
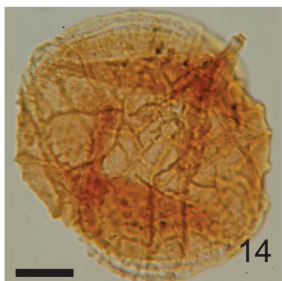
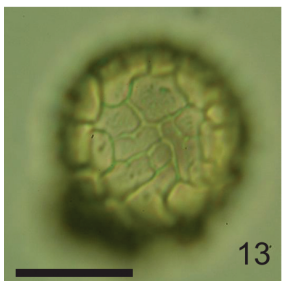
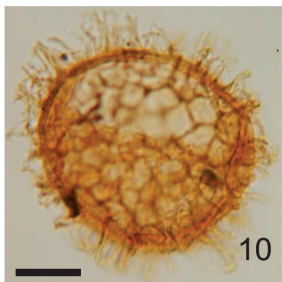
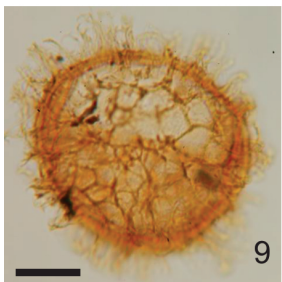
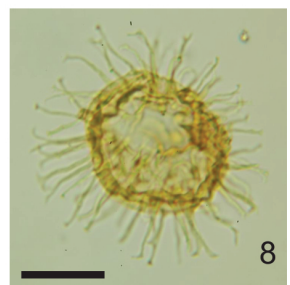
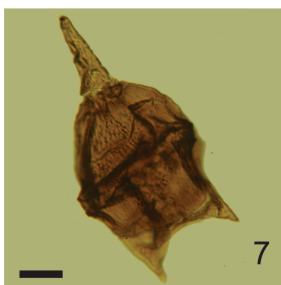
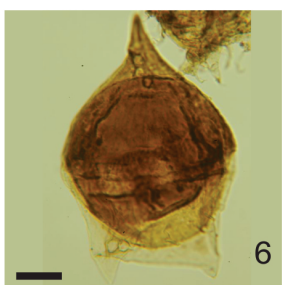
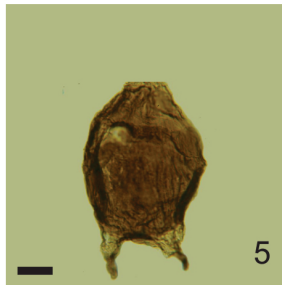
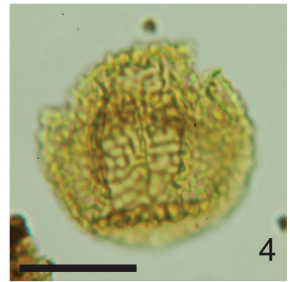
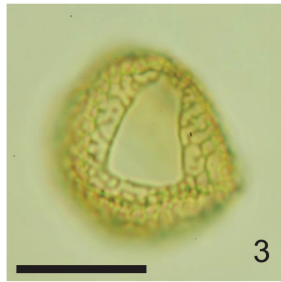
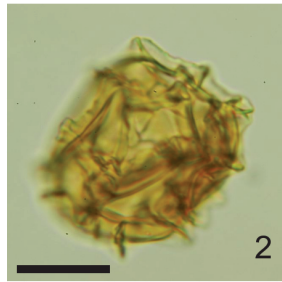
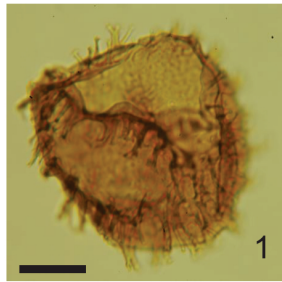


Plate 3

Dinocysts from the North Leif I-05 well. Scale bar represents 20 microns.

1. *Deflandrea phosphoritica*. 1710–1720 metres. YD17-586-2.
2. *Deflandrea* sp. B sensu Williams and Bujak 1977. 1890–1900 metres. YD17-592-2
3. *Deflandrea* sp. B sensu Williams and Bujak 1977. 1980–1990 metres. YD17-595-2.
4. *Deflandrea* sp. 2190–2200 metres. YD17-602-2.
5. *Deflandrea* sp. 2580–2590 metres. YD17-615-2.
6. *Deflandrea wetzelii*. 2175–2185 metres. P22073-01.
7. *Diphyes brevispinum*. 2010–2020 metres. YD17-596-2.
8. *Disphaerogena* sp. 2535–2545 metres. P22082-01.
9. *Elytrocysta* sp. 1560–1570 metres. YD17-581-2.
10. *Enneadocysta* “annulus”. 2130–2140 metres. YD17-600-2.
11. *Enneadocysta* cf. *arcuata*. 2130–2140 metres. YD17-600-2.
12. *Evittosphaerula* sp. 2190–2200 metres. YD17-602-2.
13. *Glaphyrocysta exuberans*. 2430–2440 metres. YD17-610-2.
14. *Glaphyrocysta pastielsii*. 1530–1540 metres. YD17-580-2.
15. *Glaphyrocysta* cf. *vicina*. 1895–1905 metres. P22066-01.
16. *Heterosphaeridium bellii*. 2730–2740 metres. P22087-01.
17. *Hystrichodinium pulchrum*. 2730–2740 metres. P22087-01.
18. *Hystrichokolpoma globulus*. 2370–2380 metres. YD17-608-2.
19. *Hystrichokolpoma globulus*. 2370–2380 metres. YD17-608-2.
20. *Hystrichosphaeridium* “complex”. 2550–2560 metres. YD17-614-2.

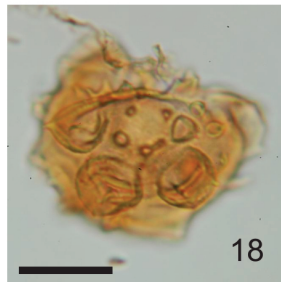
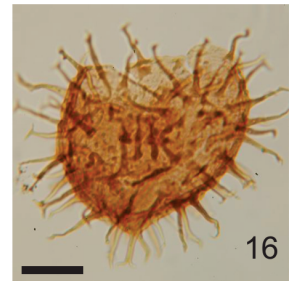
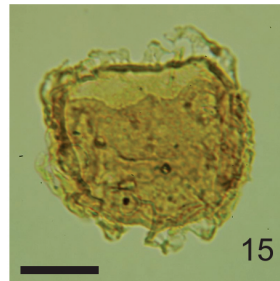
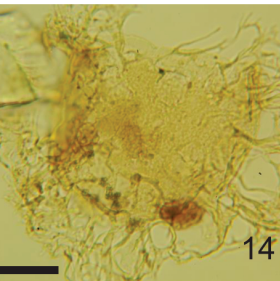
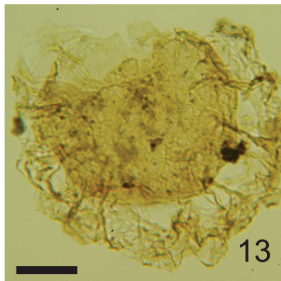
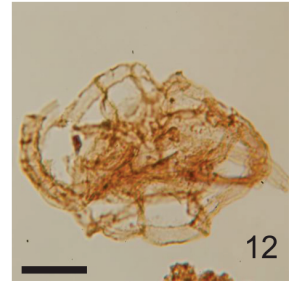
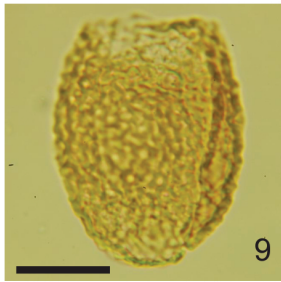
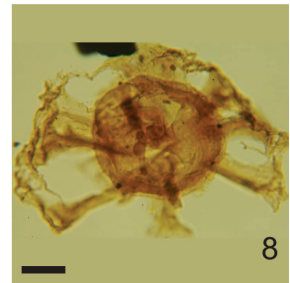
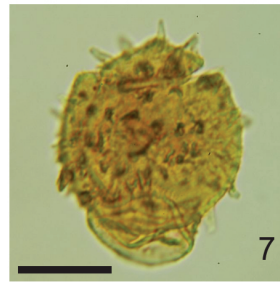
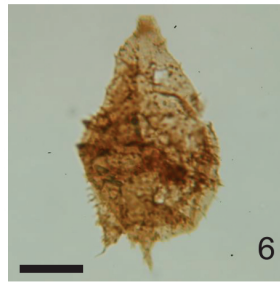
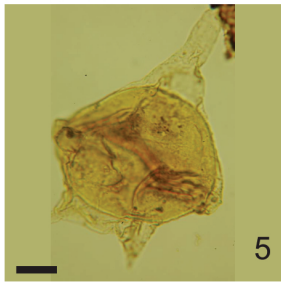
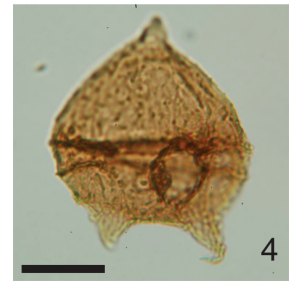


Plate 4

Dinocysts from the North Leif I-05 well. Scale bar represents 20 microns.

1. *Hystrichosphaeridium* “*pulcherrimum*”. 2520–2530 metres. YD17-613-2.
2. *Hystrichosphaeridium tubiferum*. 2400–2410 metres. YD17-609-2.
3. *Hystrichosphaeridium tubiferum*. 2400–2410 metres. YD17-609-2.
4. *Hystrichosphaeridium tubiferum*. 2400–2410 metres. YD17-609-2
5. *Hystrichosphaeridium tubiferum* var. “*perforatum*”. 2580–2590 metres. YD17-615-2.
6. *Hystrichosphaeropsis perforata*. 2580–2590 metres. P22083-01.
7. *Impagidinium* cf. *victorianum*. 2610–2620 metres. YD17-612-2.
8. *Impagidinium* cf. *victorianum*. 2610–2620 metres. YD17-612-2.
9. *Impletosphaeridium apodastum*. 2455–2465 metres. YD17-611-2.
10. *Impletosphaeridium apodastum*. 2520-2530 metres. YD17-613-2.
11. *Isabelidinium cooksoniae*. 2730–2740 metres. P22087-01.
12. *Isabelidinium cretaceum*. 2650–2660 metres. P22085-01.
13. *Isabelidinium majae*. 2535–2545 metres. P22082-01.
14. *Kleithriasphaeridium cooksoniae*. 3010–3020 metres. P22094-01.
15. *Lejeunecysta* sp. 2040–2050 metres. YD17-597-2.
16. *Microdinium saeptum*. 2700–2710 metres. YD17-619-2.
17. *Minisphaeridium latirictum*. 2190–2200 metres. YD17-602-2.
18. *Nyktericysta davisii*. 2970–2980 metres. P22093-01.
19. *Odontochitina costata*. 2730–2740 metres. P22087-01.
20. *Oligosphaeridium dictyophorum*. 2610–2620 metres. YD17-616-2.

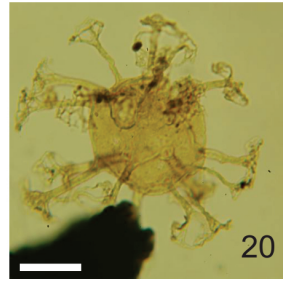
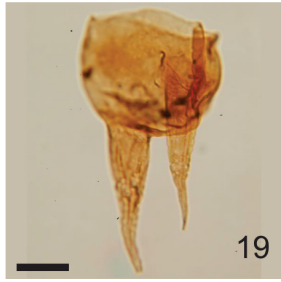
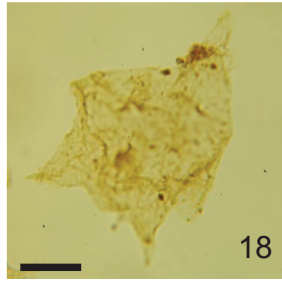
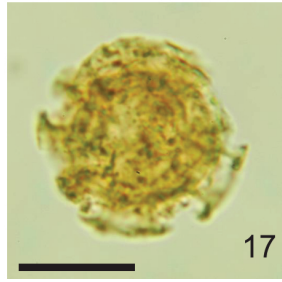
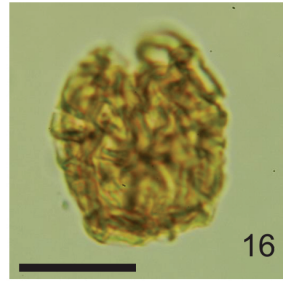
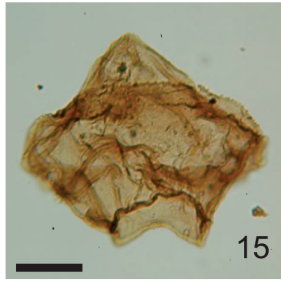
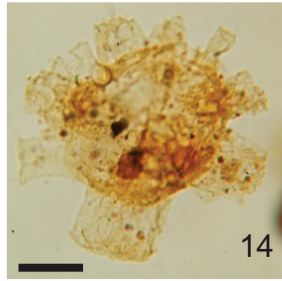
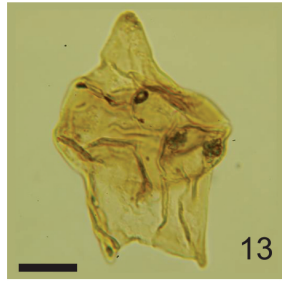
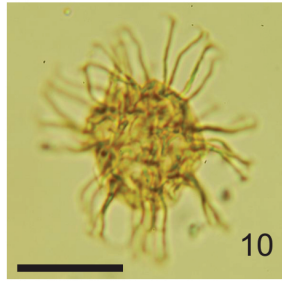
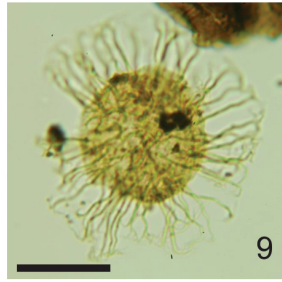
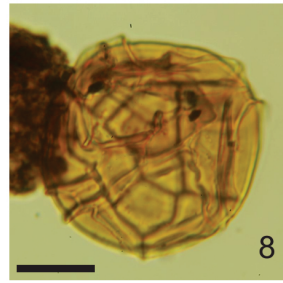
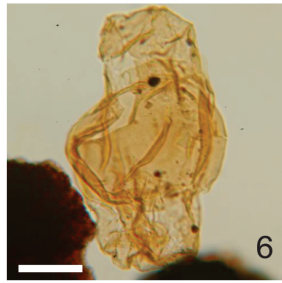
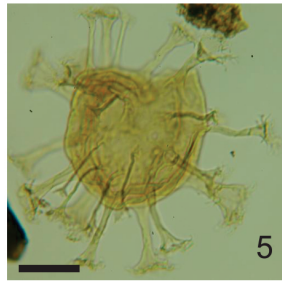
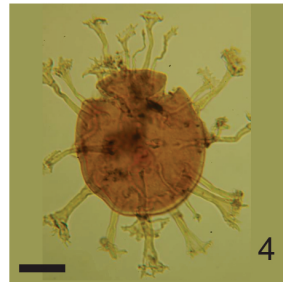


Plate 5

Dinocysts and an acritarch from the North Leif I-05 well. Scale bar represents 20 microns.

1. *Oligosphaeridium pulcherrimum*. 2700–2710 metres. YD17-619-2.
2. *Plaeocystodinium lidiae*. 2370–2380 metres. YD17-608-2.
3. *Palaeocystodinium* sp. 2455–2465 metres. YD17-611-2.
4. *Palaeoperidinium pyrophorum*. 2430–2440 metres. YD17-610-2.
5. *Palynodinium grallator*. 2580–2590 metres. YD17-615-2.
6. *Palynodinium grallator*. 2580–2590 metres. YD17-615-2.
7. *Pervosphaeridium* sp. 2175–2185 metres. P22073-01.
8. *Petalodinium condylos*. 2130–2140 metres. YD17-600-2.
9. *Petalodinium condylos*. 2130–2140 metres. YD17-600-2.
10. *Phelodinium kozlowskii*. 2400–2410 metres. YD17-609-2.
11. *Phelodinium kozlowskii*. 2520–2530 metres. YD17-613-2.
12. *Phthanoperidinium* “*hibernium*”. 1170–1180 metres. YD17-568-2.
13. *Rottnestia* sp. 2455–2465 metres. YD17-611-2.
14. *Rottnestia* sp. 2455–2465 metres. YD17-611-2.
15. *Schematophora speciosa*. 1745–1755 metres. P22062-01.
16. *Schematophora speciosa*. 1745–1755 metres. P22062-01.
17. *Schizocystia* sp., acritarch. 840–850 metres. YD17-557-2.
18. *Senoniasphaera microreticulata*. 2880–2890 metres. YD17-625-2.
19. *Spinidinium echinoideum*. 2430–2440 metres. YD17-610-2.
20. *Spiniferites scabrosus*. 2650–2660 metres. P22085-01.

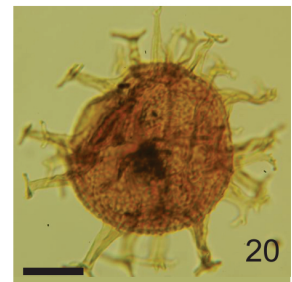
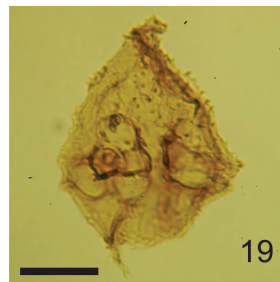
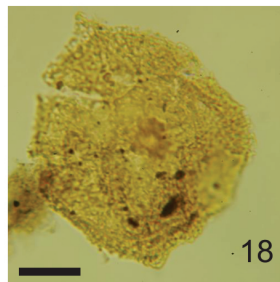
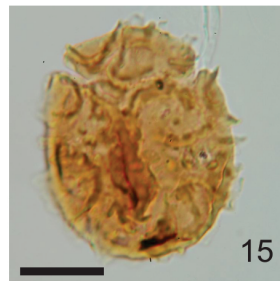
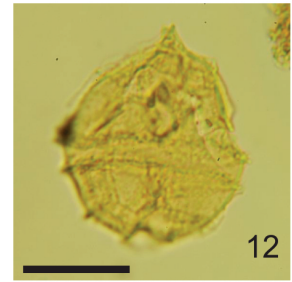
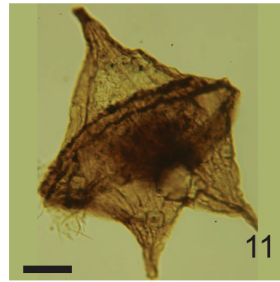
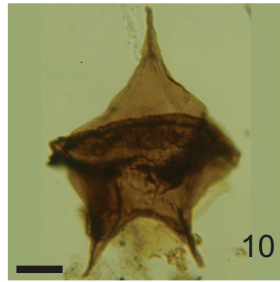
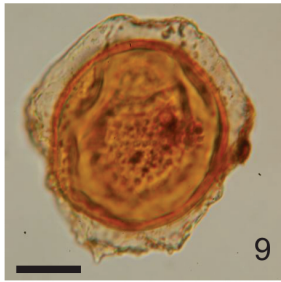
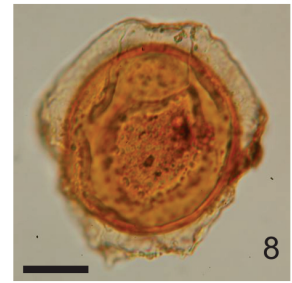
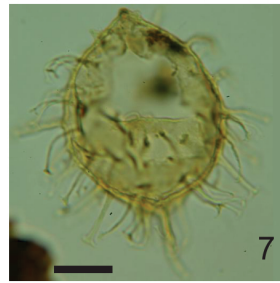
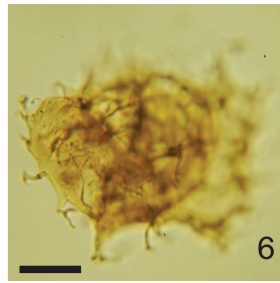
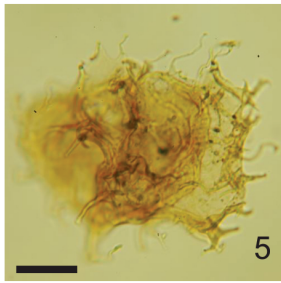
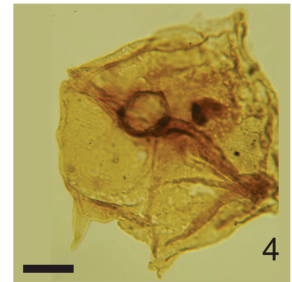
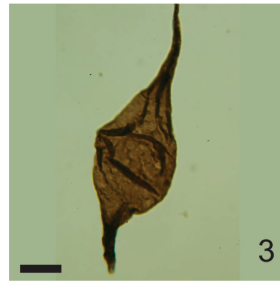


Plate 6

Dinocysts, algae and miospores from the North Leif I-05 well. Scale bar represents 20 microns.

1. *Spiniferites speciosus*. 3420–3430 metres. YD17-643-2.
2. *Spongodinium delitiense*, optical section. 2650–2660 metres. P22085-01.
3. *Spongodinium delitiense*, dorsal surface. 2650–2660 metres. P22085-01.
4. *Surculosphaeridium longifurcatum*. 2730–2740 metres. P22087-01.
5. *Trithyrodinium conservatum*. 1800–1810 metres. YD17-589-2.
6. *Trithyrodinium suspectum*. 2535–2545 metres. P22082-01.
7. *Trithyrodinium suspectum*. 2610–2620 metres. P22084-01
8. *Trithyrodinium suspectum*. 2610–2620 metres. YD17-616-2.
9. *Cometodinium whitei*. 2730–2740 metres. P22087-01.
10. *Paralecaniella indentata*. 1350–1360 metres. YD17-574-2.
11. *Tritonites inaequalis*. 1530–1540 metres. YD17-580-2.
12. *Aequitriradites spinulosus*. 3370–3380 metres. P22103-01.
13. *Appendicisporites bilateralis*. 3390–3400 metres. YD17-642-3.
14. *Appendicisporites potomacensis*, proximal view. 2850–2860 metres. P22090-01.
15. *Appendicisporites potomacensis*, distal view. 2850–2860 metres. P22090-01.
16. *Cicatricosisporites hallei*. 3335–3345 metres. P22102-01.
17. *Cicatricosisporites pseudotripartitus*. 3115 metres, conventional core. P50318 +30 μm .
18. *Cingutriletes clavus*. 2550–2560 metres. YD17-614-2.
19. *Coronatispora valdensis*. 3450–3460 metres. YD17-644-2.
20. *Costatoperforosporites foveolatus*. 3170–3180 metres. P22098-01.

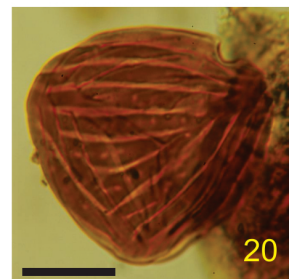
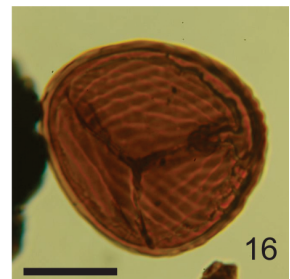
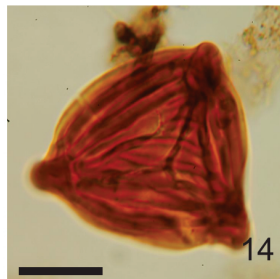
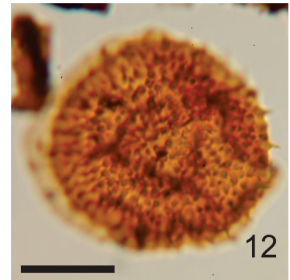
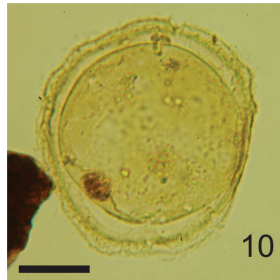
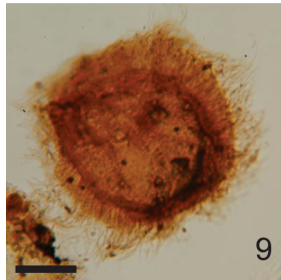
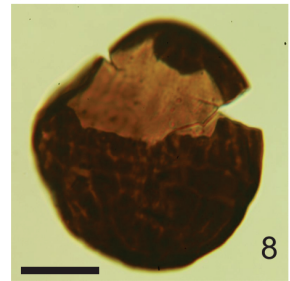
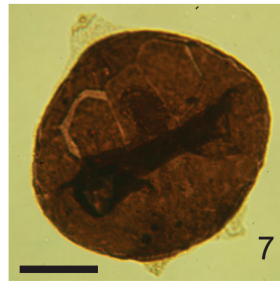
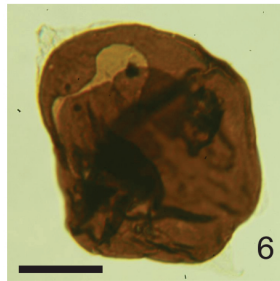
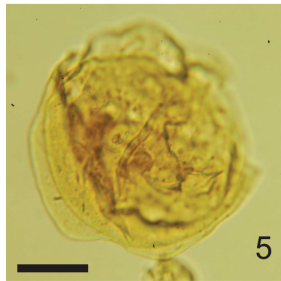
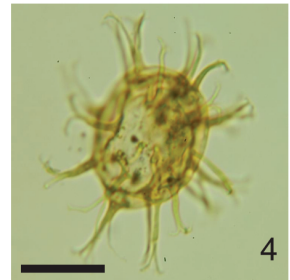
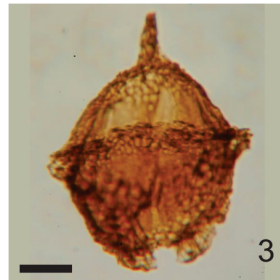
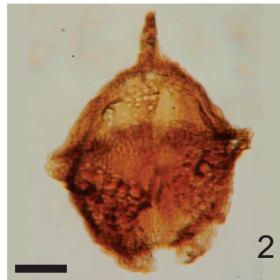
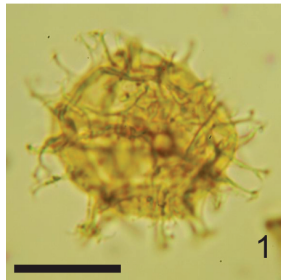


Plate 7

Miospores from the North Leif I-05 well. Scale bar represents 20 microns.

1. *Distaltriangulisporites perplexus*. 3110 metres. P50316, +30 μm .
2. *Foveotriletes* sp. 3090–3100 metres. P22096-01.
3. *Impardecispora?* cf. *apiverrucata*. 870–880 metres. YD17-558-2.
4. *Impardecispora?* cf. *apiverrucata*. 3500–3507 metres. P22107-01.
5. *Corsinopollenites oculusnoctis*. 720–730 metres. YD17-553-2.
6. *Eucommiidites troedsonii*. 3111.05 metres, conventional core. P50315, UN.
7. *Extratropipollenites* sp. 1440–1450 metres. YD17-577-2.
8. *Trudopollis* sp. 2250–2260 metres. YD17-604-2.
9. *Juglanspollenites* sp. 480–490 metres. YD17-545-2.
10. *Mancicorpus canadianus*. 1230–1240 metres. YD17-570-2.
11. *Parvisaccites amplus*. 3110.0 metres, conventional core. P50316, +30 μm .
12. *Parvisaccites amplus*. 3410–3420 metres, P22104-01.
13. *Parvisaccites radiatus*. 2790–2800 metres. YD17-622-2.
14. *Rugubivesiculites rugosus*. 3110.0, conventional core. P50316, +30 μm .
15. *Rugubivesiculites rugosus*. 3112.55 metres, conventional core. P50314, +30 μm .
16. *Rugubivesiculites rugosus*. 3295–3305 metres. P22101-01.
17. *Rugubivesiculites rugosus*. 3295–3305 metres. P22101-01.
18. *Tiliaepollenites crassipites*. 450–460 metres. YD17-544-2.
19. *Tiliaepollenites crassipites*. 450–460 metres. YD17-544-2.
20. *Tripurites* sp. 720–730 metres. YD17-555-2.

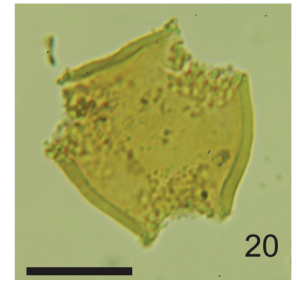
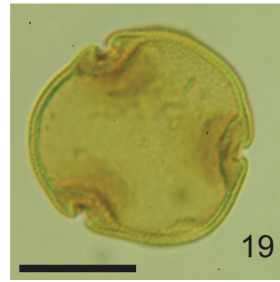
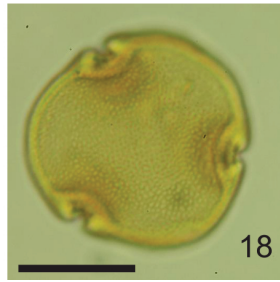
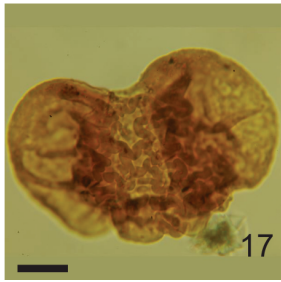
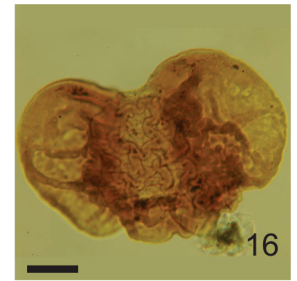
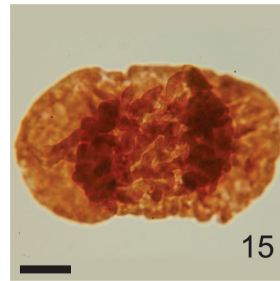
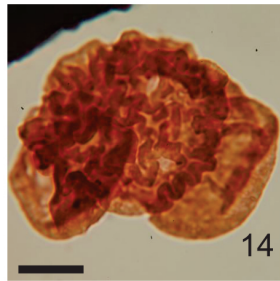
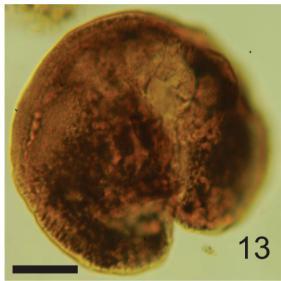
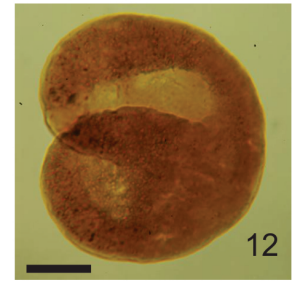
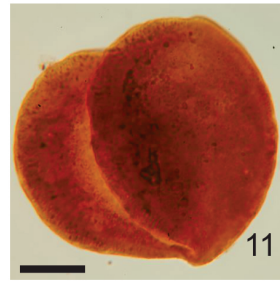
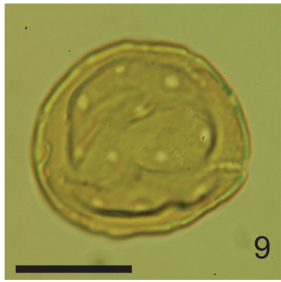
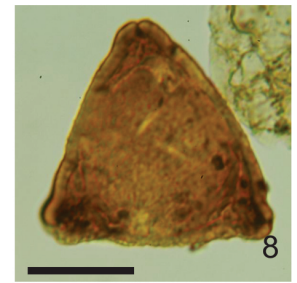
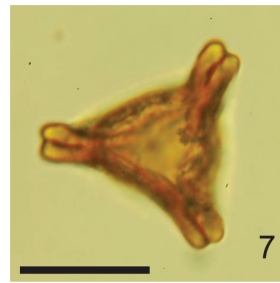
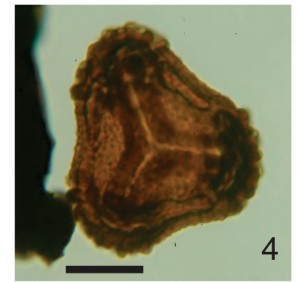
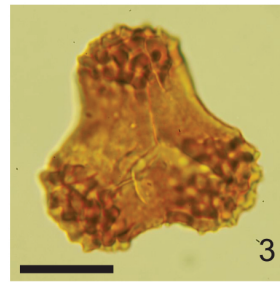
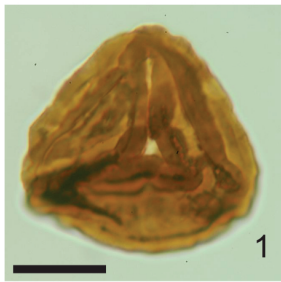


Plate 8

Miospores and other palynomorphs from the North Leif I-05 well. Scale bar represents 20 microns.

1. *Triprojectus attenuatus*. 1500–1510 metres. YD17-579-2.
2. *Triprojectus attenuatus*. 1560–1570 metres. YD17-581-2.
3. *Triprojectus attenuatus*. 1560–1570 metres. YD17-581-2.
4. *Fractisporonites*. 1710–1720 metres. YD17-586-2.
5. Root hair. 3010–3020 metres. P22094-01.
6. Incertae sedis. 810–820 metres. YD17-556-2.
7. Incertae sedis. 810–820 metres. YD17-556-2.

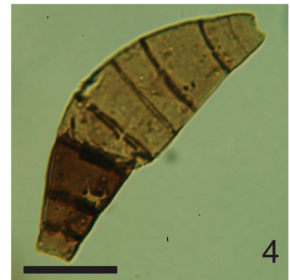
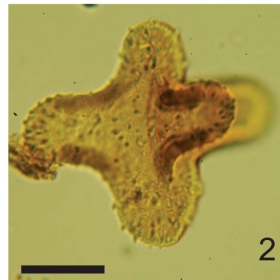
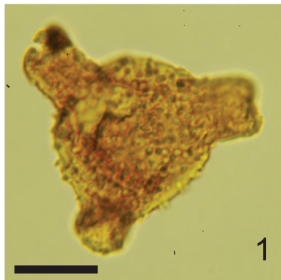


Plate 9

Dinocysts from the Skolp E-07 well. Scale bar represents 20 microns.

1. *Achomosphaera* sp. 1080–1085 metres. P50018, +30 μm .
2. *Alisogymnium* sp. 1980–1985 metres. P50054, +30 μm .
3. *Alisogymnium* sp. 2040–2045 metres. P50057, +30 μm .
4. *Isabelidinium acuminatum* sensu Ioannides 1986. 1470–1475 metres. P50031, +30 μm .
5. *Aterbidinium acutulum*. 1590–1595 metres. P50035, +30 μm .
6. *Alterbidinium acutulum*. 2340–2345 metres. P50067, UN.
7. *Alterbidinium biaperturatum*. 1260–1265 metres. P50024, +30 μm .
8. *Alterbidinium biaperturatum*. 1320–1325 metres. P50026, +30 μm .
9. *Alterbidinium majae*. 540–545 metres. P50000, +30 μm .
10. *Alterbidinium minor*. 1110–1115 metres. P50019, UN.
11. *Alterbidinium minor*. 1380–1385 metres. P50028, UN.
12. *Alterbidinium* “*obscurum*”. 990–995 metres. P50015, +30 μm .
13. *Alterbidinium* “*obscurum*”. 1200–1205 metres. P50022, +30 μm .
14. *Alterbidinium* “*skolpense*”. 1080–1085 metres. P50018, +30 μm .
15. *Alterbidinium* cf. *acutulum*. 780–785 metres. P50008, UN.
16. *Alterbidinium* cf. *acutulum*. 780–785 metres. P50008, +30 μm .
17. *Alterbidinium* sp. 780–785 metres. P50008, +30 μm .
18. *Alterbidinium* sp. 1110–1115 metres. P50019, +30 μm .
19. *Isabelidinium cretaceum*. 1110–1115 metres. P50019, +30 μm .
20. *Alterbidinium* cf. “*obscurum*”. 1140–1145 metres. P50024, +30 μm .

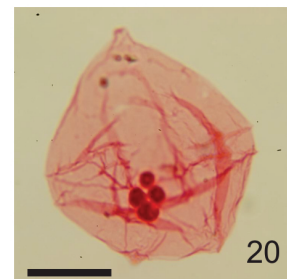
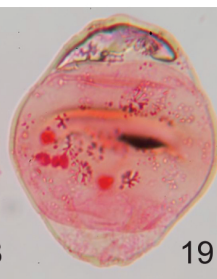
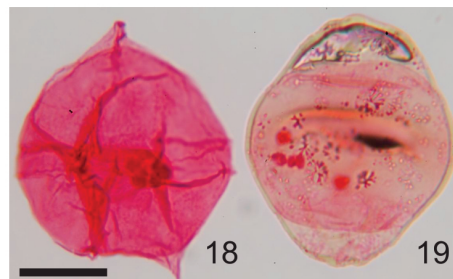
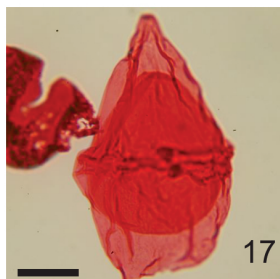
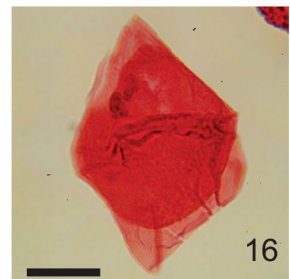
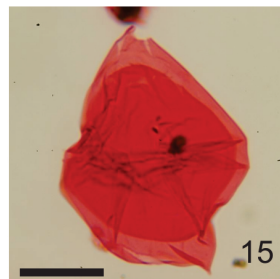
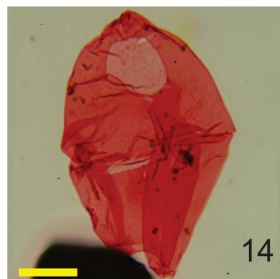
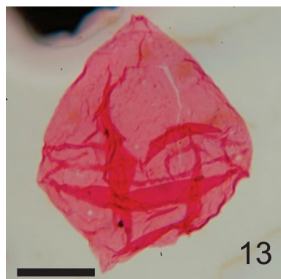
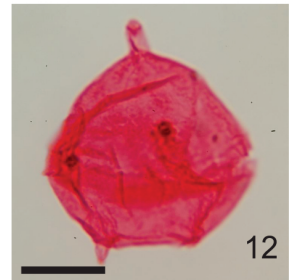
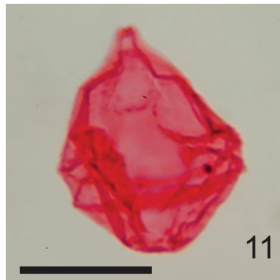
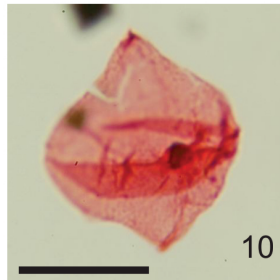
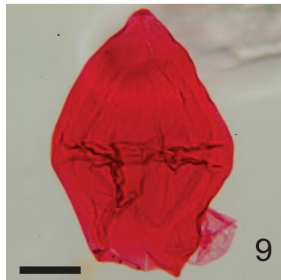
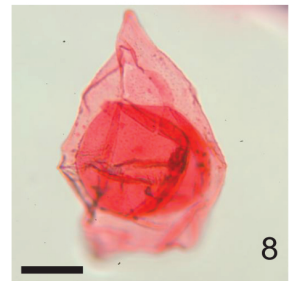
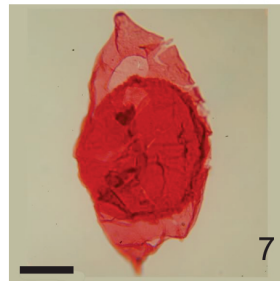
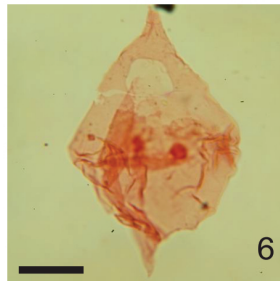
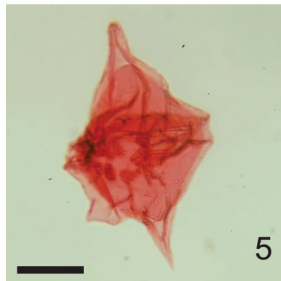
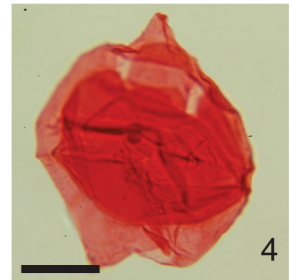
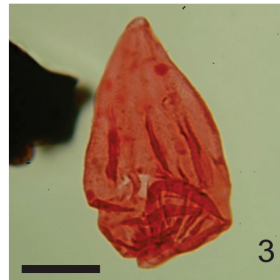
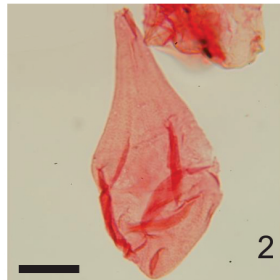
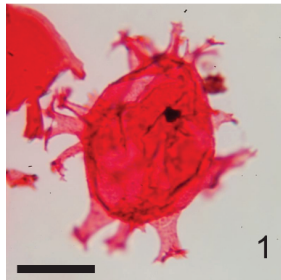


Plate 10

Dinocysts from the Skolp E-07 well. Scale bar represents 20 microns.

1. *Alterbidinium* sp. 1170–1175 metres. P50021, +30 μm .
2. *Alterbidinium* sp. 1230–1235 metres. P50023, UN.
3. *Alterbidinium* “*rotundum*”. 1650–1655 metres. P50037, +30 μm .
4. *Alterbidinium* sp. 1875–1880 metres. P50047, +30 μm .
5. *Alterbidinium* sp. 1905–1910 metres. P50049, +30 μm .
6. *Areoligera medusettiformis*, ventral surface. 1410–1415 metres. P50029, +30 μm .
7. *Areoligera medusettiformis*, dorsal surface. 1410–1415 metres. P50029, +30 μm .
8. *Batioladinium jaegeri*. 2140–2145 metres. P50060, +30 μm .
9. *Batioladinium jaegeri*. 2185–2190 metres. P50062, UN.
10. *Callaiosphaeridium asymmetricum*. 1950–1955 metres. P50052, +30 μm .
11. *Circulodinium* sp. 1260–1265 metres. P50024, +30 μm .
12. *Circulodinium* sp. 2225–2230 metres. P50063, +30 μm .
13. *Aptea* sp. 1710–1715 metres. P50039, +30 μm .
14. *Cerodinium galeota*. 1020–1025 metres. P50016, +30 μm .
15. *Cerodinium kangiliense*. 990–995 metres. P50015, +30 μm .
16. *Cerodinium striatum*. 1020–1025 metres. P50016, UN.
17. *Chatangiella amphiata*. 1740–1745 metres. P50040, +30 μm .
18. *Chatangiella madura*. 1740–1745 metres. P50040, +30 μm .
19. *Chatangiella madura*. 1845–1850 metres. P50045, +30 μm .
20. *Chatangiella verrucosa*. 1590–1695 metres. P50035, +30 μm .

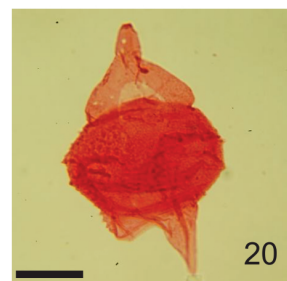
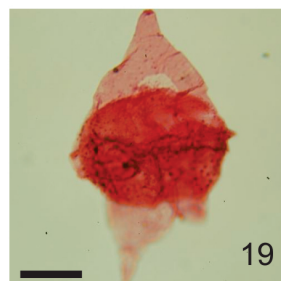
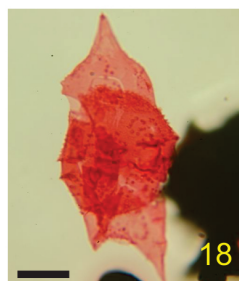
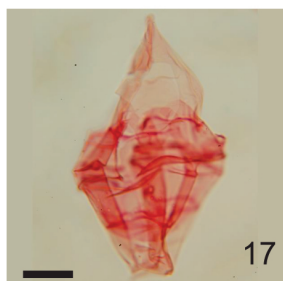
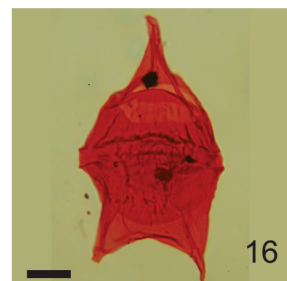
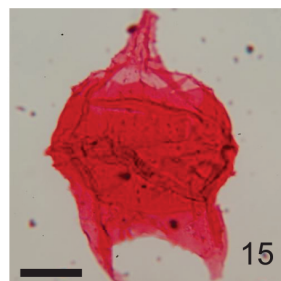
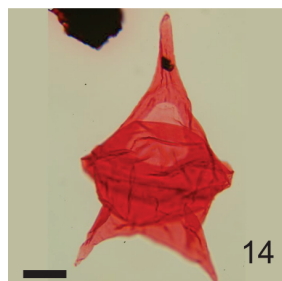
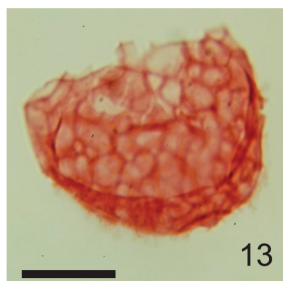
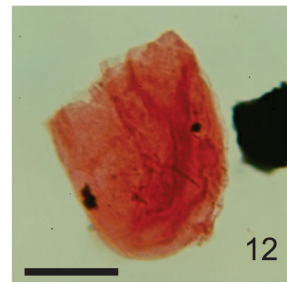
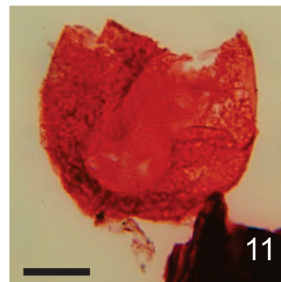
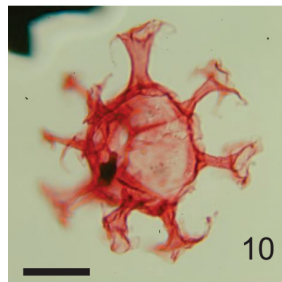
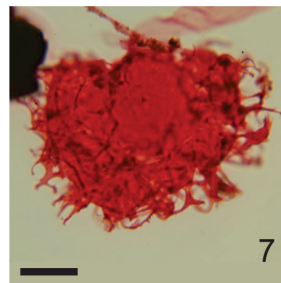
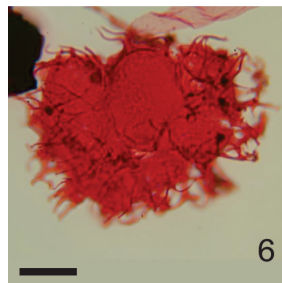
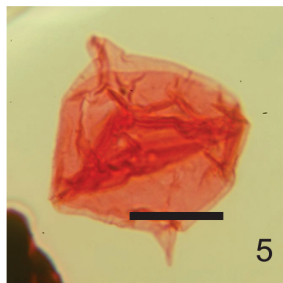
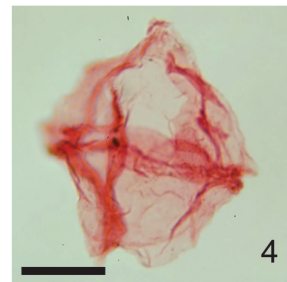
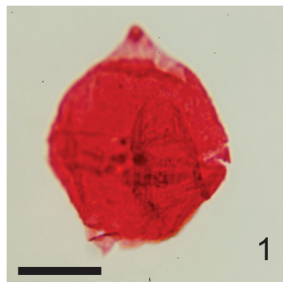


Plate 11

Dinocysts from the Skolp E-07 well. Scale bar represents 20 microns.

1. *Chatangiella verrucosa*. 1710–1715 metres. P50039, +30 μm .
2. *Chatangiella*, with deltaform archeopyle. 1935–1940 metres. P50051, +30 μm .
3. *Chlamydophorella nyei*. 1710–1715 metres. P50039, +30 μm .
4. *Chlamydophorella nyei*. 1845–1850 metres. P50045, +30 μm .
5. *Chlamydophorella* sp. 2040–2045 metres. P50057, +30 μm .
6. *Chlamydophorella nyei*. 2250–2255 metres. P50064, UN.
7. *Downiesphaeridium?* *aciculare*. 2040–2035 metres. P50057, + 30 μm .
8. *Downiesphaeridium?* *aciculare*. 2400–2405 metres. P50069, +30 μm .
9. *Cometodinium whitei*. 1905–1910 metres. P50049, +30 μm .
10. *Coronifera oceanica* 1830–1835 metres. P50044, +30 μm .
11. *Cleistosphaeridium* cf. *placacanthum* sp. 900–905 metres. P50012, UN.
12. *Cribooperidinium* sp., ventral surface. 2010–2015 metres. P50056, UN.
13. *Cyclonephelium* sp. 1140–1145 metres. P50020, +30 μm .
14. *Dapsilidinium simplex*. 1200–1205 metres. P50022, +30 μm .
15. *Dapsilidinium* sp. 1230–1235 metres. P50023, +30 μm .
16. *Deflandrea* sp. B Williams and Bujak 1977, 870–875 metres. P50011, +30 μm .
17. *Trigonopyxidia ginella*. 1890–1895 metres. P50048, +30 μm .
18. *Dinogymnium acuminatum*. 2250–2255 metres. P50064, +30 μm .
19. *Dinopterygium cladoides*. 1410–1415 metres. P50029, +30 μm .
20. *Diphyes ficusoides*. 900–905 metres. P50012, UN.

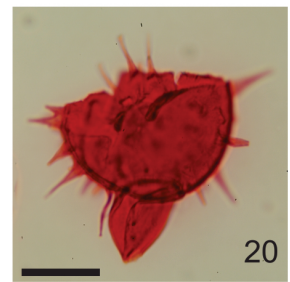
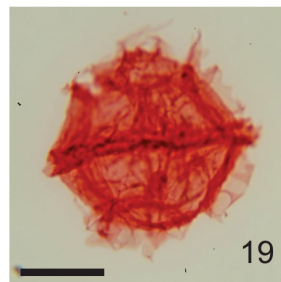
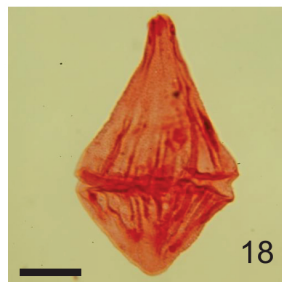
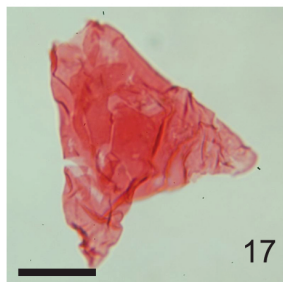
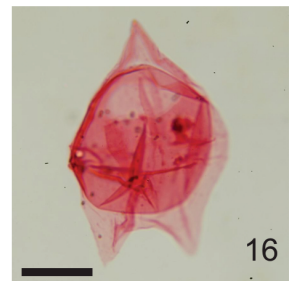
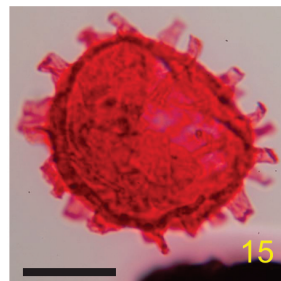
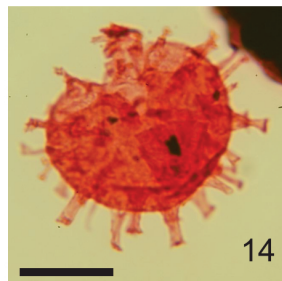
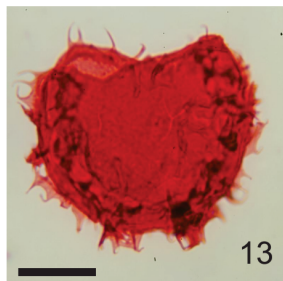
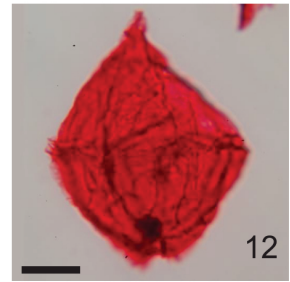
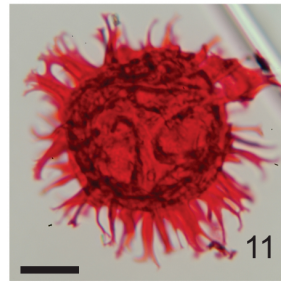
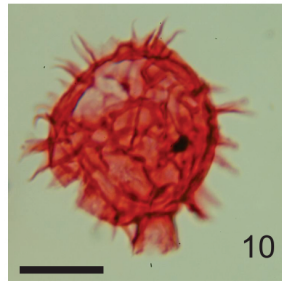
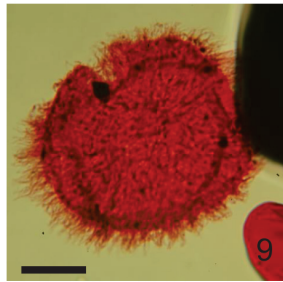
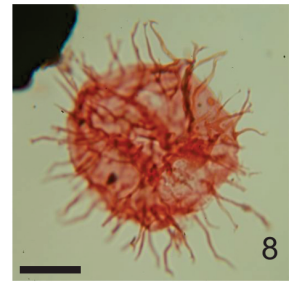
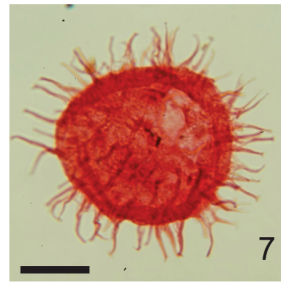
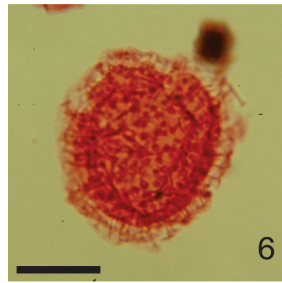
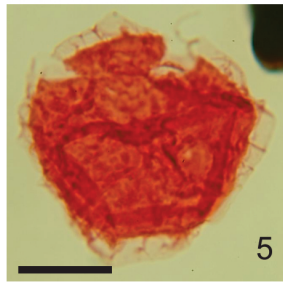
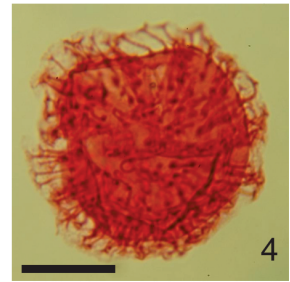
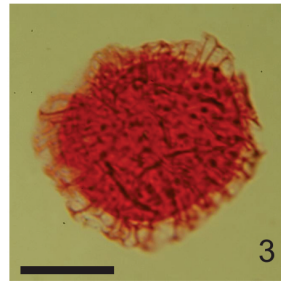
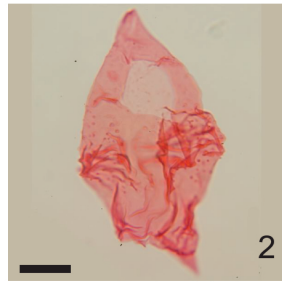
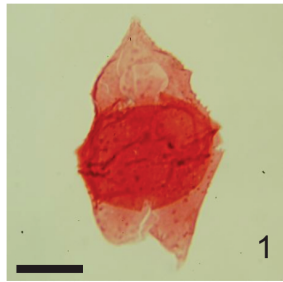


Plate 12

Dinocysts from the Skolp E-07 well. Scale bar represents 20 microns.

1. *Distatodinium* sp. 1279.35 metres, conventional core. P50335
2. *Tenua* sp. 1110–1115 metres. P50019, +30 μm .
3. *Circulodinium* sp. 1845–1850 metres. P50045, +30 μm .
4. *Druggidium* sp. 1440–1445 metres. P50030, UN.
5. *Elytrocysta druggii*. 1380–1385 metres. P50028, UN.
6. *Exochosphaeridium bifidum*. 2400–2405 metres. P50069, +30 μm .
7. *Exochosphaeridium* sp. 1530–1535 metres. P50033, +30 μm .
8. *Exochosphaeridium* sp. 1830–1835 metres. P50044, +30 μm .
9. *Fibradinium annetorpense*. 1860–1865 metres. P50046, UN.
10. *Florentinia ferox*. 1845–1850 metres. P50045, +30 μm .
11. *Gillinia hymenophora*. 1451.2 metres, conventional core. P50350, +30 μm .
12. *Gillinia hymenophora*. 1454.32 metres, conventional core. P50348.
13. *Gillinia hymenophora*. 1454.32 metres, conventional core. P50348.
14. *Gillinia* sp. 1450 metres, conventional core. P50351.
15. *Gillinia* sp. 1452.5 metres, conventional core. P50349.
16. *Gonyaulacysta eisenackii*. 2310–2315 metres. P50066, +30 μm .
17. *Heterosphaeridium bellii*. 1530–1535 metres. P50033, UN.
18. *Heterosphaeridium difficile* subsp. “*elegantulum*”. 1680–1685 metres. P50038, UN.
19. *Heterosphaeridium difficile*. 750–755 metres. P50007, +30 μm .
20. *Heterosphaeridium difficile*. 1560–1565 metres. P50034, +30 μm .

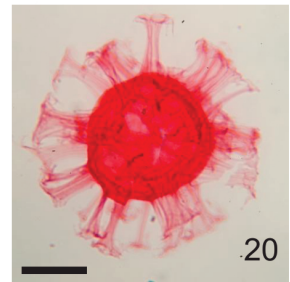
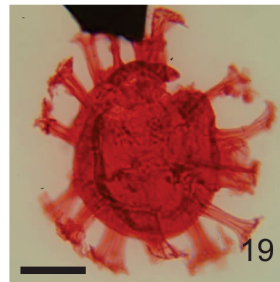
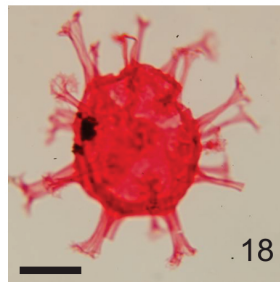
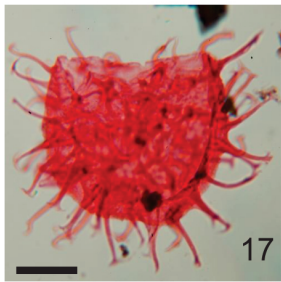
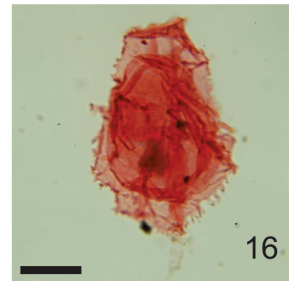
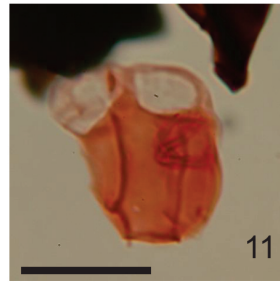
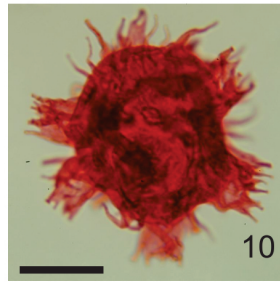
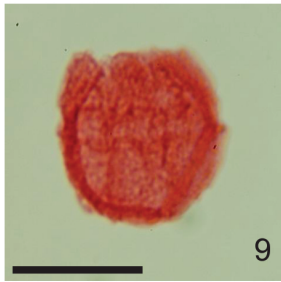
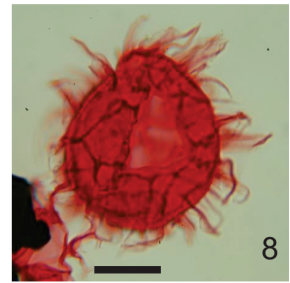
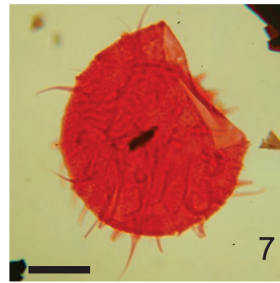
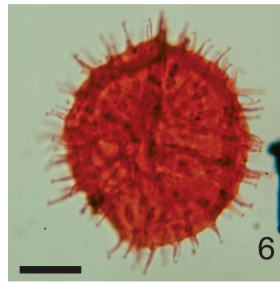
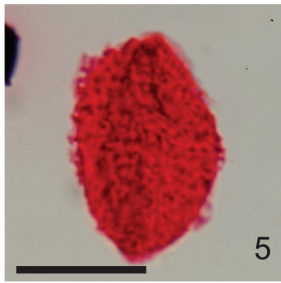
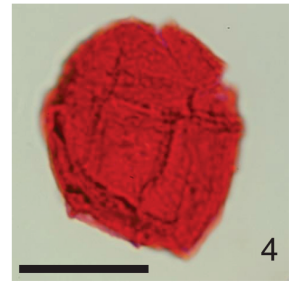
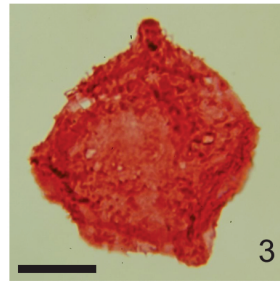
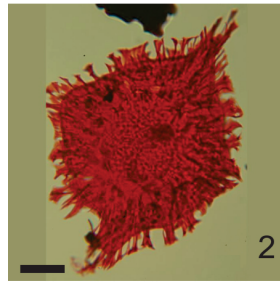


Plate 13

Dinocysts from the Skolp E-07 well. Scale bar represents 20 microns.

1. *Histiocysta palla*, lateral view. 1615–1620 metres. P50036, +30 μm .
2. *Histiocysta palla*, apical view. 1710–1715 metres. P50039, +30 μm .
3. *Hystrichosphaeridium bowerbankii*. 1320–1330 metres. P50026, +30 μm .
4. *Hystrichosphaeridium palmatum*. 2140–2145 metres. P50060, +30 μm .
5. *Hystrichosphaeridium quadratum*. 1451.2 metres, conventional core. P50350, +30 μm .
6. *Hystrichosphaeridium quadratum*. 1230–1235 metres. P50023, +30 μm .
7. *Hystrichosphaeridium* sp. 3 of McIntyre, 1974. 2040–2045 metres. P50057, +30 μm .
8. *Hystrichosphaeropsis quasricibrata*. 1470–1475 metres. P50031, +30 μm .
9. *Hystrichosphaeropsis quasricibrata*. 1590–1595 metres. P50035, +30 μm .
10. *Hystrichosphaeropsis* sp. 1860–1865 metres. P50046, +30 μm .
11. *Impagidinium* sp., dorsal surface. 1260–1265 metres. P50024, +30 μm .
12. *Impagidinium* sp., dorsal surface. 1380–1385 metres. P50028, +30 μm .
13. *Impagidinium* sp., ventral surface. 1380–1385 metres. P50028, +30 μm .
14. *Impagidinium* sp., ventral surface. 1410–1415 metres. P50029, +30 μm .
15. *Impagidinium* sp., optical section. 1410–1415 metres. P50029, +30 μm .
16. *Isabelidinium bakeri*. 1200–1205 metres. P50022, +30 μm .
17. *Isabelidinium cooksoniae*. 1170–1175 metres. P50021, +30 μm .
18. *Isabelidinium cooksoniae*. 1230–1235 metres. P50023, +30 μm .
19. *Isabelidinium cretaceum*. 1080–1085 metres. P50018, +30 μm .
20. *Isabelidinium?* “*deltacooksoniae*”. 2400–2405 metres. P50069, +30 μm .

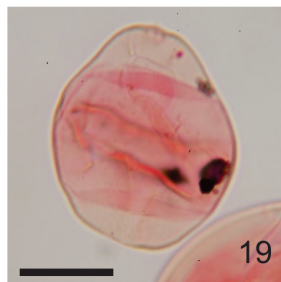
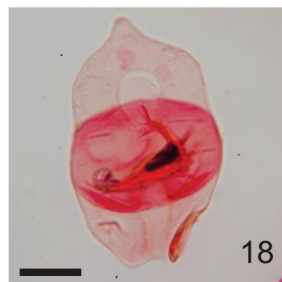
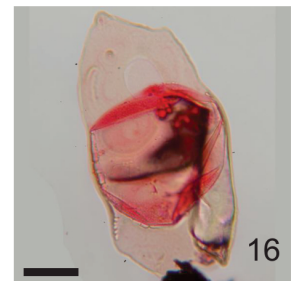
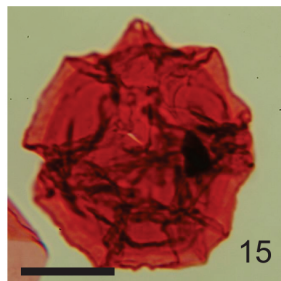
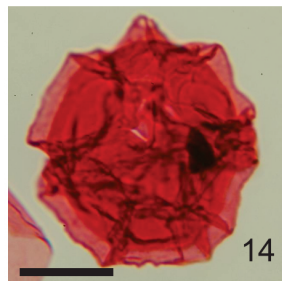
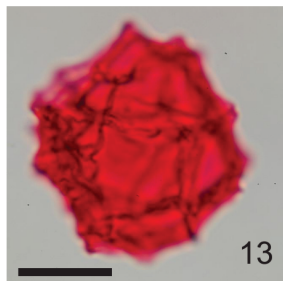
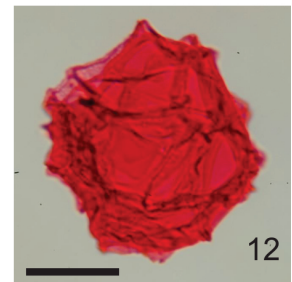
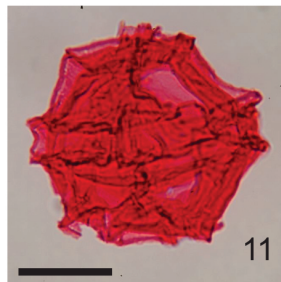
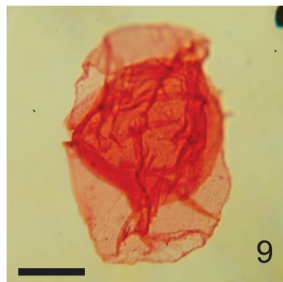
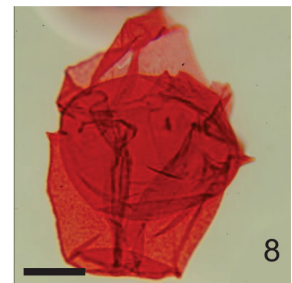
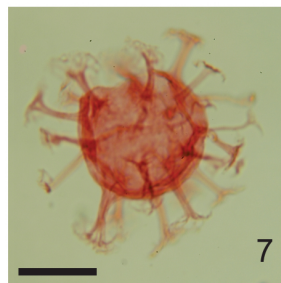
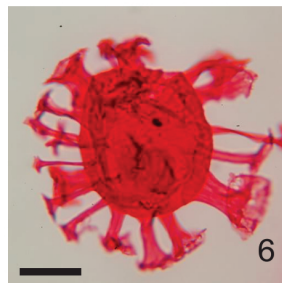
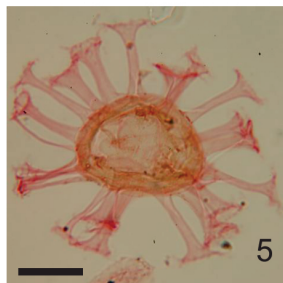
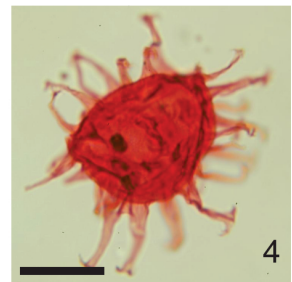
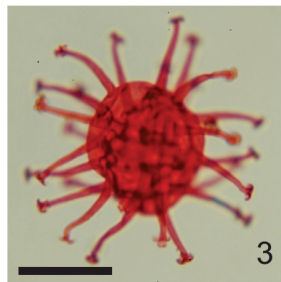
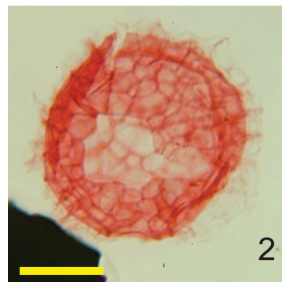
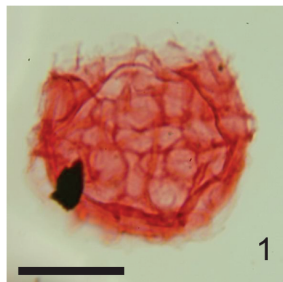


Plate 14

Dinocysts from the Skolp E-07 well. Scale bar represents 20 microns.

1. *Isabelidinium weidichii*. 1815–1825 metres. P50043, +30 μm .
2. *Kiokansium erectum*. 1260–1265 metres. P50024, +30 μm .
3. *Kiokansium polytes*. 1935–1940 metres. P50051, +30 μm .
4. *Kleithriasphaeridium loffrense*. 1590–1595 metres. P50035, +30 μm .
5. *Laciniadinium williamsii*. 1260–1265 metres. P50024, UN.
6. *Laciniadinium williamsii*. 1860–1870 metres. P50046, UN.
7. *Leberidocysta chlamydata*. 1440–1445 metres. P50030, +30 μm .
8. *Litosphaeridium* cf. *arundum*. 1650–1660 metres. P50037, +30 μm .
9. *Manumiella* sp. 630–635 metres. P50003, +30 μm .
10. *Meiourogonyaulax* sp. 1995–2000 metres. P50055, +30 μm .
11. *Membranosphaera maastrichtica*. 1530–1535 metres. P50033, UN.
12. *Membranosphaera maastrichtica*. 1287.5 metres, conventional core. P50340, UN.
13. *Microdinium mariae*. 1710–1715 metres. P50039, UN.
14. *Microdinium* cf. *ornatum*. 720–725 metres. P50006, +30 μm .
15. *Microdinium inornatum*. 1170–1175 metres. P50021, +30 μm .
16. *Microdinium* cf. *pauciscabrosum*. 1380–1390 metres. P50028, UN.
17. *Microdinium* cf. *pauciscabrosum*. 1500–1505 metres. P50032, UN.
18. *Microdinium* sp. A sensu Ioannides 1986. 1500–1505 metres. P50032, UN.
19. *Nyktericysta* sp. 630–635 metres. P50003, UN.
20. *Odontochitina costata*, operculum. 1830–1835 metres. P50044, UN.

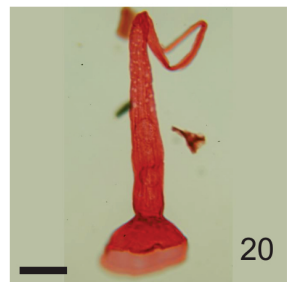
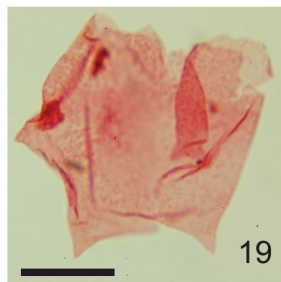
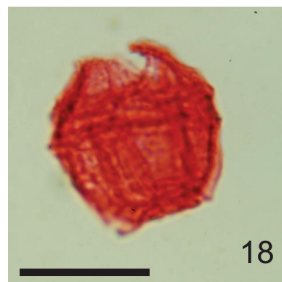
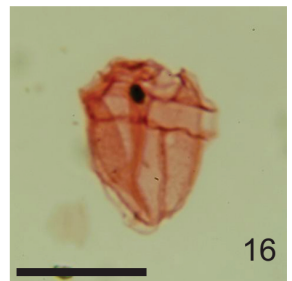
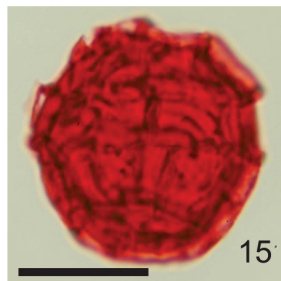
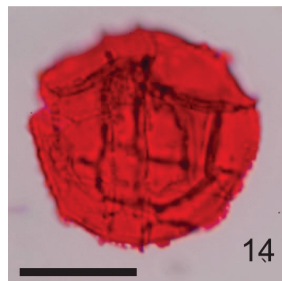
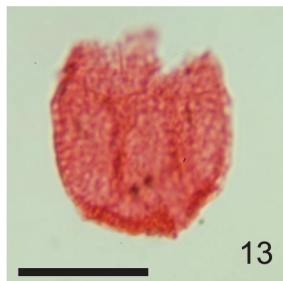
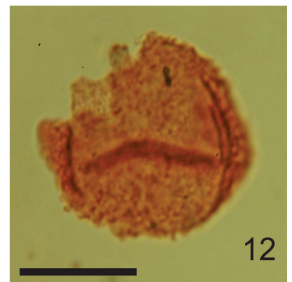
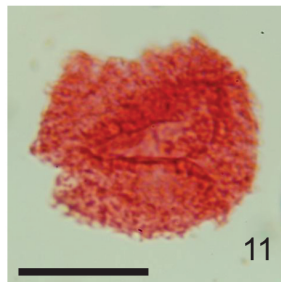
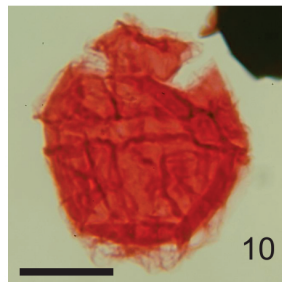
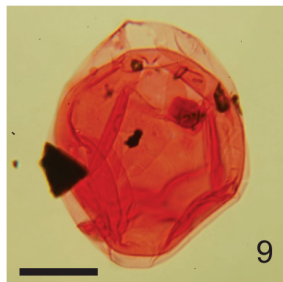
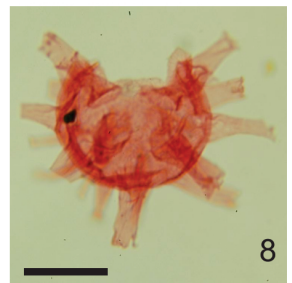
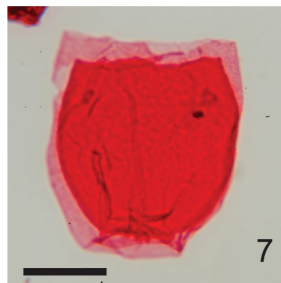
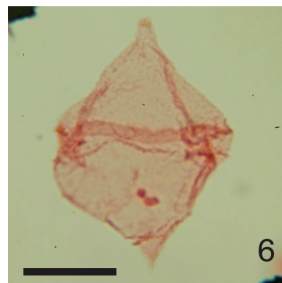
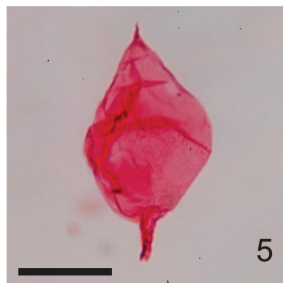
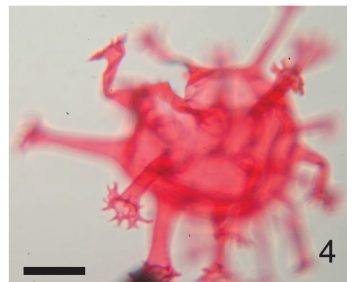
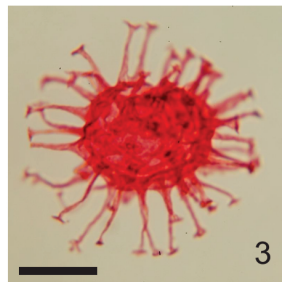
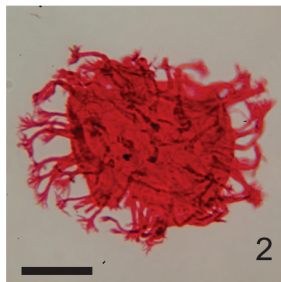
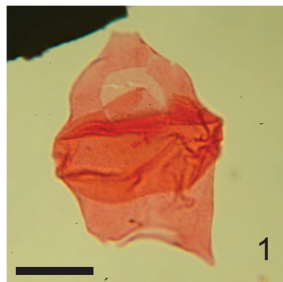


Plate 15

Dinocysts from the Skolp E-07 well. Scale bar represents 20 microns.

1. *Odontochitina porifera*. 1950–1960 metres. P50052, +30 μm
2. *Odontochitina porifera*. 2160–2165 metres. P50061, +30 μm .
3. *Odontochitina* “*skolpensis*”. 1920–1930 metres. P50050, +30 μm .
4. *Oligosphaeridium dictyophorum*, upper surface. 1230–1235 metres. P50023, +30 μm .
5. *Oligosphaeridium dictyophorum*, optical section. 1260–1265 metres. P50024, +30 μm .
6. *Oligosphaeridium dictyophorum*, lower section. 1260–1265 metres. P50024, +30 μm .
7. *Oligosphaeridium complex*. 2310–2315 metres. P50066, +30 μm .
8. *Oligosphaeridium dictyophorum*. 1995–2000 metres. P50055, +30 μm .
9. *Oligosphaeridium pulcherrimum*. 1350–1355 metres. P50027, +30 μm .
10. *Ovoidinium scabrosum*. 2530–2535 metres. P50078, +30 μm .
11. *Ovoidinium verrucosum*. 2185–2190 metres. P50062, +30 μm .
12. *Palaeoperidinium pyrophorum*. 1050–1055 metres. P50017, +30 μm .
13. *Palaeoperidinium pyrophorum*. 1680–1685 metres. P50038, UN.
14. *Palaeotetradinium* sp. 1170–1180 metres. P50021, UN.
15. *Palynodinium grallator*. 1020–1025 metres. P50016, +30 μm .
16. *Palynodinium grallator*. 1020–1025 metres. P50016, +30 μm .
17. *Palynodinium grallator*. 1080–1085 metres. P50018, UN.
18. *Psaligonyaulax deflandrei*. 2340–2345 metres. P50067, +30 μm
19. *Psaligonyaulax* sp. 2140–2145 metres. P50060, +30 μm .
20. *Pterodinium* sp., upper surface. 1450 metres, conventional core. P50351.

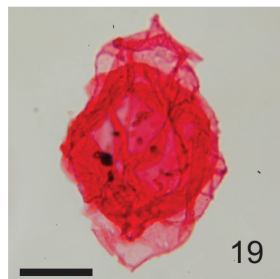
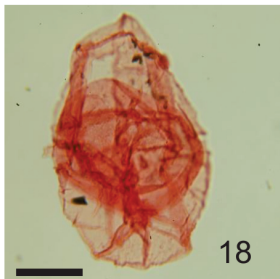
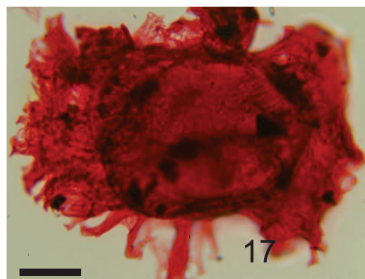
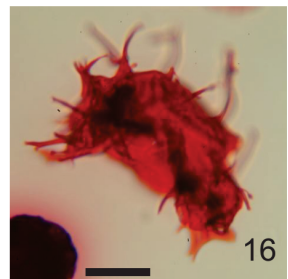
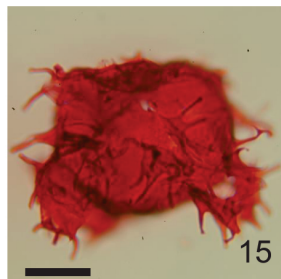
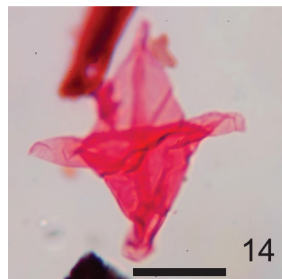
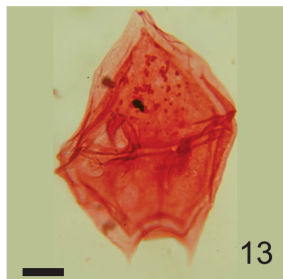
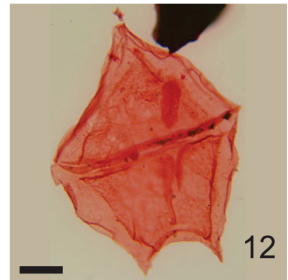
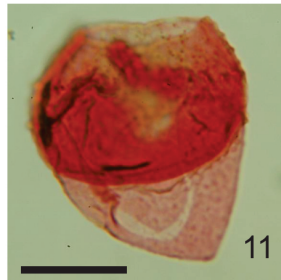
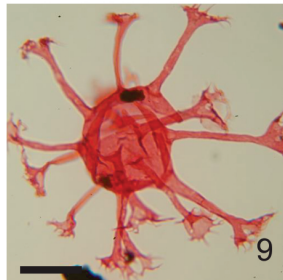
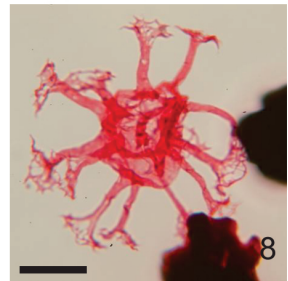
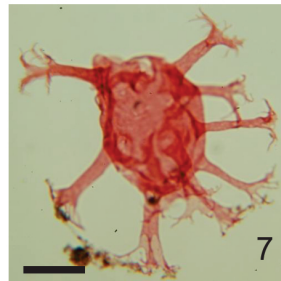
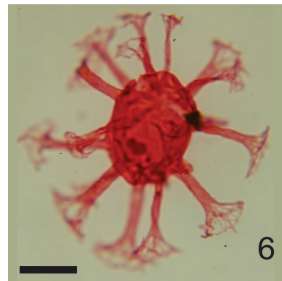
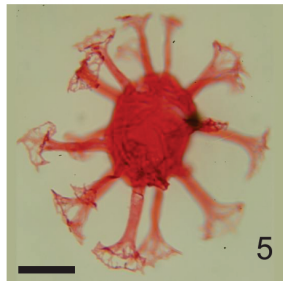
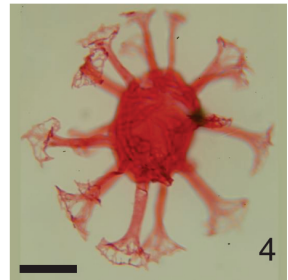
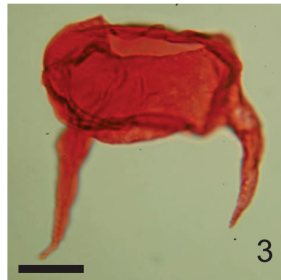
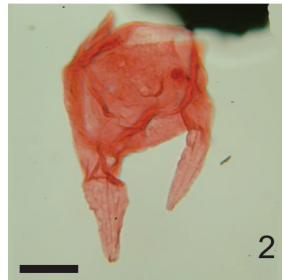
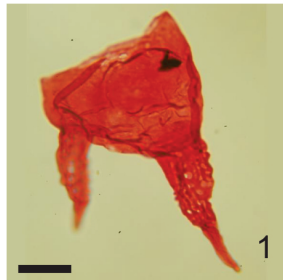


Plate 16

Dinocysts and acritarchs from the Skolp E-07 well. Scale bar represents 20 microns.

1. *Pterodinium* sp., optical section. 1450 metres, conventional core. P50351.
2. *Pterodinium* sp., lower surface. 1450 metres, conventional core. P50351.
3. *Schizocystia* sp., acritarch. 1350–1355 metres. P50027, UN.
4. *Schizocystia* sp., acritarch. 1950–1955 metres. P50052, +30 μm .
5. *Senegalinium* sp. 1290–1295 metres. P50025, UN.
6. *Senoniasphaera inornata*. 1020–1025 metres. P50016, +30 μm .
7. *Senoniasphaera* sp. 1470–1475 metres. P50031, +30 μm .
8. *Sepispinula* sp., some processes are joined distally. 1965–1970 metres. P50053, +30 μm .
9. *Spinidinium uncinatum*. 1470–1475 metres. P50031, +30 μm .
10. *Spinidinium* sp. 1020–1025 metres. P50016, +30 μm .
11. *Spinidinium densispinatum*. 1020–1025 metres. P50016, +30 μm .
12. *Spinidinium echinoideum*. 1320–1325 metres. P50026, +30 μm .
13. *Spiniferites porosus*. 1140–1145 metres. P50020, +30 μm .
14. *Spiniferites* cf. *porosus*. 1170–1175 metres. P50021, +30 μm .
15. *Spiniferites scabrosus*. 1935–1940 metres. P50051, +30 μm .
16. *Spiniferites speciosus*. 2400–2405 metres. P50069, +30 μm .
17. *Spongodinium grossum*. 1920–1925 metres. P50050, +30 μm .
18. *Spongodinium obscurum*, operculum. 2160–2165 metres. P50061, +30 μm .
19. *Stephodinium coronatum*. 1905–1910 metres. P50049, +30 μm .
20. *Tenua* sp. 1380–1385 metres. P50028, +30 μm .

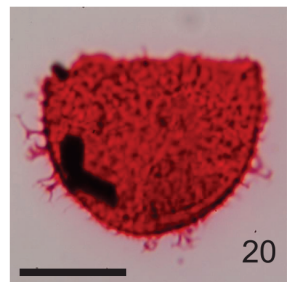
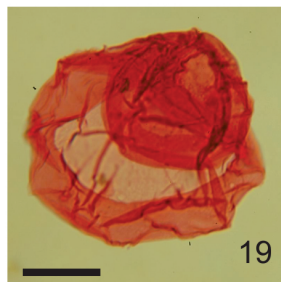
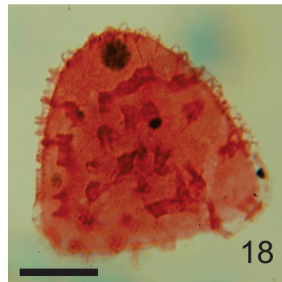
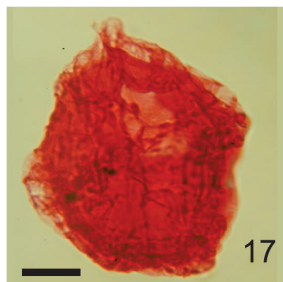
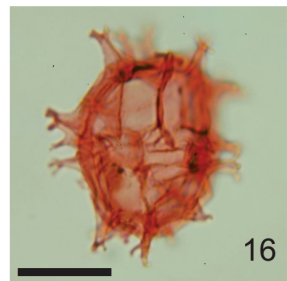
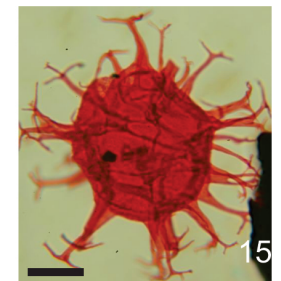
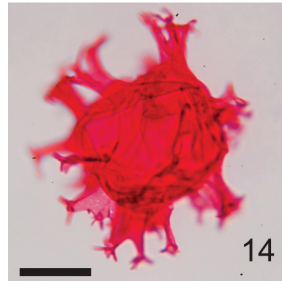
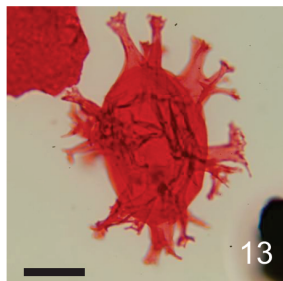
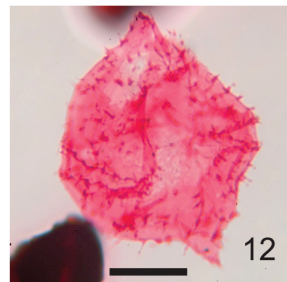
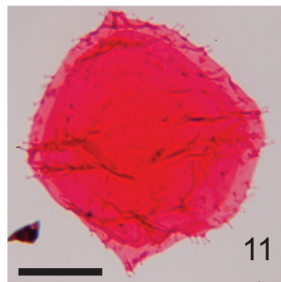
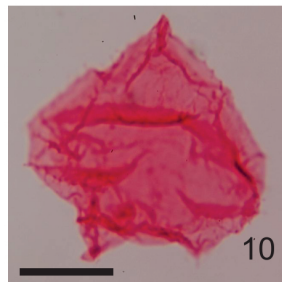
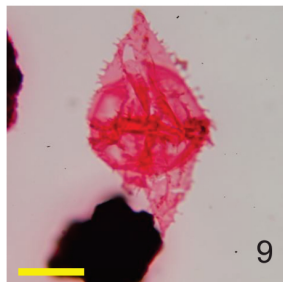
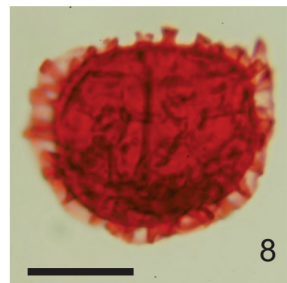
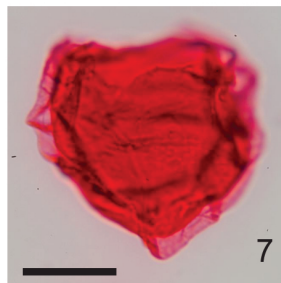
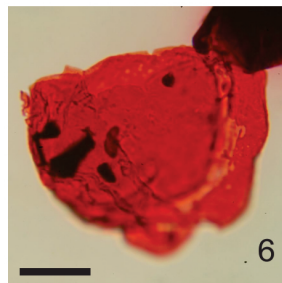
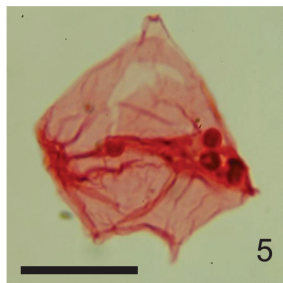
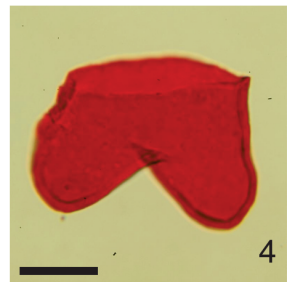
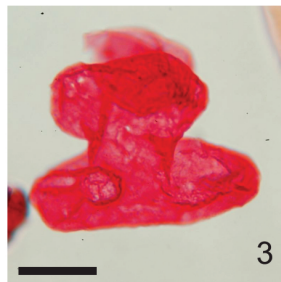


Plate 17

Dinocysts and miospores from the Skolp E-07 well. Scale bar represents 20 microns.

1. *Circulodinium* cf. *distinctum*. 2365–2370 metres. P50068, +30 μm .
2. *Tenua hystrix*. 2400–2405 metres. P50069, +30 μm .
3. *Thalassiphora fenestrata*. 630–635 metres. P50003, +30 μm .
4. *Trichodinium castanea*, right lateral view. 1740–1745 metres. P50040, UN.
5. *Trichodinium castanea*, upper right lateral view. 2160–2165 metres. P50061, +30 μm .
6. *Trichodinium castanea*, lower right lateral view. 2160–2165 metres. P50061, +30 μm .
7. *Trigonopyxidia ginella*. 1320–1325 metres. P50026, +30 μm .
8. *Trithyrodinium conservatum*. 840–845 metres. P50010, +30 μm .
9. *Trithyrodinium conservatum*. 900–905 metres. P50012, UN.
10. *Trithyrodinium evittii*. 1020–1025 metres. P50016, +30 μm .
11. *Whitecliffia* sp. 1140–1145 metres. P50020, +30 μm .
12. *Appendicisporites erdtmanii*. 2280–2285 metres. P50065, +30 μm .
13. *Appendicisporites tricornitatus*. 2680–2685 metres. P50085, +30 μm .
14. *Ornamentifera echinata*. 2530–2535 metres. P50078, +30 μm .
15. *Camarozonosporites insignis*. 840–845 metres. P50010, +30 μm .
16. *Cicatricosisporites annulatus*. 2310–2315 metres. P50066, +30 μm .
17. *Cicatricosisporites subrotundus*. 2880–2890 metres. P50092, +30 μm .
18. *Ruffordiaspora* sp. 2610–2615 metres. P50083, +30 μm .
19. *Cicatricosisporites auritus*. 2515–2520 metres. P50077, +30 μm .
20. *Cicatricosisporites auritus*. 2935–2940 metres. P50094, +30 μm .

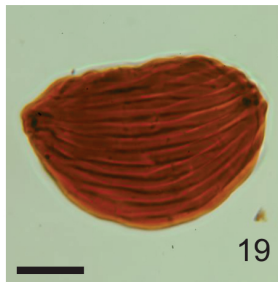
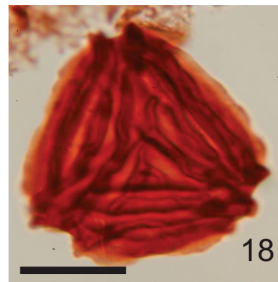
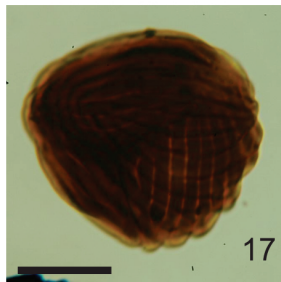
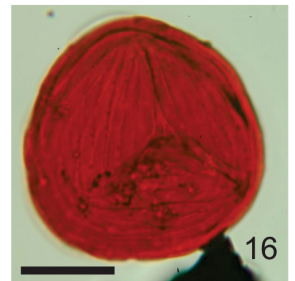
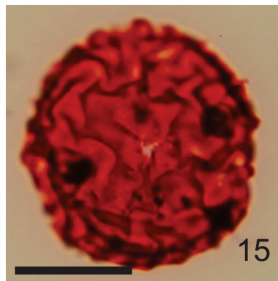
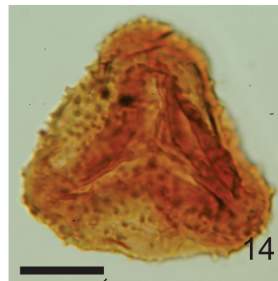
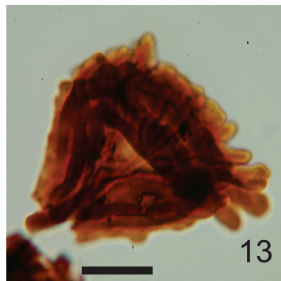
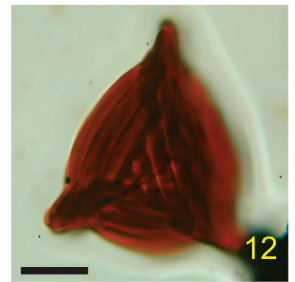
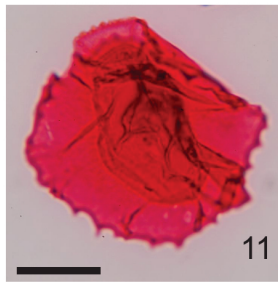
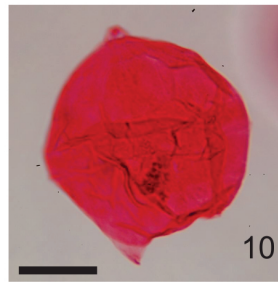
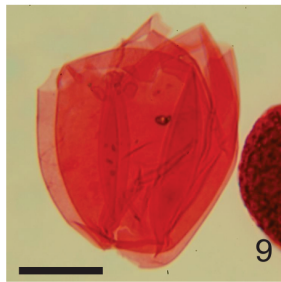
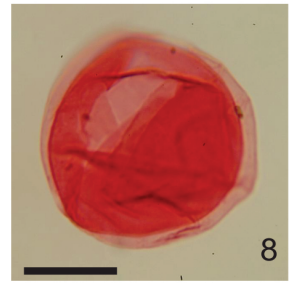
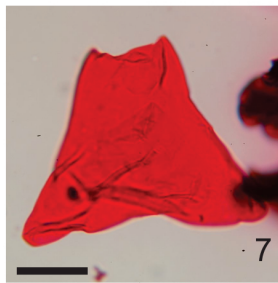
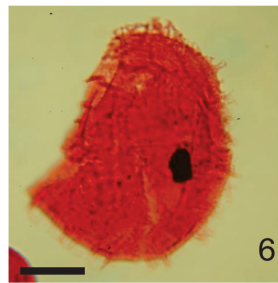
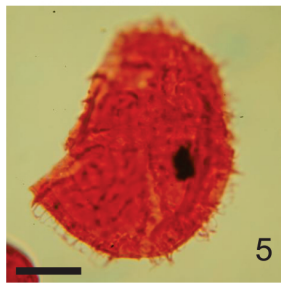
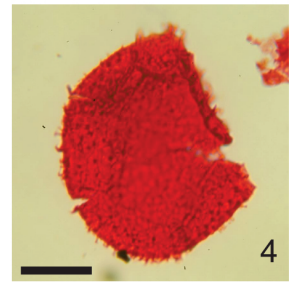
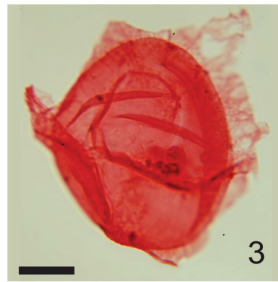
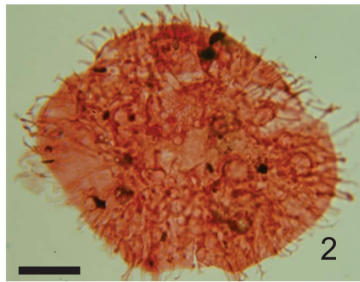
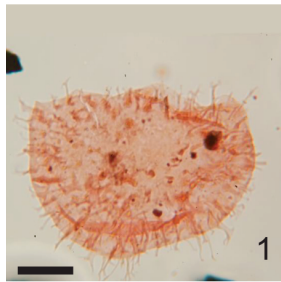


Plate 18

Miospores from the Skolp E-07 well. Scale bar represents 20 microns.

1. *Cingutriletes* sp. 1680–1685 metres. P50038, +30 μm .
2. *Cingutriletes* sp. 1935–1940 metres. P50051, +30 μm .
3. *Cingutriletes* sp. 1980–1985 metres. P50054, +30 μm .
4. *Contignisporites cooksoniae*. 2140–2145 metres. P50060, +30 μm .
5. *Distaltriangulisporites perplexus*. 1890–1895 metres. P50048, +30 μm .
6. *Distaltriangulisporites perplexus*. 1995–2000 metres. P50055, +30 μm .
7. *Distaltriangulisporites perplexus*. 2530–2535 metres. P50078, +30 μm .
8. *Distaltriangulisporites perplexus*. 2310–2315 metres. P50066, +30 μm .
9. *Foveotriletes* sp. 1200–1205 metres. P50022, +30 μm .
10. *Sestrosporites pseudoalveolatus*. 2140–2145 metres. P50060, +30 μm .
11. *Gleicheniidites senonicus*. 1860–1865 metres. P50046, +30 μm .
12. *Matonisporites* sp. 2310–2315 metres. P50066, +30 μm .
13. *Matonisporites* sp. 2445–2450 metres. P50072, +30 μm .
14. *Plicatella problematicus*. 2550–2555 metres. P50079, +30 μm .
15. *Plicatella problematicus*. 2595–2600 metres. P50082, +30 μm .
16. *Rugutriletes* sp. 1110–1115 metres. P50019, +30 μm .
17. *Rugutriletes* sp. 1765–1770 metres. P50041, +30 μm .
18. *Rugutriletes* sp. 1965–1970 metres. P50053, +30 μm .
19. *Rugutriletes* sp. 2010–2015 metres. P50056, UN.
20. *Rugutriletes* sp. 2595–2600 metres. P50082, +30 μm .

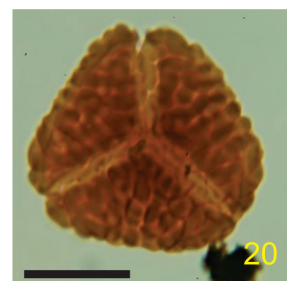
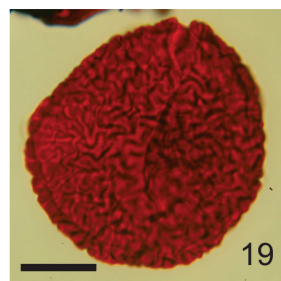
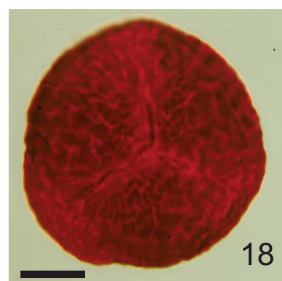
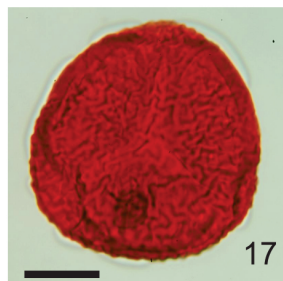
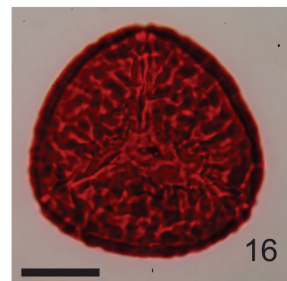
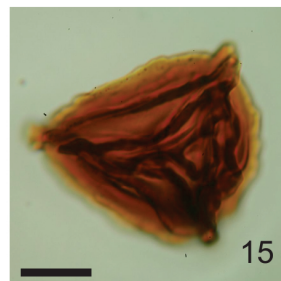
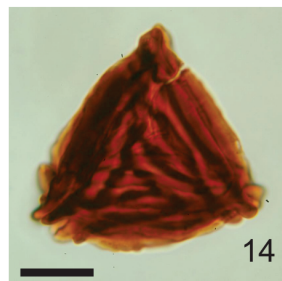
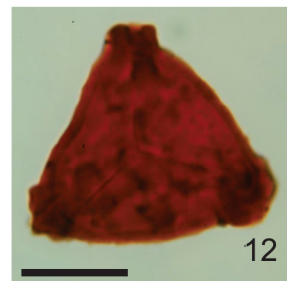
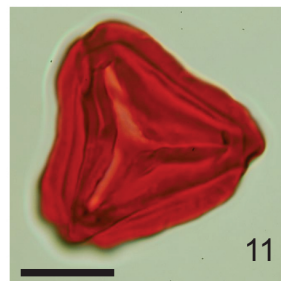
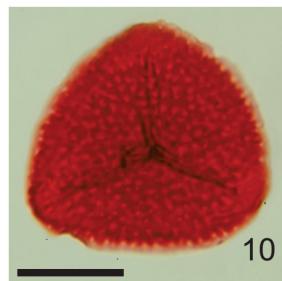
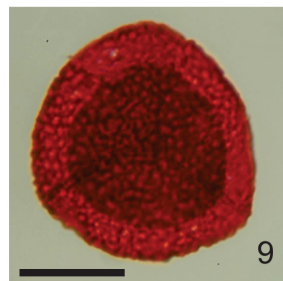
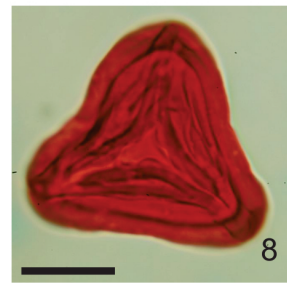
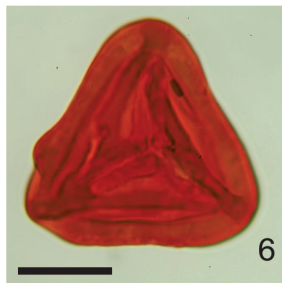
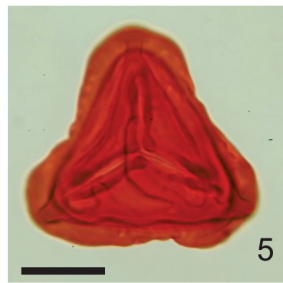
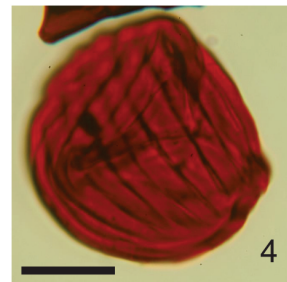
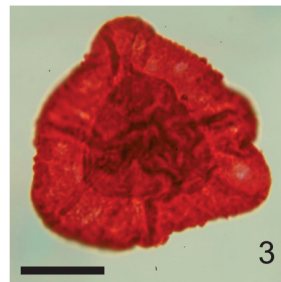
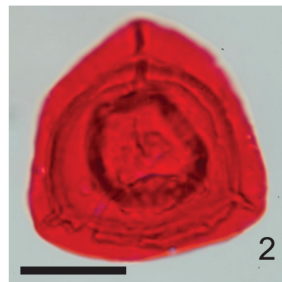
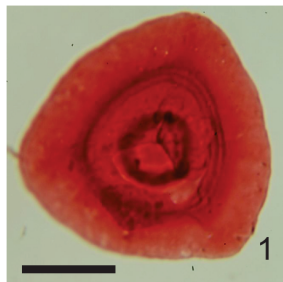


Plate 19

Dinocysts and miospores from the Skolp E-07 well. Scale bar represents 20 microns.

1. *Triporites* sp. 2880–2885 metres. P50092, +30 μm .
2. *Zebrasporites* sp. 2160–2165 metres. P50061, +30 μm .
3. *Triprojectus* cf. *magnus*. 1110–1115 metres. P50019, +30 μm .
4. *Triprojectus granulatus*. 1170–1175 metres. P50021, +30 μm .
5. *Triprojectus* sp. 1170–1175 metres. P50021, +30 μm .
6. *Boisduvalia clavitites*. 630–635 metres. P50003, +30 μm .
7. *Brevitricolpites* sp. 930–935 metres. P50013, +30 μm .
8. *Caryapollenites veripites*. 870–875 metres. P50011, UN.
9. *Extratropipollenites* sp. 2340–2345. P50037, UN.
10. *Extratropipollenites* sp. 1450 metres, conventional core. P50351.
11. *Gothanipollis* sp. 1170–1175 metres. P50021, +30 μm .
12. Tricolporate pollen. 780–785 metres. P50008, UN.
13. *Kurtzipites* sp. 1740–1745 metres. P50040, +30 μm .
14. *Nyssapollenites* sp. 1050–1055 metres. P50017, +30 μm .
15. *Parvisaccites radiatus*. 2918.77 metres. P50352.
16. *Proteacidites* sp. 2310–2315 metres. P50066, UN.
17. *Pterocaryapollenites* sp. 600–605 metres. P50002, UN.
18. *Pterocaryapollenites* sp. 1500–1505 metres. P50032, UN.
19. *Rugubivesiculites reductus*. 2965–2970 metres. P50095, +30 μm .
20. *Spinatriporites* sp. 630–635 metres. P50003, +30 μm .

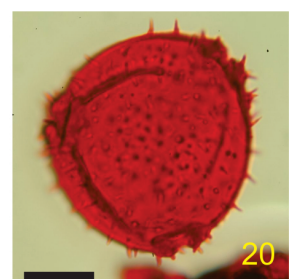
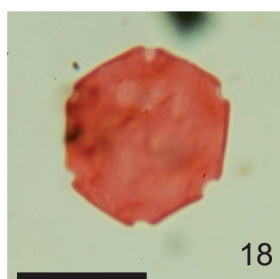
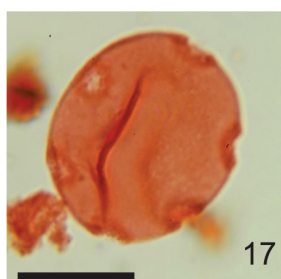
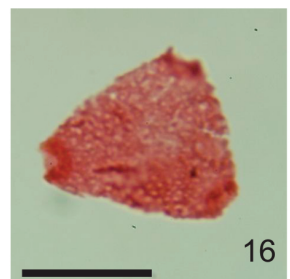
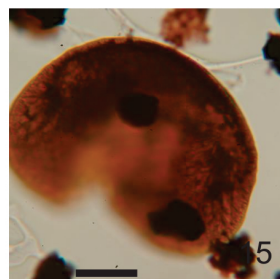
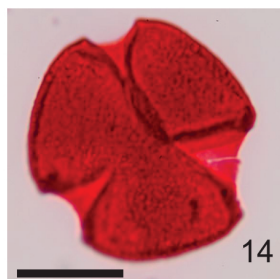
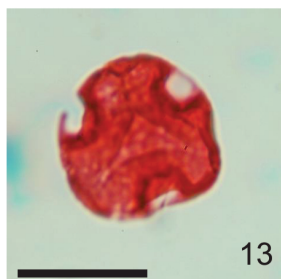
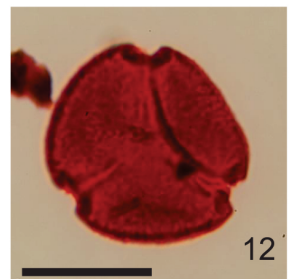
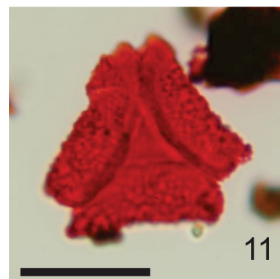
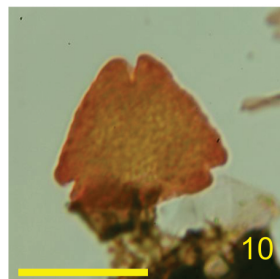
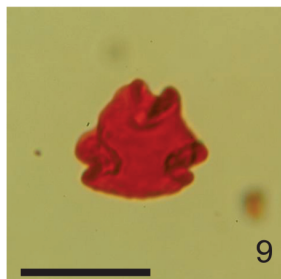
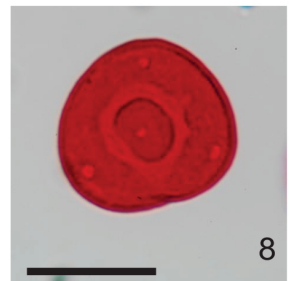
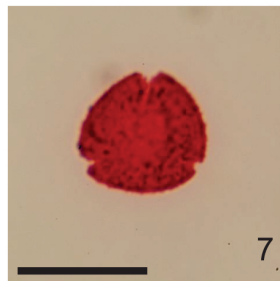
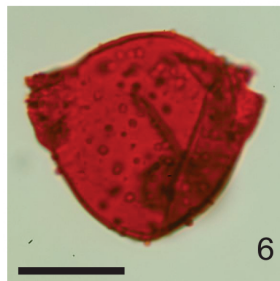
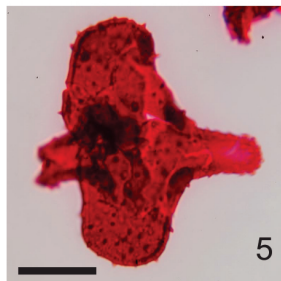
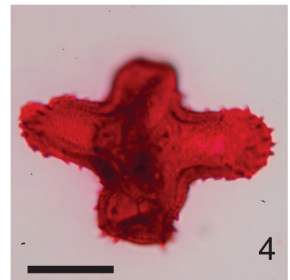
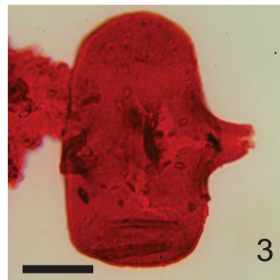
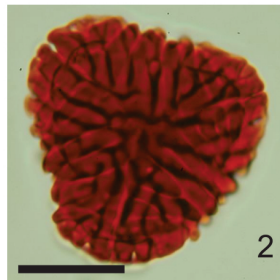
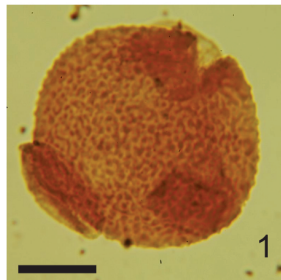


Plate 20

Dinocysts and miospores from the Skolp E-07 well. Scale bar represents 20 microns.

1. Tetrasaccate pollen. 540-545 metres. P50000, UN.
2. *Bombacacidites* sp. 900–905 metres. P50012, UN.
3. *Nyssapollenites* sp. 1020–1025 metres. P50016, +30 μm .
4. *Triporopollenites* sp. 1451.2 metres. P50350.
5. *Triporopollenites* sp. 990–995 metres. P50015, +30 μm
6. *Triprojectus dispositus*. 2140–2145 metres. P50060, +30 μm .
7. *Trudopollis* sp. 1276.5 metres, conventional core. P50338.
8. *Trudopollis* sp. 960–965 metres. P50014, +30 μm .
9. *Momipites wyomingensis*. 1140-1145 metres. P50020, UN.
10. *Extratriporopollenites* sp. 1320–1325 metres. P50026, UN.
11. *Wodehouseia gracilis*. 1020–1025 metres. P50016, +30 μm .
12. *Wodehouseia spinata*. 1200–1205 metres. P50022, +30 μm .
13. *Fimbriaesporis*” sensu Williams and Brideaux 1975. 630–635 metres. P50003, +30 μm .
14. *Fromea chytra*. 1281.5 metres, conventional core. P50344.
15. *Fromea chytra*. 1276.5 metres, conventional core. P50337.
16. *Fromea fragilis*. 1965–1975 metres. P50053, +30 μm
17. *Fromea quadrata*. 2250–2255 metres. P50064, UN.
18. *Horologinella* sp. 870–875 metres. P50011, UN.
19. *Micrhystridium* sp. 1170–1175 metres. P50021, UN.
20. *Micrhystridium* sp. 1260–1265 metres. P50024, UN.

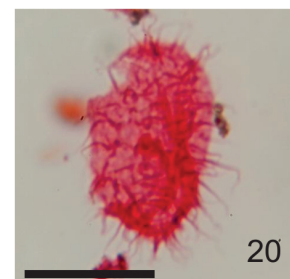
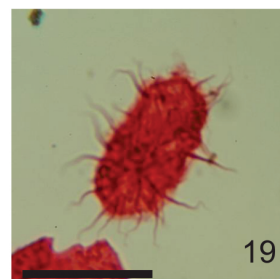
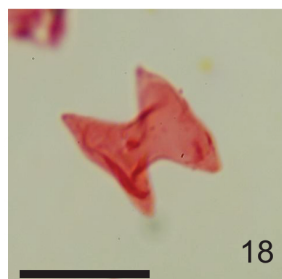
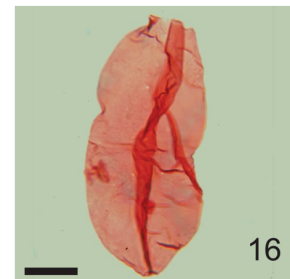
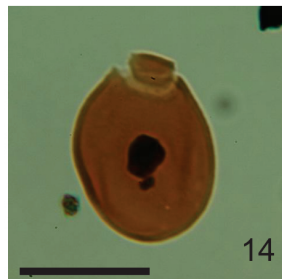
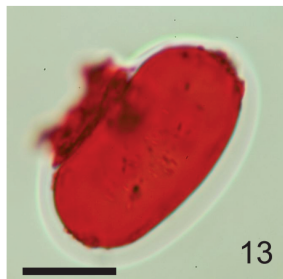
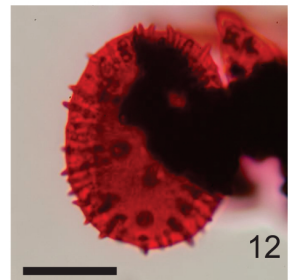
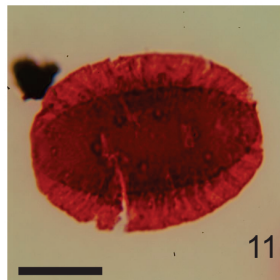
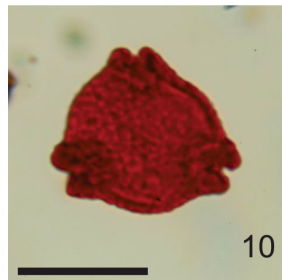
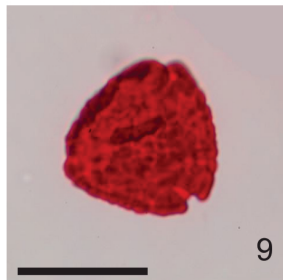
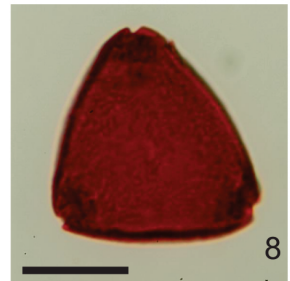
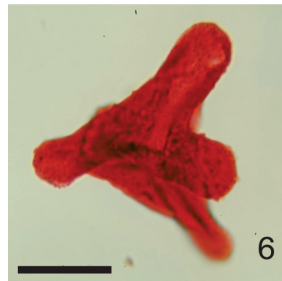
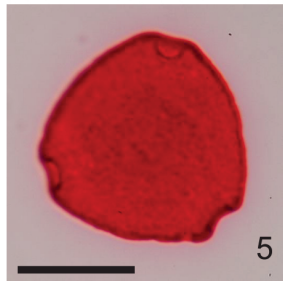
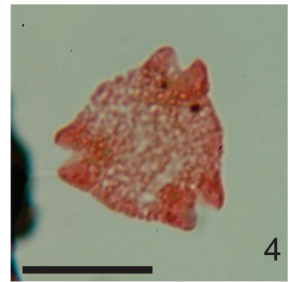
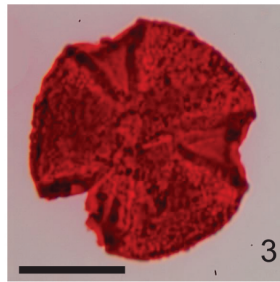
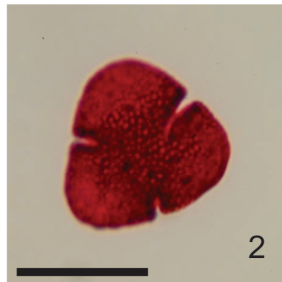
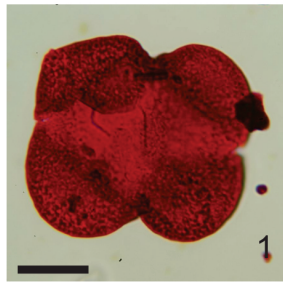


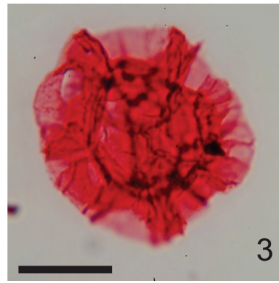
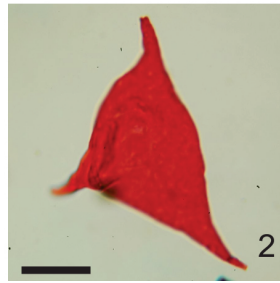
Plate 21

Dinocysts and miospores from the Skolp E-07 well. Scale bar represents 20 microns.

1. *Micrhystridium* sp. 1440-1445 metres. P50030, +30 μm .
2. *Veryhachium trispinosum*. 1560–1565 metres. P50034, UN.
3. *Cymatiosphaera* sp. 1350–1355 metres. P50027, +30 μm .
4. Fungal hypha. 1276.5 metres, conventional core. P50337.

Skolp E-07

Plate 21



APPENDIX A

PLATE	FIGURE	TAXON	DEPTH (M)	GSC (P) OR GEUS (YD) NUMBER & SLIDE TYPE	SLIDE CO-ORDINATES
1	1	<i>Adnatosphaeridium vittatum</i>	2130-2140	YD17-600-2	14.6 X 93.7
1	2	<i>Adnatosphaeridium vittatum</i>	2400-2410	YD17-609-2	15.0 X 107.1
1	3	<i>Adnatosphaeridium robustum</i>	2220-2230	YD17-603-2	7.6 X 93.5
1	4	<i>Alisocysta margarita</i>	2335-2345	P22077-01	20.6 X 103.2
1	5	<i>Alisocysta margarita</i>	2335-2345	P22077-01	20.6 X 103.2
1	6	<i>Alisocysta margarita</i>	2335-2345	P22077-01	15.5 X 104.3
1	7	<i>Alisocysta margarita</i>	2455-2465	YD17-611-2	10.5 X 97.8
1	8	<i>Alisocysta margarita</i>	2455-2465	YD17-611-2	10.5 X 97.8
1	9	<i>Alterbidinium acutululum</i>	2730-2740	YD17-620-2	3.0 X 101.8
1	10	<i>Alterbidinium</i> sp.	2455-2465	YD17-611-2	18.8 X 104.0
1	11	<i>Apectodinium homomorphum</i>	2040-2050	YD17-597-2	5.2 X 110.8
1	12	<i>Apectodinium parvum</i>	2160-2170	YD17-601-2	4.0 X 89.00
1	13	<i>Areoligera gippingensis</i>	2335-2345	P22077-01	16.5 X 120.0
1	14	<i>Areoligera gippingensis</i>	2335-2345	P22077-01	16.5 X 109.6
1	15	<i>Areoligera gippingensis</i>	2335-2345	P22077-01	16.5 X 109.6
1	16	<i>Areoligera gippingensis</i>	2340-2350	YD17-607-2	15.0 X 112.4
1	17	<i>Areoligera gippingensis</i>	2340-2350	YD17-607-2	15.0 X 112.4
1	18	<i>Axiodinium augustum</i>	2250-2260	YD17-604-2	23.0 X 95.0
1	19	<i>Caligodinium aceras</i>	2730-2740	YD17-620-2	10.0 X 96.6
1	20	<i>Cerbia</i> cf. <i>tabulata</i>	2700-2710	YD17-619-2	5.0 X 96.8
2	1	<i>Cerbia</i> cf. <i>tabulata</i>	2700-2710	YD17-619-2	7.0 X 98.0
2	2	<i>Impagidinium</i> sp.	2700-2710	YD17-619-2	19.7 x 107.3
2	3	<i>Cerebrocysta bartonensis</i>	1800-1810	YD17-589-2	17.0 X 99.0
2	4	<i>Cerebrocysta</i> sp.	2010-2020	YD17-596-2	16.6 X 111.0
2	5	<i>Cerodinium diebelii</i>	2700-2710	YD17-619-2	15.7 X 105.6
2	6	<i>Cerodinium speciosum</i>	2580-2590	YD17-615-2	6.8 X 98.0
2	7	<i>Cerodinium striatum</i>	2520-2530	YD17-613-2	6.4 X 104.3
2	8	<i>Cleistosphaeridium elegantulum</i>	1885-1895	P22066-01	21.5 X 107.2
2	9	<i>Cometodinium</i> sp.	2730-2740	P22087-01	12.8 X 107.6
2	10	<i>Cometodinium</i> sp.	2730-2740	P22087-01	12.8 X 107.6
2	11	<i>Operculodinium</i> sp.	2535-2545	P22082-01	6.0 X 114.7
2	12	<i>Corrudinium</i> sp.	600-610	YD17-549-2	9.0 X 103.0
2	13	<i>Corrudinium</i> sp.	600-610	YD17-549-2	9.0 X 103.0
2	14	<i>Cribroperidinium</i> cf. <i>orthoceras</i>	430-440	P22029-01	5.7 X 114.7
2	15	<i>Cribroperidinium</i> sp.	2445-2455	P22080-01	16.5 X 112.0
2	16	<i>Tenua hystrix</i>	2930-2940	P22092-01	14.7 X 116.5
2	17	<i>Cyclonephelium compactum</i>	2930-2940	P22092-01	15.0 X 111.4
2	18	<i>Cyclonephelium vannophorum</i>	3390-3400	YD17-642-2	11.0 x 103.1
2	19	<i>Danea californica</i>	2520-2530	YD17-613-2	8.2 x 107.1
2	20	<i>Deflandrea oebisfeldensis</i>	2520-2530	YD17-613-2	8.5 x 109.2
3	1	<i>Deflandrea</i> cf. <i>phosphoritica</i>	1710-1720	YD17-586-2	16.5 x 99.9

3	2	<i>Deflandrea</i> sp. B	1890-1900	YD17-592-2	16.4 x 91.2
3	3	<i>Deflandrea</i> sp. B	1980-1990	YD17-595-2	7.5 x 91.7
3	4	<i>Deflandrea</i> sp.	2190-2200	YD17-602-2	6.2 x 92.6
3	5	<i>Deflandrea</i> sp.	2580-2590	YD17-615-2	21.0 x 99.2
3	6	<i>Deflandrea wetzellii</i>	2175-2185	P22073-01	6.1 x 107.8
3	7	<i>Diphyes brevispinum</i>	2010-2020	YD17-596-2	22.0 x 93.5
3	8	<i>Disphaerogena</i> sp.	2535-2545	P22082-01	14.0 x 104.6
3	9	<i>Elytrocysta</i> sp.	1560-1570	YD17-581-2	1.2 x 96.2
3	10	<i>Enneadocysta</i> "annulus"	2130-2140	YD17-600-2	16.1 x 104.9
3	11	<i>Enneadocysta</i> cf. <i>arcuata</i>	2130-2140	YD17-600-2	17.7 x 104.9
3	12	<i>Evittosphaerula</i> sp.	2190-2200	YD17-602-2	14.0 x 111.9
3	13	<i>Glaphyrocysta exuberans</i>	2430-2440	YD17-610-2	19.0 x 101.8
3	14	<i>Glaphyrocysta pastielsii</i>	1530-1540	YD17-580-2	5.0 x 105.0
3	15	<i>Glaphyrocysta</i> cf. <i>vicina</i>	1895-1905	P22066-01	6.0 x 115.2
3	16	<i>Heterosphaeridium bellii</i>	2730-2740	P22087-01	6.4 x 117.2
3	17	<i>Hystrichodinium pulchrum</i>	2730-2740	P22087-01	3.5 x 115.3
3	18	<i>Hystrichokolpoma globulus</i>	2370-2380	YD17-608-2	17.0 x 92.7
3	19	<i>Hystrichokolpoma globulus</i>	2370-2380	YD17-608-2	17.0 x 92.7
3	20	<i>Hystrichosphaeridium</i> "complex"	2550-2560	YD17-614-2	5.1 x 106.0
4	1	<i>Hystrichosphaeridium</i> "pulcherrimum"	2520-2530	YD17-613-2	23.0 x 103.0
4	2	<i>Hystrichosphaeridium tubiferum</i>	2400-2410	YD17-609-2	2.3 x 95.5
4	3	<i>Hystrichosphaeridium tubiferum</i>	2400-2410	YD17-609-2	2.3 x 95.5
4	4	<i>Hystrichosphaeridium tubiferum</i>	2400-2410	YD17-609-2	21.5 x 107.4
4	5	<i>Hystrichosphaeridium tubiferum</i> var. "perforatum"	2580-2590	YD17-615-2	8.0 x 103.7
4	6	<i>Hystrichosphaeropsis perforata</i>	2580-2590	P22083-01	12.0 x 114.7
4	7	<i>Impagidinium</i> cf. <i>victorianum</i>	2610-2620	YD17-612-2	14.7 x 104.2
4	8	<i>Impagidinium</i> cf. <i>victorianum</i>	2610-2620	YD17-612-2	14.7 x 104.2
4	9	<i>Impletosphaeridium apodastum</i>	2455-2465	YD17-611-2	7.0 x 104.0
4	10	<i>Impletosphaeridium apodastum</i>	2520-2530	YD17-613-2	21.0 x 92.9
4	11	<i>Isabelidinium cooksoniae</i>	2730-2740	P22087-01	8.6 x 115.1
4	12	<i>Isabelidinium cretaceum</i>	2650-2660	P22085-01	10.0x 102.6
4	13	<i>Isabelidinium majae</i>	2535-2545	P22082-01	6.8 x 113.9
4	14	<i>Kleithriasphaeridium cooksoniae</i>	3010-3020	P22094-01	18.7 x 104.7
4	15	<i>Lejeunecysta</i> sp.	2040-2050	YD17-597-2	9.0 x 111.1
4	16	<i>Microdinium saeptum</i>	2700-2710	YD17-619-2	13.0 x 105.3
4	17	<i>Minisphaeridium latirictum</i>	2190-2200	YD17-602-2	17.0 x 100.1
4	18	<i>Nyktericysta davisii</i>	2970-2980	P22093-01	17.3 x 112.8
4	19	<i>Odontochitina costata</i>	2730-2740	P22087-01	14.3 x 102.0
4	20	<i>Oligosphaeridium dictyophorum</i>	2610-2620	YD17-616-2	13.4 xx 93.0
5	1	<i>Oligosphaeridium pulcherrimum</i>	2700-2710	YD17-619-2	15.2 x 01.6
5	2	<i>Palaeocystodinium lidiae</i>	2370-2380	YD17-608-2	9.0 x 97.0
5	3	<i>Palaeocystodinium</i> sp.	2455-2465	YD17-611-2	11.0 x 96.8
5	4	<i>Palaeoperidinium pyrophorum</i>	2430-2440	YD17-610-2	4.1 x 93.0
5	5	<i>Palynodinium grillator</i>	2580-2590	YD17-615-2	21.7 x 100.3
5	6	<i>Palynodinium grillator</i>	2580-2590	YD17-615-2	21.7 x 00.3
5	7	<i>Pervosphaeridium</i> sp.	2175-2185	P22073-01	12.3 x 114.4

5	8	<i>Petalodinium condylos</i>	2130-2140	YD17-600-2	13.3 x 95.0
5	9	<i>Petalodinium condylos</i>	2130-2140	YD17-600-2	13.3 x 95.0
5	10	<i>Phelodinium kozlowskii</i>	2400-2410	YD17-609-2	11.3 x 94.2
5	11	<i>Phelodinium kozlowskii</i>	2520-2530	YD17-613-2	6.4 x 104.3
5	12	<i>Phthanoperidinium "hibernium"</i>	1170-1180	YD17-568-2	6.7 x 101.0
5	13	<i>Rottnestia</i> sp.	2455-2465	YD17-611-2	20.4 x 110.2
5	14	<i>Rottnestia</i> sp.	2455-2465	YD17-611-2	20.4 x 110.2
5	15	<i>Schematophora speciosa</i>	1745-1755	P22062-01	14.8 x 109.8
5	16	<i>Schematophora speciosa</i>	1745-1755	P22062-01	14.8 x 109.8
5	17	<i>Schizocystia</i> sp.	840-850	YD17-557-2	15.6 x 92.0
5	18	<i>Senoniasphaera microreticulata</i>	2880-2890	YD17-625-2	18.6 x 96.7
5	19	<i>Spinidinium echinoideum</i>	2430-2440	YD17-610-2	1.2 x 93.2
5	20	<i>Spiniferites scabrosus</i>	2650-2660	P22085-01	3.1 x 99.0
6	1	<i>Spiniferites speciosus</i>	3420-3430	YD17-643-2	11.1 x 98.7
6	2	<i>Spongodinium delitiense</i>	2650-2660	P22085-01	10.6 x 115.0
6	3	<i>Spongodinium delitiense</i>	2650-2660	P22085-01	10.6 x 115.0
6	4	<i>Surculosphaeridium longifurcatum</i>	2730-2740	P22087-01	14.4 x 107.2
6	5	<i>Trithyrodinium conservatum</i>	1800-1810	YD17-589-2	9.0 x 98.8
6	6	<i>Trithyrodinium suspectum</i>	2535-2545	P22082-01	16.5 x 113.1
6	7	<i>Trithyrodinium suspectum</i>	2610-2620	P22084-01	22.5 x 117.5
6	8	<i>Trithyrodinium suspectum</i>	2610-2620	YD17-616-2	2.1 x 95.0
6	9	<i>Cometodinium whitei</i>	2730-2740	P22087-01	21.1 x 105.5
6	10	<i>Paralecaniella indentata</i>	1350-1360	YD17-574-2	9.8 x 103.9
6	11	<i>Tritonites inaequalis</i>	1530-1540	YD17-580-2	7.5 x 103.0
6	12	<i>Aequitriradites spinulosus</i>	3370-3380	P22103-01	10.0 x 113.0
6	13	<i>Appendicisporites bilateralis</i>	3390-3400	YD17-642-3	11.0 x 97.0
6	14	<i>Appendicisporites potomacensis</i>	2850-2860	P22090-01	13.0 x 115.0
6	15	<i>Appendicisporites potomacensis</i>	2850-2860	P22090-01	13.0 x 115.0
6	16	<i>Cicatrissporites hallei</i>	3335-3345	P22102-01	19.3 x 101.6
6	17	<i>Cicatricosisporites pseudotripartitus</i>	3115	P50318 +30	19.7 x 92.7
6	18	<i>Cinguliriletes clavus</i>	2550-2560	YD17-614-2	20.5 x 93.2
6	19	<i>Coronatispora valdensis</i>	3450-3460	YD17-644-2	4.8 x 98.3
6	20	<i>Costatoperforosporites foveolatus</i>	3170-3180	P22098-01	19.4 x 113.2
7	1	<i>Distaltriangulisporites perplexus</i>	3110	P50316 +30	22.5 x 93.7
7	2	<i>Foveotriletes</i> sp.	3090-3100	P22096-01	14.0 x 104.3
7	3	<i>Impardecispora?</i> cf. <i>apiverrucata</i>	870-880	YD17-558-2	8.2 x 103.1
7	4	<i>Impardecispora?</i> cf. <i>apiverrucata</i>	3500-3507	P22107-01	18.0 x 107.8
7	5	<i>Corsinipollenites oculusnoctis</i>	720-730	YD17-553-2	16.0 x 116.3
7	6	<i>Eucommiidites troedsonii</i>	3111.05	P50315 UN	17.0 x 83.7
7	7	<i>Extratropopollenites</i> sp.	1440-1450	YD17-577-2	8.0 x 98.6
7	8	<i>Trudopollis</i> sp.	2250-2260	YD17-604-2	21.0 x 93.8
7	9	<i>Juglanspollenites</i> sp.	480-490	YD17-545-2	17.8 x 94.1
7	10	<i>Mancicorpus canadianus</i>	1230-1240	YD17-570-2	12.0 x 91.0
7	11	<i>Parvisaccites amplus</i>	3110	P50316 +30	20.3 x 9.0
7	12	<i>Pavisaccites amplus</i>	3410-3420	P22104-01	2.0 x 115.1
7	13	<i>Parvisaccites radiatus</i>	2790-2800	YD17-622-2	16.0 x 102.7

7	14	<i>Rugubivesiculites rugosus</i>	3110	P50316 +30	16.0 x 91.0
7	15	<i>Rugubivesiculites rugosus</i>	3112.55	P50314 +30	18.2 x 91.0
7	16	<i>Rugubivesiculites rugosus</i>	3295-3305	P22101-01	10.5 x 103.8
7	17	<i>Rugubivesiculites rugosus</i>	3295-3305	P22101-01	10.5 x 103.8
7	18	<i>Tiliaepollenites crassipites</i>	450-460	YD17-544-2	23.5 x 108.6
7	19	<i>Tiliaepollenites crassipites</i>	450-460	YD17-544-2	23.5 x 108.6
7	20	<i>Triporites</i> sp.	720-730	YD17-555-2	6.8 x 106.0
8	1	<i>Triprojectus attenuatus</i>	1500-1510	YD17-579-2	11.4 x 99.0
8	2	<i>Triprojectus attenuatus</i>	1560-1570	YD17-581-2	20.4 x 94.7
8	3	<i>Triprojectus attenuatus</i>	1560-1570	YD17-581-2	4.0 x 98.0
8	4	<i>Fractisporonites</i>	1710-1720	YD17-586-2	18.5 x 102.8
8	5	Root hair	3010-3020	P22094-01	18.0 x 110.8
8	6	Incertae sedis	810-820	YD17-556-2	17.8 x 108.6
8	7	Incertae sedis	810-820	YD17-556-2	17.8 x 108.6
9	1	<i>Achomosphaera</i> sp.	1080-1085	P50018 +30	15.0 x 93.1
9	2	<i>Alisogymnium</i> sp.	1980-1985	P50054 +30	10.5 x 93.6
9	3	<i>Alisogymnium</i> sp.	2040-2045	P50057 +30	19.0 x 95.3
9	4	<i>Isabelidinium acuminatum</i>	1470-1475	P50031 +30	5.1 x 105.4
9	5	<i>Alterbidinium acutulum</i>	1590-1595	P50035 +30	5.5 x 97.2
9	6	<i>Alterbidinium acutulum</i>	2340-2345	P50067 UN	20.8 x 93.3
9	7	<i>Alterbidinium biaperturatum</i>	1260-1265	P50024 +30	10.0 x 96.0
9	8	<i>Alterbidinium biaperturatum</i>	1320-1325	P50026 +30	20.6 x 99.0
9	9	<i>Alterbidinium majae</i>	540-545	P50000 +30	9.4 x 93.0
9	10	<i>Alterbidinium minor</i>	1110-1115	P50019 UN	8.7 x 92.9
9	11	<i>Alterbidinium minor</i>	1380-1385	P50028 UN	13.0 x 92.2
9	12	<i>Alterbidinium "obscurum"</i>	990-995	P50015 +30	17.0 x 95.2
9	13	<i>Alterbidinium "obscurum"</i>	1200-1205	P50022 +30	18.0 x 92.6
9	14	<i>Alterbidinium "skolpense"</i>	1080-1085	P50018 +30	10.5 x 96.0
9	15	<i>Alterbidinium</i> cf. <i>acutulum</i>	780-785	P50008 UN	15.8 x 93.0
9	16	<i>Alterbidinium</i> cf. <i>acutulum</i>	780-785	P50008 +30	7.2 x 94.3
9	17	<i>Alterbidinium</i> sp.	780-785	P50008 +30	9.0 x 96.0
9	18	<i>Alterbidinium</i> sp.	1110-1115	P50019 +30	13.7 x 97.0
9	19	<i>Isabelidinium cretaceum</i>	1110-1115	P50019 +30	13.7 x 97.0
9	20	<i>Alterbidinium</i> cf. <i>"obscurum"</i>	1140-1145	P50024 +30	12.0 x 93.8
10	1	<i>Alterbidinium</i> sp.	1170-1175	P50021 +30	19.0 x 92.9
10	2	<i>Alterbidinium</i> sp.	1230-1235	P50023 UN	6.0 x 93.8
10	3	<i>Alterbidinium "rotundum"</i>	1650-1655	P50037 +30	17.0 x 95.0
10	4	<i>Alterbidinium</i> sp.	1875-1880	P50047 +30	18.5 x 96.6
10	5	<i>Alterbidinium</i> sp.	1905-1910	P50049 +30	13.8 x 90.3
10	6	<i>Areoligera medusettiformis</i>	1410-1415	P50029 +30	18.1 x 95.7
10	7	<i>Areoligera medusettiformis</i>	1410-1415	P50029 +30	18.1 x 95.7
10	8	<i>Batioladinium jaegeri</i>	2140-2145	P50060 +30	16.0 x 94.0
10	9	<i>Batioladinium jaegeri</i>	2185-2190	P50062 UN	8.0 x 94.0
10	10	<i>Callaiosphaeridium asymmetricum</i>	1950-1955	P50052 +30	6.7 x 98.3
10	11	<i>Circulodinium</i> sp.	1260-1265	P50024 +30	12.8 x 92.8
10	12	<i>Circulodinium</i> sp.	2225-2230	P50063 +30	10.5 x 98.0

10	13	<i>Aptea</i> sp.	1710-1715	P50039 +30	11.8 x 93.7
10	14	<i>Cerodinium galeota</i>	1020-1025	P50016 +30	8.5 x 102.5
10	15	<i>Cerodinium kangliense</i>	990-995	P50015 +30	9.8 x 93.8
10	16	<i>Cerodinium striatum</i>	1020-1025	P50016 UN	23.2 x 93.8
10	17	<i>Chatangiella amphiota</i>	1740-1745	P50040 +30	17.1 x 94.0
10	18	<i>Chatangiella madura</i>	1740-1745	P50040 +30	14.8 x 93.0
10	19	<i>Chatangiella madura</i>	1845-1850	P50045 +30	5.0 x 97.7
10	20	<i>Chatangiella verrucosa</i>	1590-1595	P50035 +30	16.0 x 96.8
11	1	<i>Chatangiella verrucosa</i>	1710-1715	P50039 +30	14.8 x 99.3
11	2	<i>Chatangiella</i> (deltaform)	1935-1940	P50051 +30	7.5 x 97.8
11	3	<i>Chlamydophorella nyei</i>	1710-1715	P50039 +30	15.4 x 94.0
11	4	<i>Chlamydophorella nyei</i>	1845-1850	P50045 +30	20.8 x 94.6
11	5	<i>Chlamydophorella</i> sp.	2040-2045	P50057 +30	16.0 x 97.3
11	6	<i>Chlamydophorella nyei</i>	2250-2255	P50064 UN	13.7 x 96.8
11	7	<i>Downiesphaeridium aciculare</i>	2040-2045	P50057 +30	9.1 x 100.0
11	8	<i>Downiesphaeridium aciculare</i>	2400-2405	P50069 +30	14.4 x 97.0
11	9	<i>Cometodinium whitei</i>	1905-1910	P50049 +30	4.0 x 96.6
11	10	<i>Coroniferaoceanica</i>	1830-1835	P50044 +30	10.7 x 93.8
11	11	<i>Cleistosphaeridium</i> cf. <i>placacanthum</i>	900-905	P50012 UN	3.0 x 105.7
11	12	<i>Cribroperidinium</i> sp.	2010-2015	P50056 UN	1.1 x 97.1
11	13	<i>Cyclonephelium</i> sp.	1140-1145	P50020 +30	20.0 x 95.7
11	14	<i>Dapsilidinium simplex</i>	1200-1205	P50022 +30	4.2 x 93.0
11	15	<i>Dapsilidinium</i> sp.	1230-1235	P50023 UN	12.5 x 104.0
11	16	<i>Deflandrea</i> sp. B Williams and Bujak 1977	870-875	P50011 +30	16.0 x 94.0
11	17	<i>Trigonopyxidia ginella</i>	1890-1895	P50048 +30	9.0 x 93.0
11	18	<i>Dinogymnium acuminatum</i>	2250-2255	P50064 +30	10.0 x 96.0
11	19	<i>Dinopterygium cladoides</i>	1410-1415	P50029 +30	16.2 x 94.1
11	20	<i>Dipyces ficusoides</i>	900-905	P50012 UN	12.1 x 98.5
12	1	<i>Distatodinium</i> sp.	1279.35	P50335	9.5 x 94.2
12	2	<i>Tenua</i> sp.	1110-1115	P50019 +30	23.0 x 98.0
12	3	<i>Circulodinium</i> sp.	1845-1850	P50045 +30	11.0 x 96.7
12	4	<i>Druggidium</i> sp.	1440-1445	P50030 UN	19.8 x 97.0
12	5	<i>Elytrocysta druggii</i>	1380-1385	P50028 UN	13.5 x 93.3
12	6	<i>Exochosphaeridium bifidum</i>	2400-2405	P50069 +30	11.0 x 95.1
12	7	<i>Exochosphaeridium</i> sp.	1530-1535	P50033 +30	11.8 x 96.8
12	8	<i>Exochosphaeridium</i> sp.	1830-1835	P50044 +30	5.8 x 95.6
12	9	<i>Fibradinium annetorpense</i>	1860-1865	P50046 UN	4.8 x 95.3
12	10	<i>Florentinia ferox</i>	1845-1850	P50045 +30	13.7 x 94.6
12	11	<i>Gillinia hymenophora</i>	1451.2	P50350 +30	19.3 x 91.1
12	12	<i>Gillinia hymenophora</i>	1454.32	P50348	15.0 x 91.3
12	13	<i>Gillinia hymenophora</i>	1454.32	P50348	15.0 x 91.3
12	14	<i>Gillinia</i> sp.	1450	P50351	21.8 x 91.2
12	15	<i>Gillinia</i> sp.	1452.5	P50349	16.6 x 80.5
12	16	<i>Gonyaulacysta eisenackii</i>	2310-2315	P50066 +30	15.5 x 106.9
12	17	<i>Heterosphaeridium bellii</i>	1530-1535	P50033 UN	21.7 x 95.4
12	18	<i>Heterosphaeridium difficile</i> subsp. " <i>elegantulum</i> "	1680-1685	P50038 +30	12.4 x 92.8

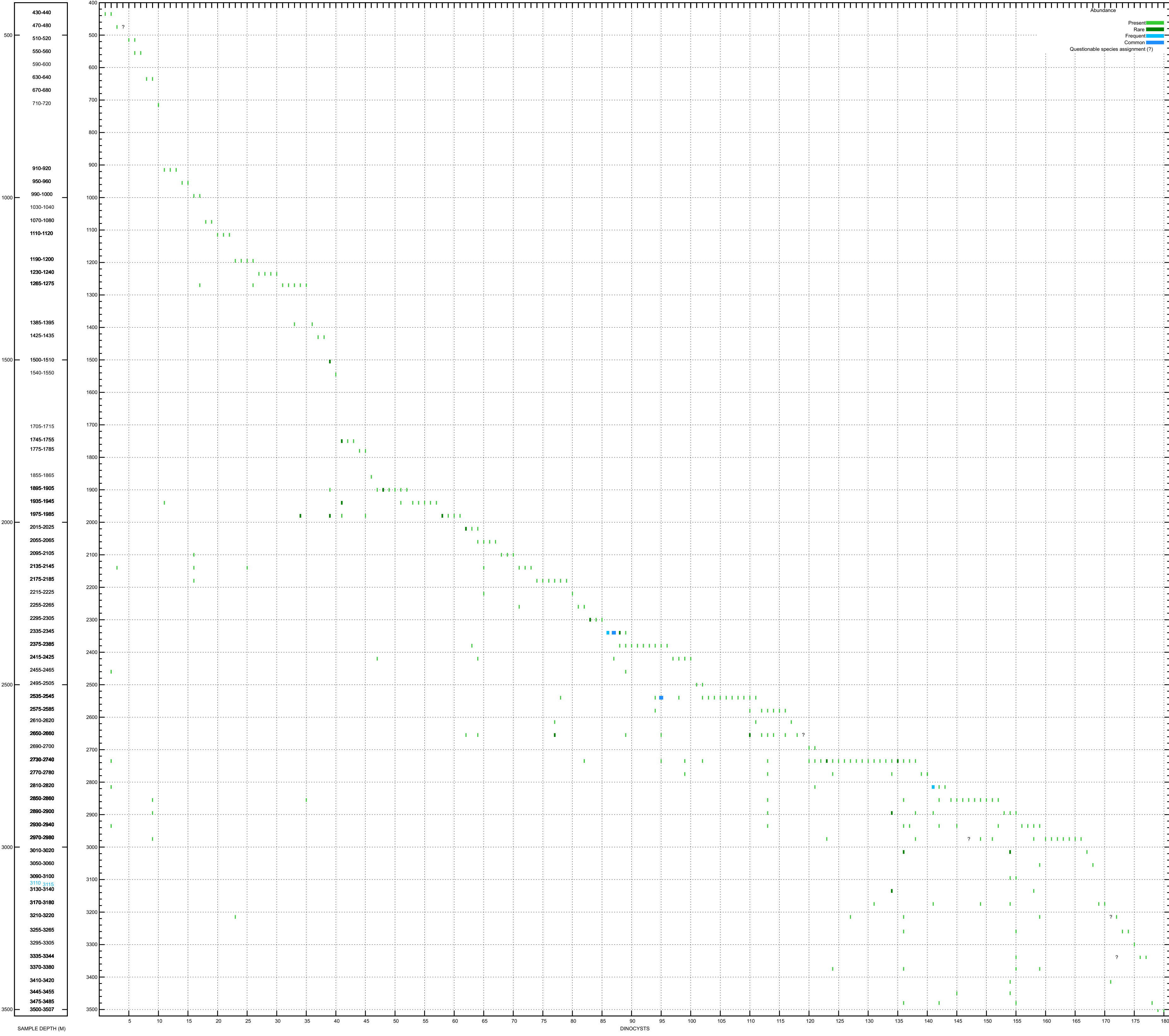
12	19	<i>Heterosphaeridium difficile</i>	750-755	P50007 +30	5.0 x 93.1
12	20	<i>Heterosphaeridium difficile</i>	1560-1565	P50034 +30	11.5 x 96.1
13	1	<i>Histiocysta palla</i>	1615-1620	P50036 +30	17.1 x 96.0
13	2	<i>Histiocysta palla</i>	1710-1715	P50039 +30	19.0 x 95.9
13	3	<i>Hystrichosphaeridium bowerbankii</i>	1320-1325	P50026 +30	8.8 x 96.0
13	4	<i>Hystrichosphaeridium palmatum</i>	2140-2145	P50060 +30	5.0 x 96.9
13	5	<i>Hystrichosphaeridium quadratum</i>	1451.2	P50350 +30	18.5 x 94.2
13	6	<i>Hystrichosphaeridium quadratum</i>	1230-1235	P50023 +30	17.3 x 98.0
13	7	<i>Hystrichosphaeridium</i> sp. 3 McIntyre 1974	2040-2045	P50057 +30	8.4 x 100.2
13	8	<i>Hystrichosphaeropsis quasacribrata</i>	1470-1475	P50031 +30	9.5 x 106.4
13	9	<i>Hystrichosphaeropsis quasacribrata</i>	1590-1595	P50035 +30	5.6 x 97.8
13	10	<i>Hystrichosphaeropsis quasacribrata</i>	1860-1865	P50046 +30	20.0 x 94.3
13	11	<i>Impagidinium</i> sp.	1260-1265	P50024 +30	6.3 x 96.0
13	12	<i>Impagidinium</i> sp.	1380-1385	P50028 +30	2.0 x 96.2
13	13	<i>Impagidinium</i> sp.	1380-1385	P50028 +30	2.0 x 96.2
13	14	<i>Impagidinium</i> sp.	1410-1415	P50029 +30	18.0 x 97.0
13	15	<i>Impagidinium</i> sp.	1410-1415	P50029 +30	18.0 x 97.0
13	16	<i>Isabelidinium bakeri</i>	1200-1205	P50022 +30	8.7 x 93.0
13	17	<i>Isabelidinium cooksoniae</i>	1170-1175	P50021 +30	14.7 x 92.8
13	18	<i>Isabelidinium cooksoniae</i>	1230-1235	P50023 +30	18.6 x 100.7
13	19	<i>Isabelidinium cretaceum</i>	1080-1085	P50018 +30	10.0 x 93.2
13	20	<i>Isabelidinium "deltacooksoniae"</i>	2400-2405	P50069 +30	21.4 x 93.0
14	1	<i>Isabelidinium weidichii</i>	1815-1820	P50043 +30	16.1 x 93.7
14	2	<i>Kiokansium erectum</i>	1260-1265	P50024 +30	15.0 x 95.1
14	3	<i>Kiokansium polypes</i>	1935-1940	P50051 +30	9.4 x 92.8
14	4	<i>Kleithriasphaeridium loffrense</i>	1590-1595	P50035 +30	6.0 x 99.8
14	5	<i>Laciniadinium williamsii</i>	1260-1265	P50024 UN	16.8 x 93.0
14	6	<i>Laciniadinium williamsii</i>	1860-1865	P50046 UN	14.7 x 93.0
14	7	<i>Leberidocysta chlamydata</i>	1440-1445	P50030 +30	10.4 x 101.4
14	8	<i>Litosphaeridium</i> cf. <i>arundum</i>	1650-1655	P50037 +30	13.5 x 96.0
14	9	<i>Manumiella</i> sp.	630-635	P50003 +30	4.3 x 102.5
14	10	<i>Meiourougonyaulax</i> sp.	1995-2000	P50055 +30	16.0 x 94.0
14	11	<i>Membranosphaera maastrichtica</i>	1530-1535	P50033 UN	13.2 x 96.1
14	12	<i>Membranosphaera maastrichtica</i>	1287.5	P50340 UN	8.5 x 81.0
14	13	<i>Microdinium mariae</i>	1710-1715	P50039 UN	9.9 x 94.3
14	14	<i>Microdinium</i> cf. <i>ornatum</i>	720-725	P50006 +30	7.0 x 96.1
14	15	<i>Microdinium inornatum</i>	1170-1175	P50021 +30	7.0 x 92.6
14	16	<i>Microdinium</i> sp.	1380-1385	P50028 UN	19.0 x 93.1
14	17	<i>Microdinium</i> cf. <i>pauciscabrosum</i>	1500-1505	P50032 UN	11.0 x 94.1
14	18	<i>Microdinium</i> sp. A sensu Ioannides 1986	1500-1505	P50032 UN	15.8 x 94.0
14	19	<i>Nyktericysta davisii</i>	630-635	P50003 +30	17.5 x 96.1
14	20	<i>Odontochitina costata</i> (operculum)	1830-1835	P50044 UN	13.0 x 93.0
15	1	<i>Odontochitina porifera</i>	1950-1955	P50052 +30	5.6 x 93.8
15	2	<i>Odontochitina porifera</i>	2160-2165	P50061 +30	16.5 x 95.1
15	3	<i>Odontochitina "skolpensis"</i>	1920-1925	P50050 +30	19.8 x 96.0
15	4	<i>Oligosphaeridium dictyophorum</i>	1230-1235	P50023 +30	7.1 x 100.7

15	5	<i>Oligosphaeridium dictyophorum</i>	1260-1265	P50024 +30	7.1 x 93.8
15	6	<i>Oligosphaeridium dictyophorum</i>	1260-1265	P50024 +30	7.1 x 93.8
15	7	<i>Oligosphaeridium complex</i>	2310-2315	P50066 +30	19.0 x 95.8
15	8	<i>Oligosphaeridium dictyophorum</i>	1995-2000	P50055 +30	18.0 x 94.3
15	9	<i>Oligosphaeridium pulcherrimum</i>	1350-1355	P50027 +30	19.6 x 92.8
15	10	<i>Ovoidinium scabrosum</i>	2530-2535	P50078 +30	12.0 x 95.8
15	11	<i>Ovoidinium verrucosum</i>	2185-2190	P50062 +30	20.8 x 98.0
15	12	<i>Palaeoperidinium pyrophorum</i>	1050-1055	P50017 +30	14.6 x 96.0
15	13	<i>Palaeoperidinium pyrophorum</i>	1680-1685	P50038 UN	18.2 x 94.2
15	14	<i>Palaeotetradinium sp.</i>	1170-1175	P50021 UN	10.0 x 95.3
15	15	<i>Palynodinium grillator</i>	1020-1025	P50016 +30	7.8 x 101.0
15	16	<i>Palynodinium grillator</i>	1020-1025	P50016 +30	12.2 x 102.3
15	17	<i>Palynodinium grillator</i>	1080	P50018 UN	8.8 x 92.8
15	18	<i>Psaligonyaulax deflndrei</i>	2340-2345	P50067 +30	4.4 x 102.1
15	19	<i>Psaligonyaulax sp.</i>	2140-2145	P50060 +30	15.5 x 98.0
15	20	<i>Pterodinium sp.</i>	1450	P50351	9.0 x 83.5
16	1	<i>Pterodinium sp.</i>	1450	P50351	9.0 x 83.5
16	2	<i>Pterodinium sp.</i>	1450	P50351	9.0 x 83.5
16	3	<i>Schizocystia sp.</i>	1350-1355	P50027 UN	21.2 x 93.5
16	4	<i>Schizocystia sp.</i>	1950-1955	P50052 +30	10.1 x 96.0
16	5	<i>Senegalinium sp.</i>	1290-1295	P50025 UN	6.8 x 94.0
16	6	<i>Senoniasphaera inornata</i>	1020-1025	P50016 +30	16.4 x 103.0
16	7	<i>Senoniasphaera sp.</i>	1470-1475	P50031 +30	21.1 x 104.2
16	8	<i>Sepispinula sp.</i>	1965-1970	P50053 +30	90.5 x 94.2
16	9	<i>Spinidinium uncinatum</i>	1470-1475	P50031 +30	16.3 x 104.7
16	10	<i>Spinidinium sp.</i>	1020-1025	P50016 +30	13.8 x 93.0
16	11	<i>Spinidinium densispinatum</i>	1020-1025	P50016 +30	14.9 x 103.3
16	12	<i>Spinidinium echinoideum</i>	1320-1325	P50026 +30	6.0 x 100.0
16	13	<i>Spiniferites porosus</i>	1140-1145	P50020 +30	14.7 x 92.7
16	14	<i>Spiniferites cf. porosus</i>	1170-1175	P50021 +30	12.2 x 97.6
16	15	<i>Spiniferites scabrosus</i>	1935-1940	P50051 +30	18.0 x 96.5
16	16	<i>Spiniferites speciosus</i>	2400-2405	P50069 +30	4.8 x 95.0
16	17	<i>Spongiodinium grossum</i>	1920-1925	P50050 +30	4.0 x 96.3
16	18	<i>Spongiodinium obscurum</i>	2160-2165	P50061 +30	10.1 x 98.3
16	19	<i>Stephodinium coronatum</i>	1905-1910	P50049 +30	15.0 x 92.7
16	20	<i>Tenua sp.</i>	1380-1385	P50028 +30	12.8 x 96.0
17	1	<i>Circulodinium cf. distinctum</i>	2365-2370	P50068 +30	16.9 x 96.0
17	2	<i>Tenua hystrix</i>	2400-2405	P50069 +30	19.6 x 93.1
17	3	<i>Thalassiphora fenestrata</i>	630-635	P50003 +30	3.5 x 98.2
17	4	<i>Trichodinium castanea</i>	1740-1745	P50040 UN	10.5 x 93.7
17	5	<i>Trichodinium castanea</i>	2160-2165	P50061 +30	7.5 x 99.4
17	6	<i>Trichodinium castanea</i>	2160-2165	P50061 +30	7.5 x 99.4
17	7	<i>Trigonopyxidia ginella</i>	1320-1325	P50026 +30	16.8 x 96.0
17	8	<i>Trithyrodinium conservatum</i>	840-845	P50010 +30	14.3 x 98.9
17	9	<i>Trithyrodinium conservatum</i>	900-905	P50012 UN	10.7 x 103.1
17	10	<i>Trithyrodinium evittii</i>	1020-1025	P50016 +30	18.3 x 93.3

17	11	<i>Whitecliffia</i> sp.	1140-1145	P50020 +30	13.8 x 93.1
17	12	<i>Appendicisporites erdtmanii</i>	2280-2285	P50065 +30	18.0 x 108.0
17	13	<i>Appendicisporites tricornitatus</i>	2680-2685	P50085 +30	6.0 x 92.6
17	14	<i>Ornamentifera echinata</i>	2530-2535	P50078 +30	16.7 x 95.7
17	15	<i>Camazonosporites insignis</i>	840-845	P50010 +30	9.0 x 109.0
17	16	<i>Cicatricosporites annulatus</i>	2310-2315	P50066 +30	18.3 x 92.88
17	17	<i>Cicatricosporites subrotundus</i>	2880-2885	P50092 +30	10.0 x 93.0
17	18	<i>Ruffordiaspora</i> sp.	2610-2615	P50083 +30	8.3 x 97.3
17	19	<i>Cicatricosporites auritus</i>	2515-2520	P50077 +30	19.5 x 98.2
17	20	<i>Cicatricosporites auritus</i>	2935-2940	P50094 +30	12.8 x 92.7
18	1	<i>Cingutriteles</i> sp.	1680-1685	P50038 +30	15.0 x 100.0
18	2	<i>Cingutriteles</i> sp.	1935-1940	P50051 +30	6.4 x 92.9
18	3	<i>Cingutriteles</i> sp.	1980-1985	P50054 +30	11.4 x 97.0
18	4	<i>Contignisporites cooksoniae</i>	2140-2145	P50060 +30	6.0 x 97.7
18	5	<i>Distaltriangulisporites perplexus</i>	1890-1895	P50048 +30	14.1 x 97.8
18	6	<i>Distaltriangulisporites perplexus</i>	1995-2000	P50055 +30	19.3 x 93.4
18	7	<i>Distaltriangulisporites perplexus</i>	2530-2535	P50078 +30	15.0 x 94.1
18	8	<i>Distaltriangulisporites perplexus</i>	2310-2315	P50066 +30	22.0 x 99.0
18	9	<i>Foveotriteles</i> sp.	1200-1205	P50022 +30	7.8 x 93.3
18	10	<i>Sestrosporites pseudoalveolatus</i>	2140-2145	P50060 +30	21.8 x 93.0
18	11	<i>Gleicheniidites senonicus</i>	1860-1865	P50046 +30	22.8 x 97.4
18	12	<i>Matonisporites</i> sp.	2310-2315	P50066 +30	18.2 x 95.1
18	13	<i>Matonisporites</i> sp.	2445-2450	P50072 +30	2.5 x 97.2
18	14	<i>Plicatella problematicus</i>	2550-2555	P50079 +30	20.4 x 95.0
18	15	<i>Plicatella problematicus</i>	2595-2600	P50082 +30	13.1 x 95.2
18	16	<i>Rugutriteles</i> sp.	1110-1115	P50019 +30	17.5 x 98.1
18	17	<i>Rugutriteles</i> sp.	1765-1770	P50041 +30	3.5 x 97.6
18	18	<i>Rugutriteles</i> sp.	1965-1970	P50053 +30	21.0 x 92.8
18	19	<i>Rugutrietes</i> sp.	2010-2015	P50056 UN	19.4 x 95.0
18	20	<i>Rugutriteles</i> sp.	2595-2600	P50082 +30	16.6 x 99.0
19	1	<i>Tripurites</i> sp.	2880-2885	P50092 +30	21.5 x 98.6
19	2	<i>Zebrasporites</i> sp.	2160-2165	P50061 +30	21.4 x 98.1
19	3	<i>Tripurites</i> cf. <i>magnus</i>	1110-1115	P50019 +30	9.5 x 95.6
19	4	<i>Tripurites granulatus</i>	1170-1175	P50021 +30	14.7 x 94.2
19	5	<i>Tripurites</i> sp.	1170-1175	P50021 +30	9.1 x 94.2
19	6	<i>Boisduvalia clavitites</i>	630-635	P50003 +30	4.9 x 104.2
19	7	<i>Brevitricolpites</i> sp.	930-935	P50013 UN	17.0 x 103.0
19	8	<i>Caryapollenites veripites</i>	870-875	P50011 UN	16.8 x 93.0
19	9	<i>Extratropopollenites</i> sp.	2340-2345	P50037 UN	8.0 x 97.0
19	10	<i>Extratropopollenites</i> sp.	1450	P50351	16.1 x 83.6
19	11	<i>Gothanipollis</i> sp.	1170-1175	P50021 UN	14.6 x 92.5
19	12	Tricolporate pollen	780-785	P50008 UN	18.0 x 93.0
19	13	<i>Kurtzipites</i> sp.	1740-1745	P50040 +30	13.0 x 93.0
19	14	<i>Nyssapollenites</i> sp.	1050-1055	P50017 +30	14.7 x 97.0
19	15	<i>Parvisaccites radiatus</i>	2918.77	P50352	17.2 x 83.7
19	16	<i>Proteacidites</i> sp.	2310-2315	P50066 UN	20.6 x 95.0

19	17	<i>Pterocaryapollenites</i> sp.	600-605	P50002 UN	15.0 x 95.0
19	18	<i>Pterocaryapollenites</i> sp.	1500-1505	P50032 UN	4.1 x 95.7
19	19	<i>Rugubivesiculites reductus</i>	2965-2970	P50095 +30	5.0 x 95.8
19	20	<i>Spinatriporites</i> sp.	630-635	P50003 +30	5.4 x 102.1
20	1	Tetrasaccate pollen	540-545	P50000 UN	22.0 x 94.7
20	2	<i>Bombacacidites</i> sp.	900-905	P50012 UN	12.0 x 93.0
20	3	<i>Nyssapollenites</i> sp.	1020-1025	P50016 +30	17.5 x 100.7
20	4	<i>Triporopollenites</i> sp.	1451.2	P50350	21.5 x 92.0
20	5	<i>Triporopollenites</i> sp.	990-995	P50015 +30	9.6 x 92.6
20	6	<i>Triprojectus dispositus</i>	2140-2145	P50060 +30	17.5 x 98.0
20	7	<i>Trudopollis</i> sp.	1276.5	P50338	9.0 x 91.1
20	8	<i>Trudopollis</i> sp.	960-965	P50014 +30	20.8 x 100.8
20	9	<i>Momipites wyomingensis</i>	1140-1145	P50020 UN	108.0 x 93.4
20	10	<i>Extratriporopollenites</i> sp.	1320-1325	P50026 UN	18.0 x 92.6
20	11	<i>Wodehouseia gracilis</i>	1020-1025	P50016 +30	10.0 x 93.1
20	12	<i>Wodehouseia spinata</i>	1200-1205	P50022 +30	9.2 x 94.1
20	13	" <i>Fimbriaesporis</i> " sensu Williams and Brideaux 1975	630-635	P50003 +30	20.1 x 100.0
20	14	<i>Fromea chytra</i>	1281.5	P50344	16.4 x 91.2
20	15	<i>Fromea chytra</i>	1276.5	P50337	4.4 x 80.9
20	16	<i>Fromea fragilis</i>	1965-1970	P50053 +30	2.0 x 94.0
20	17	<i>Fromea quadrata</i>	2250-2255	P50064 UN	7.8 x 93.4
20	18	<i>Horologinella</i> sp.	870-875	P50011 UN	18.0 x 92.6
20	19	<i>Micrhystridium</i> sp.	1170-1175	P50021 UN	21.0 x 94.0
20	20	<i>Micrhystridium</i> sp.	1260-1265	P50024 UN	20.0 x 93.4
21	1	<i>Micrhystridium</i> sp.	1440-1445	P50030 +30	5.0 x 92.7
21	2	<i>Veryhachium trispinosum</i>	1560-1565	P50034 UN	16.5 x 94.0
21	3	<i>Cymatiosphaera</i> sp.	1350-1355	P50027 +30	10.1 x 94.2
21	4	Fungal hypha	1276.5	P50337	4.1 x 91.1

North Leif I-05 (Dartmouth slides)



SAMPLE DEPTH (M) 430-440 470-480 510-520 550-560 590-600 630-640 670-680 710-720 910-920 950-960 990-1000 1030-1040 1070-1080 1110-1120 1190-1200 1230-1240 1265-1275 1385-1395 1425-1435 1500-1510 1540-1550 1705-1715 1745-1755 1775-1785 1855-1865 1895-1905 1935-1945 1975-1985 2015-2025 2065-2085 2095-2105 2135-2145 2175-2185 2215-2225 2255-2265 2295-2305 2335-2345 2375-2385 2415-2425 2455-2465 2495-2505 2535-2545 2575-2585 2610-2620 2650-2660 2690-2700 2730-2740 2770-2780 2810-2820 2850-2860 2890-2900 2930-2940 2970-2980 3010-3020 3050-3060 3090-3100 3110-3120 3130-3140 3170-3180 3210-3220 3255-3265 3295-3305 3335-3344 3370-3380 3410-3420 3445-3455 3475-3485 3500-3505

400 500 600 700 800 900 1000 1100 1200 1300 1400 1500 1600 1700 1800 1900 2000 2100 2200 2300 2400 2500 2600 2700 2800 2900 3000 3100 3200 3300 3400 3500

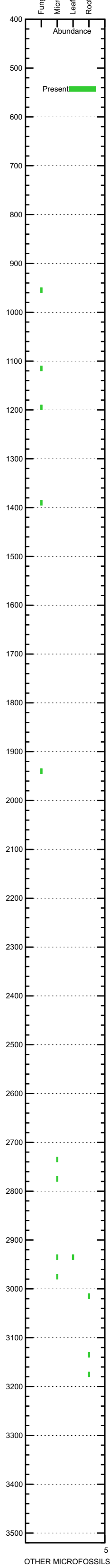
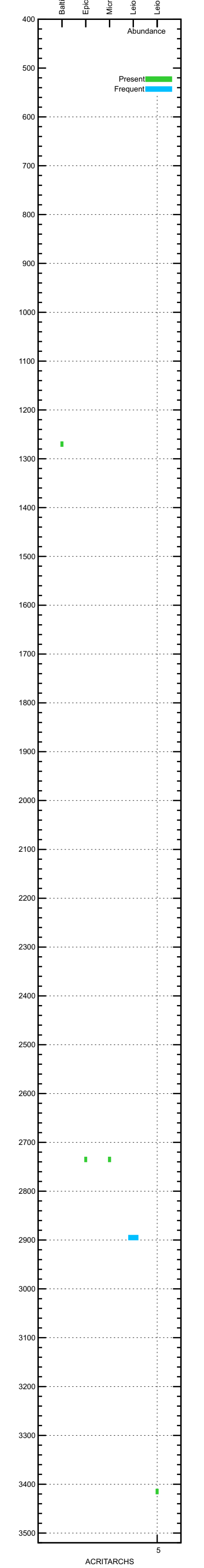
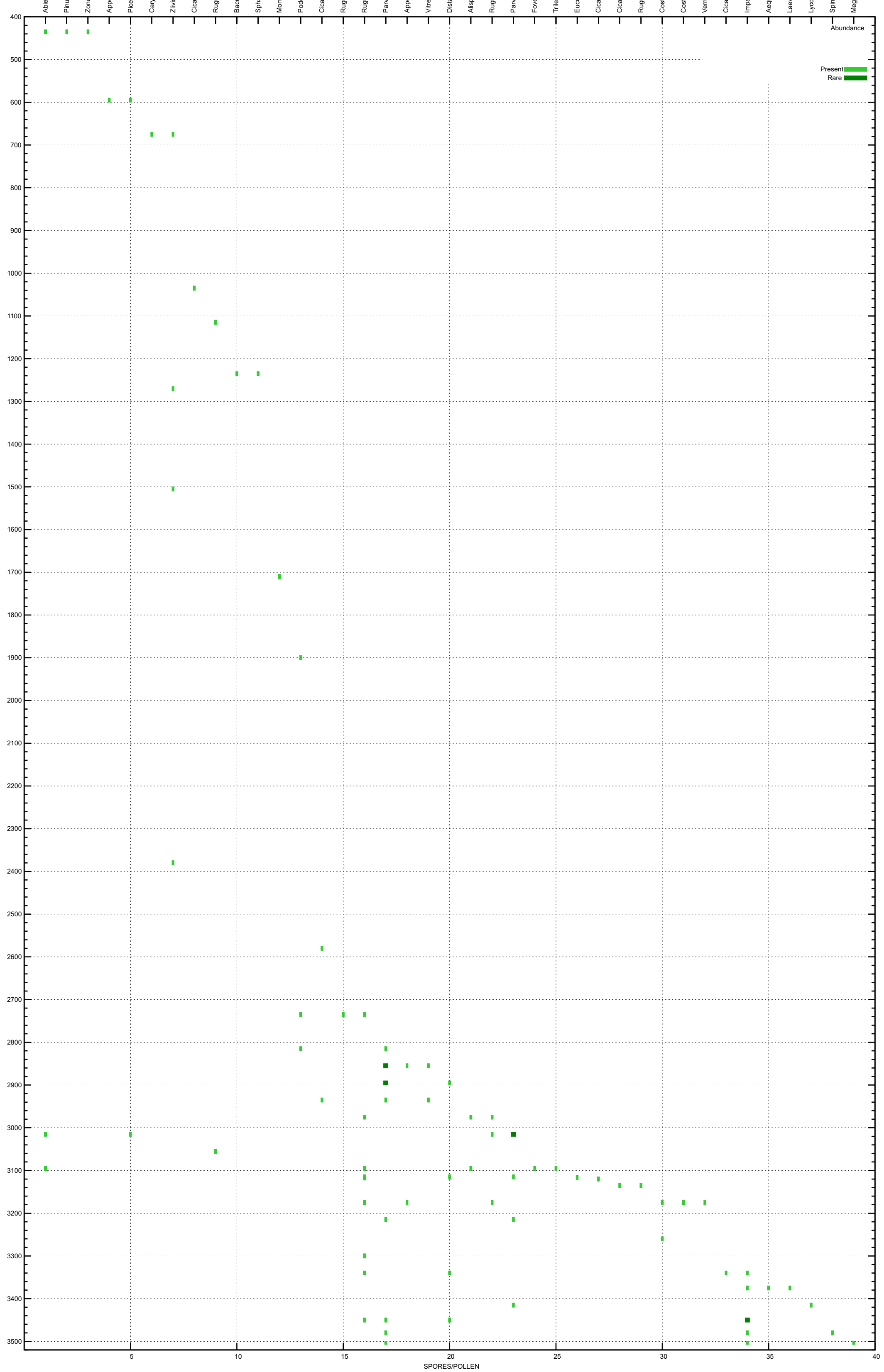
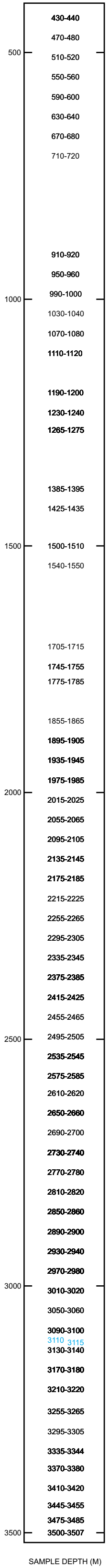
5 10 15 20 25 30 35 40 45 50 55 60 65 70 75 80 85 90 95 100 105 110 115 120 125 130 135 140 145 150 155 160 165 170 175 180

Abundance

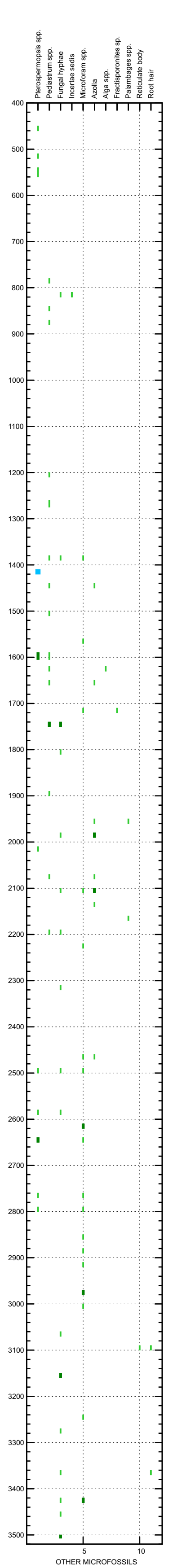
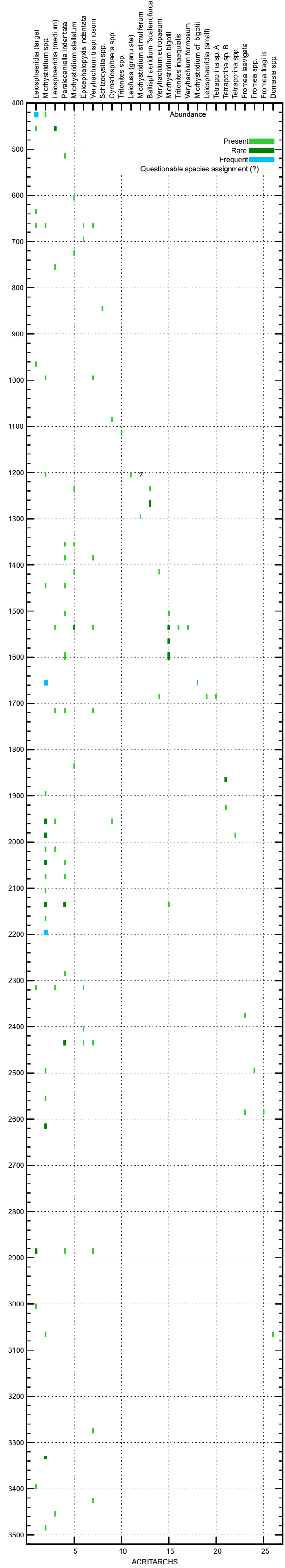
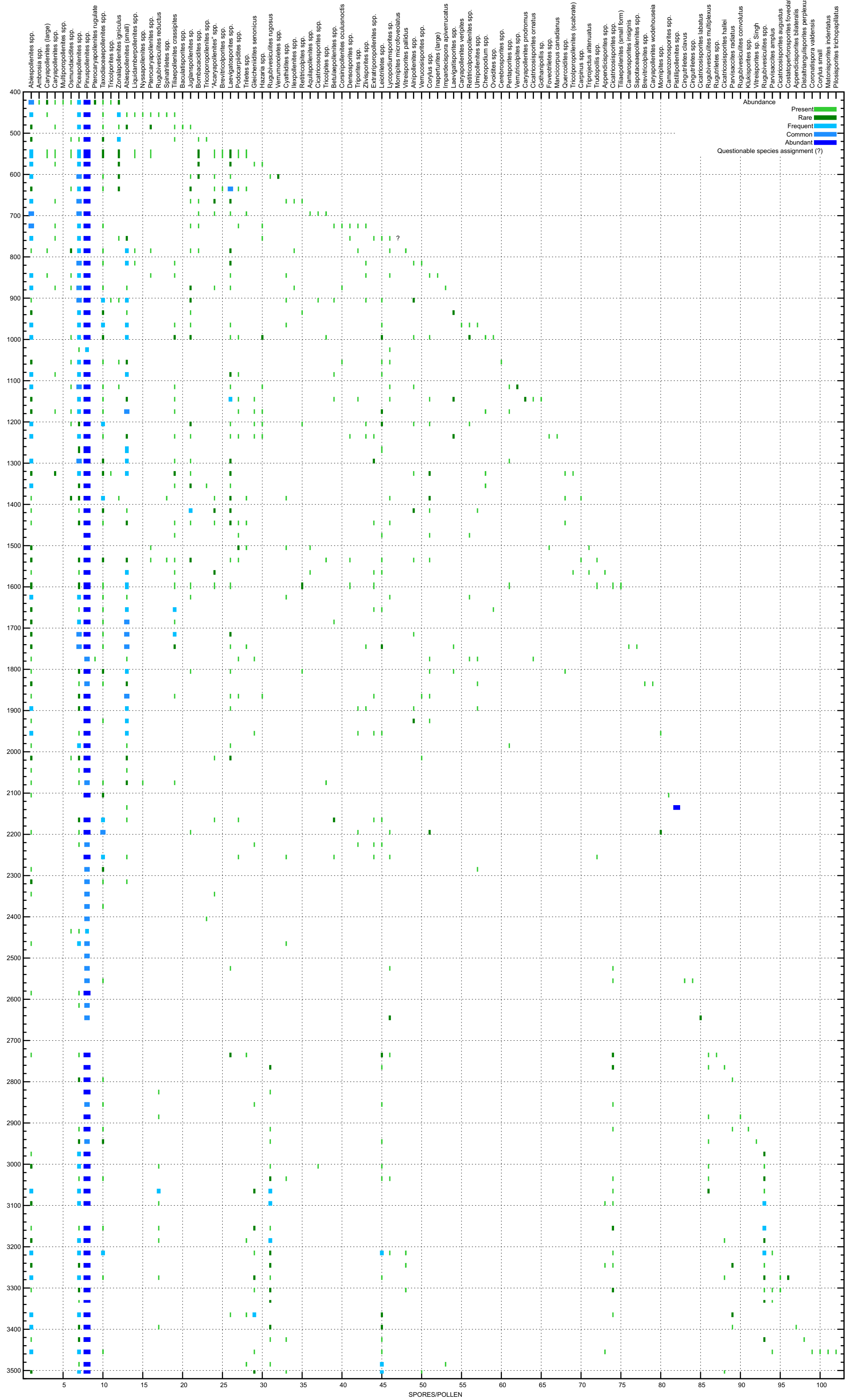
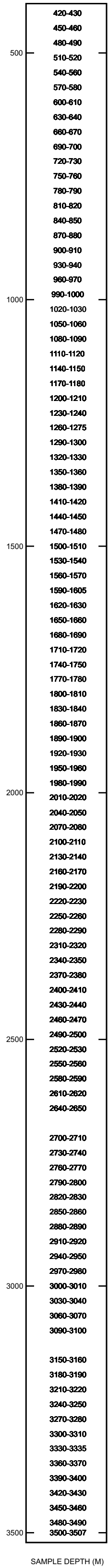
Present
Rare
Frequent
Common
Questionable species assignment (?)

DINOCYSTS

North Leif I-05 (Dartmouth slides)



North Leaf I-05 (GEUS slides)



North Leif I-05 Palynomorph Ratios

